



---

**Universidad de Valladolid**

Facultad de Ciencias

## Trabajo Fin de Grado

Grado en Química

**Comprehensive analysis of Isobutyraldehyde: millimetre-wave spectroscopy as an approach to ISM detection**

*Autor:*

*Juan Carlos del Valle Morales*

*Tutor/es:*

*José Luis Alonso Hernández*





# COMPRENHENSIVE ANALYSIS OF ISO-BUTYRALDEHYDE: MILLIMETRE-WAVE SPECTROSCOPY AS AN APPROACH TO ISM DETECTION

GRUPO DE ESPECTROSCOPIA MOLECULAR

FACULTAD DE CIENCIAS

UNIVERSIDAD DE VALLADOLID

UVa

VALLADOLID

2021









## AGRADECIMIENTOS

El trabajo recogido en la presente memoria ha sido realizado bajo la dirección del profesor José Luis Alonso Hernández, director del Grupo de Espectroscopía Molecular (GEM), a quien quiero expresar en primer lugar mi agradecimiento por su dedicación y por haberme brindado la oportunidad de trabajar y aprender en su grupo.

Querría también agradecer el apoyo y la ayuda que me han brindado a lo largo de este trabajo a Lucie Kolesniková y Miguel Sanz, que han colaborado activamente en este proyecto y cuyo consejo ha sido de gran importancia.

A todos los miembros del GEM: Santiago, Raúl, Gabriela e Iker, por su acogida en el grupo y su apoyo.

A mi familia, a mis amigos y a mi pareja no tengo palabras suficientes para agradecerles todo el cariño y el apoyo que me han dado.



# INDEX

<b>TERMINOLOGY</b> .....	<b>1</b>
<b>ABSTRACT</b> .....	<b>2</b>
<b>INTRODUCTION</b> .....	<b>3</b>
+ <i>SPECTROSCOPY AND MOLECULAR DETECTION IN SPACE: BRIEF HISTORICAL REVIEW</i> .....	3
+ <i>THE ROLE OF MILLIMETER-WAVE SPECTROSCOPY IN SPACIAL SEARCH</i> .....	4
+ <i>MOTIVATION</i> .....	6
<b>OBJECTIVES AND WORKING PLAN</b> .....	<b>7</b>
+ <i>OBJECTIVES:</i> .....	7
+ <i>WORKING PLAN:</i> .....	7
<b>THEORETICAL BASIS</b> .....	<b>8</b>
+ <i>ENERGIES OF THE SEMI-RIGID ASYMMETRIC TOP</i> .....	8
+ <i>SELECTION RULES AND LINE INTENSITY</i> .....	10
+ <i>COMPUTATIONAL METHODS</i> .....	12
<b>EXPERIMENTAL METHODOLOGY</b> .....	<b>13</b>
+ <i>FREQUENCY MODULATION MILLIMETER-WAVE SPECTROSCOPIES</i> .....	13
+ <i>EXPERIMENTAL:</i> .....	14
<b>SPECTRA ANALYSIS AND RESULTS</b> .....	<b>16</b>
+ <i>PREVIOUS WORKS ON ISO-BUTYRALDEHYDE</i> .....	16
+ <i>SPECTRAL RANGE SELECTION</i> .....	17
+ <i>GAUCHE ROTAMER: RESULTS</i> .....	18
+ <i>TRANS ROTAMER: RESULTS</i> .....	23
+ <i>GAUCHE-TRANS ENERGETIC DIFFERENCE</i> .....	27
<b>CONCLUSIONS</b> .....	<b>28</b>
<b>BIBLIOGRAPHY</b> .....	<b>29</b>
<b>IMAGES, TABLES AND EQUATIONS</b> .....	<b>32</b>
+ <i>LIST OF IMAGES:</i> .....	32
+ <i>LIST OF EQUATIONS:</i> .....	33
+ <i>LIST OF TABLES:</i> .....	34
<b>SUPPORTING INFORMATION</b> .....	<b>35</b>
+ <i>GAUCHE CONFORMER: LIST OF TRANSITIONS</i> .....	35
+ <i>TRANS ROTAMER: LIST OF TRANSITIONS</i> .....	55
+ <i>TRANS CONFORMER: LOOMIS-WOOD PLOTS</i> .....	58



## TERMINOLOGY

**AABS:** Assignment and Analysis of Broadband Spectra

**ALMA:** Atacama Large Millimeter/sub-Millimeter Array

**AMC:** Amplifier Multiplier Chains

**CARMA:** Combined Array for Research in Millimetre-wave Astronomy

**COM:** Complex Organic Molecule

**DRM:** Double Resonance Modulation

**GEM:** Grupo de Espectroscopía Molecular (University of Valladolid)

**GPIB:** General-Purpose Instrumentation Bus

**HIFI:** Heterodyne Instrument for HERSCHEL – formerly known as FIRST

**IRAM:** Institut de Radioastronomie Millimétrique

**ISM:** Interstellar Medium

**MW:** Microwave

**MMW:** Millimetre Microwave Region

**Orion-KL:** Kleinmann-Low Nebula

**QOD:** Quasi-Optical Detector

**SEM:** Stark Effect Modulation

**Sgr-B2:** Sagittarius B2

**SPCAT/SPFIT (PROSPE):** Programs for Rotational Spectroscopy

## **ABSTRACT**

Iso-butyraldehyde is a strong candidate for ISM search, for which GEM is willing to provide spectroscopical information. Out of four possible rotational conformations, only the gauche and trans rotamers are stable. In a 75 to 325 GHz frequency range analysis, more than 3800 transitions corresponding to the most stable (gauche) specie in the vibrational ground state were assigned. Only 394 transitions of the trans conformer could be assigned as a result of a mismatching between the observed and predicted frequencies.

The high number of observed transitions led to precise determination of rotational, quartic and first complete set of sextic centrifugal distortion constants using Watson's-A Hamiltonian reduction. These accurate parameters could allow the detection of iso-butyraldehyde in the ISM.

## INTRODUCTION

### + SPECTROSCOPY AND MOLECULAR DETECTION IN SPACE: BRIEF HISTORICAL REVIEW

Nowadays, there is a huge interest in unveiling the secrets of space. Its chemical composition remains mostly unknown, though many efforts are put into elucidating which substances are present in it. The combination of radio astronomy and spectroscopy has proven to be very effective in the search and detection of molecular species in outer space since the first half of the XX<sup>th</sup> century, and today it is probably the most effective way to gather data from the ISM.

Spectroscopy begins its journey back in the second half of the XVII<sup>th</sup> century, when Sir Isaac Newton<sup>1</sup> diffracted a beam of sunlight using a prism, observing how it decomposed in all the colours that conform the visible spectrum. Besides the characteristic colours of the rainbow, he stated that many dark lines were present.

These discrete black lines were catalogued and measured in 1814 by J. von Fraunhofer<sup>2</sup>. In another experiment using the light emitted by the nearby red-star Betelgeuse, he observed a change in the pattern of black lines, concluding that it depended on the object being studied.

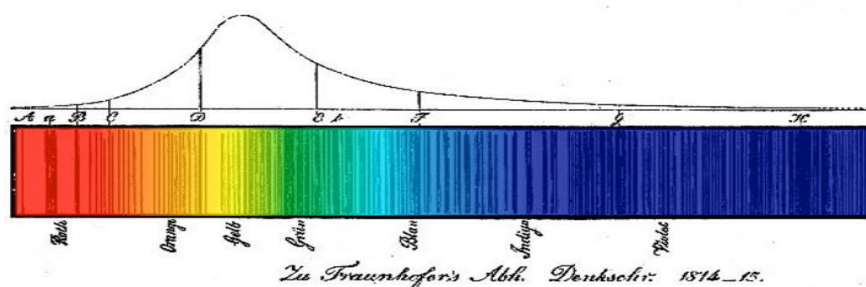


*Image 1. Fraunhofer's Betelgeuse spectrum. Note the black lines in the upper part signalling absorption zones<sup>3</sup>.*

The German scientists Kirchhoff and Bunsen further studied these lines using the combustion of different metals<sup>4</sup>. The nature of the absorption phenomena was not understood until the XX<sup>th</sup> century, when the first hypothesis of the quantum-mechanic behaviour of matter were proposed.

In 1864, Maxwell proposed that light could be described as an electromagnetic wave moving at the speed of light<sup>5,6</sup>. But it was at the beginning of the XX<sup>th</sup> century, when the electromagnetic spectrum was completely observed. Spectroscopy took a huge leap forward: observations could be done beyond human-eye barriers.

Herschel very rightly affirmed that space could be composed of molecules already present on Earth<sup>7</sup>, which was far later verified by Huggins, who observed the spectrum of several astronomical bodies<sup>8</sup> in a quite rudimentary experiment.

In 1931, Jansky showed that radiation at a frequency of 20.5 MHz received with a direction-sensitive antenna was not emitted by the sun<sup>9</sup>. This enabled the detection of molecules in the ISM as we know today: in 1937 methylidyne (CH)<sup>10</sup>, its monocation (CH<sup>+</sup>)<sup>10</sup> and the cyano radical (CN\*)<sup>11, 12, 13</sup> were discovered. Ammonia, which was the first molecule observed by rotational spectroscopy in 1934<sup>14</sup>, was detected in 1968 in space<sup>15</sup>.



As years went by and technology evolved, many more species were observed: until September 2018, 204 individual molecular species comprising 16 different elements have been detected in the ISM<sup>16</sup>.

### + THE ROLE OF MILLIMETER-WAVE SPECTROSCOPY IN SPACIAL SEARCH

“Millimetre band” is a common designation for the part of the radio-wave electromagnetic spectrum between 30 and 300 GHz. In this particular region, rotational transitions involving fundamental and excited vibrational states take place, which can be used as a molecule “fingerprint”. Astronomical interferometers are capable of providing data in these frequencies, so that through comparison, lines corresponding to a particular molecules can be detected.

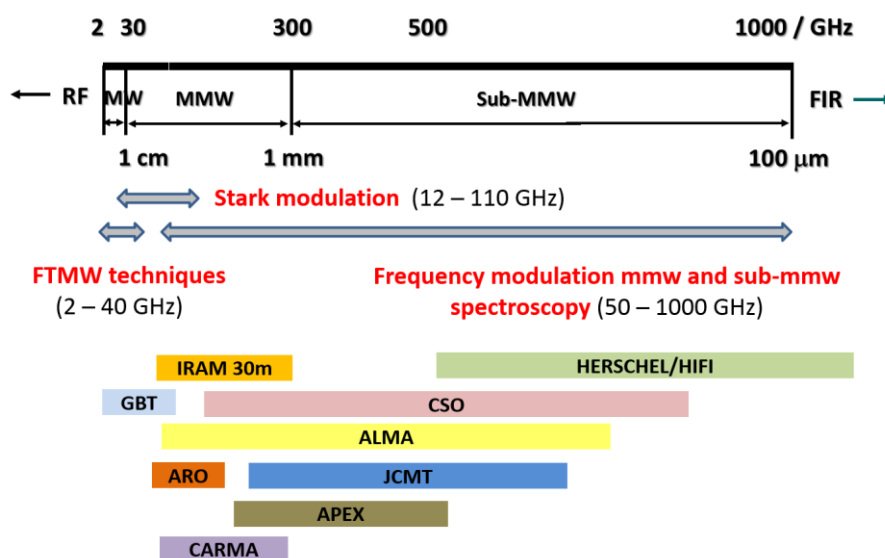


Image 2: laboratory and various astronomical interferometers coverage.

Conventional microwave spectroscopy yields precise data in the low frequency region. However, the presence of transitions involving vibrational excited states or affected by centrifugal distortion, suggest that it is not appropriate to extrapolate the results: precise data valid for ISM searching purposes can only be obtained through millimetre spectroscopy.

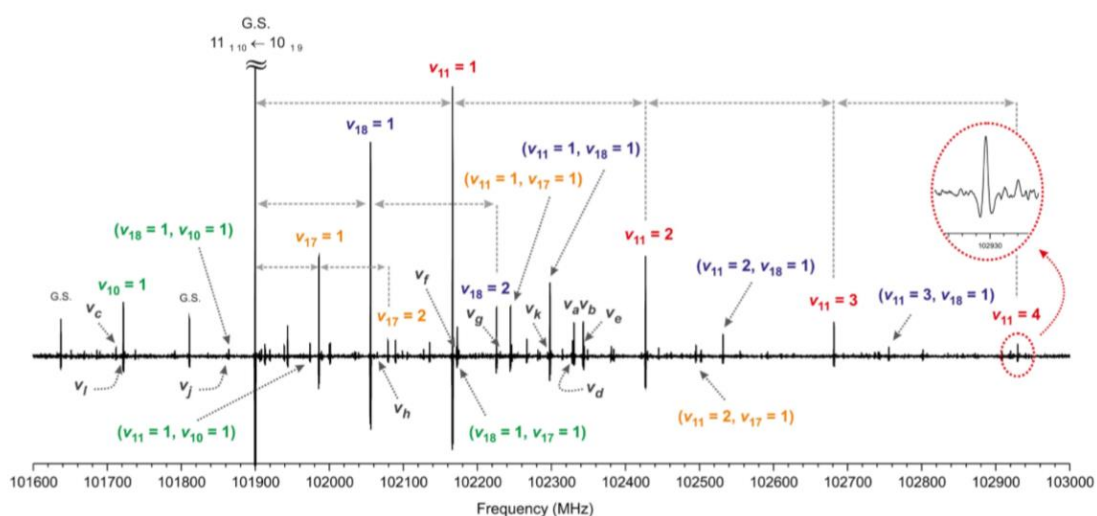
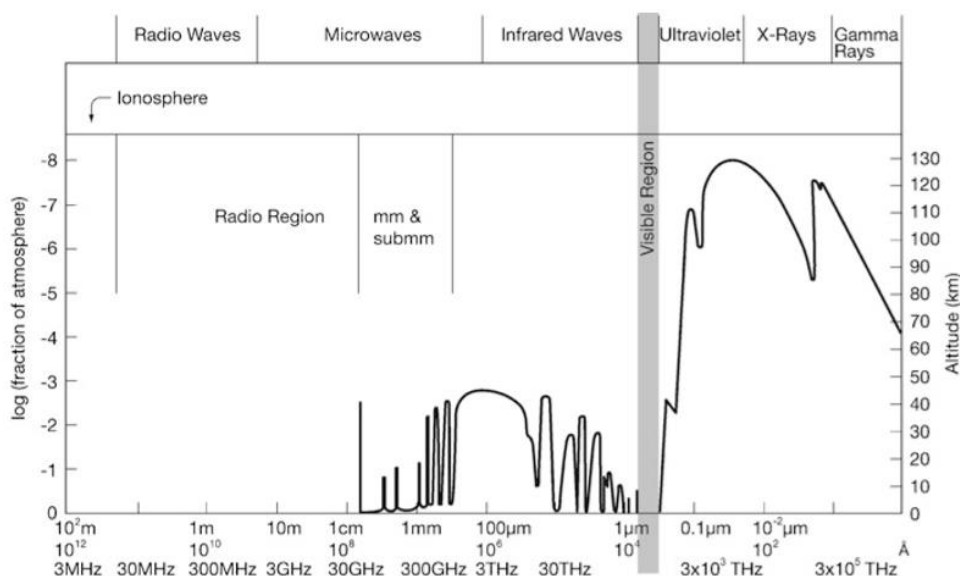


Image 3: excited vibrational states of aminoacetonitrile. Up to 29 excited states and many 13-C satellites were detected in the millimetre region<sup>17</sup>.

The use of millimetre waves is not only beneficial from a spectroscopical perspective, but also the configuration of these spectrometers has a lot to say. Resolution depends on the diameter of the antenna and the frequency of the radiation: high resolution is achieved in vast apparatus (or an array of multiple interferometers) operating between 80 and 900 GHz<sup>9, 18</sup>.

Atmospheric absorption is also another important issue since the electromagnetic waves do not trespass the atmosphere in the same way. At low frequencies, free electrons in the ionosphere block the transmission, whereas resonant absorption of the lowest rotation bands of molecules present in the atmosphere (water, CO...) do so at higher frequencies.



**Image 4: atmospheric absorption graphic.** The operation of astronomical interferometers is submitted to the radiation absorption.

The spectra obtained by these antennas, contain a huge amount of transitions involving many species. A good agreement between this data and transitions observed on Earth, indicate the detection of a molecule. To simplify future research, lines corresponding to already identified particles are subtracted.

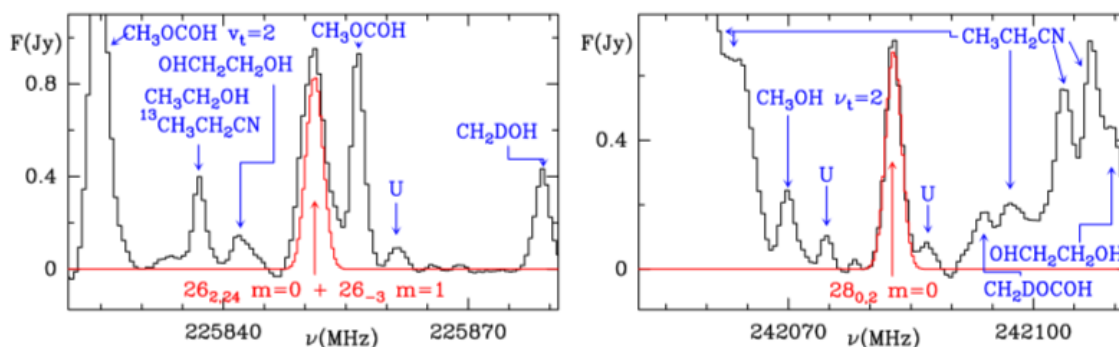


**Image 5: Orion KL selected spectra.** Note the presence of three unidentified lines, six different molecules, deuterium and 13-C isotopologues and two excited vibrational states.

Two observatories are remarkably important due to the quality of their data: IRAM (Institute de Radiastronomie Millimétrique) and ALMA (Atacama Large Millimeter/sub-Millimeter Array).

- IRAM<sup>20</sup>: result of Spanish, French and German collaboration operates two interferometers in Pico Veleta (Granada, Spain) and the French Alps.

- ALMA<sup>21</sup>: operates 64 interferometers in the Atacama Desert in a joint international effort for astronomical research.

## **+ MOTIVATION**

Spectroscopy is probably the most useful tool for astronomers to study the universe: it can detect chemical compositions, physical properties... Even though there's still a long way to go, this technique has unveiled many secrets of the ISM, especially about its composition.

Some regions in space known as "hot cores" are very active star-forming regions with very complex chemical compositions. Formed of dust clouds, when they begin to collapse, gas-phase particles condense on ice grains. Reactants move along their surface until they meet and give birth to a new molecule. Cosmic-rays spot heating or collisions release them back to space<sup>22</sup>. Sagittarius B2 (Sgr B2) and the Kleinmann-Low Nebula (Orion-KL) usually serve as searching fields.

Sgr B2 (about 100 pc from the centre of the Milky Way) is the most massive star-forming area in our Galaxy. In a routine survey using the HIFI instrument on the Herschel Space Observatory comprising the 480-1910 GHz spectral range, more than 8000 spectral features corresponding to 72 isotopologues from 4 different molecules were identified<sup>23</sup>.

As we see from this example, some regions are efficient enough to form moderately complex organic molecules (COM's). Recently, new research has reported that some COM's (isobutyraldehyde included) can be produced using ultra-high vacuum surface-science chambers at extremely low temperatures (recreating ISM conditions), thus making our molecule a potential candidate for ISM search<sup>24</sup>.

GEM has performed an exhaustive work in this field, conducting numerous researches and even achieving detection including acrylic acid<sup>25</sup>, aminoacetonitrile<sup>17</sup>, ethyl cyanide<sup>26</sup>, propenal<sup>27</sup>, and propinal<sup>28</sup> or vinyl cyanide<sup>29</sup>.

Since 2012 our group is a Unit Associated to CSIC, involved in an international endeavour to advance in our molecular understanding of the universe. In an intern communication with CSIC Professor Cernicharo, we could get to know that if an alkyl cyanide is detected in space, its corresponding aldehyde is usually found a few years later. As iso-propyl cyanide had already been detected<sup>30</sup> and later deeply studied by GEM<sup>31</sup>, we were very deeply encouraged to proceed with this study.

Though iso-butyraldehyde was previously studied by Stiefvater et al. (1986)<sup>32</sup>, as we mentioned earlier, it is not appropriate to extrapolate the results in the low frequency region to the millimetre-region as rotational energy levels are distorted by excited vibrational levels, their combinations and centrifugal effects. Millimetre-wave spectroscopy is the only technique that can provide precise results at high frequencies.



## OBJECTIVES AND WORKING PLAN

### + OBJECTIVES:

Our main goal is to provide data for future detection of iso-butyaldehyde in the ISM. Therefore, we will proceed with a spectroscopic analysis in the millimetre region from 75-325 GHz, yielding very precise rotational parameters. Future work with this data will be focused on interferometer survey comparison.

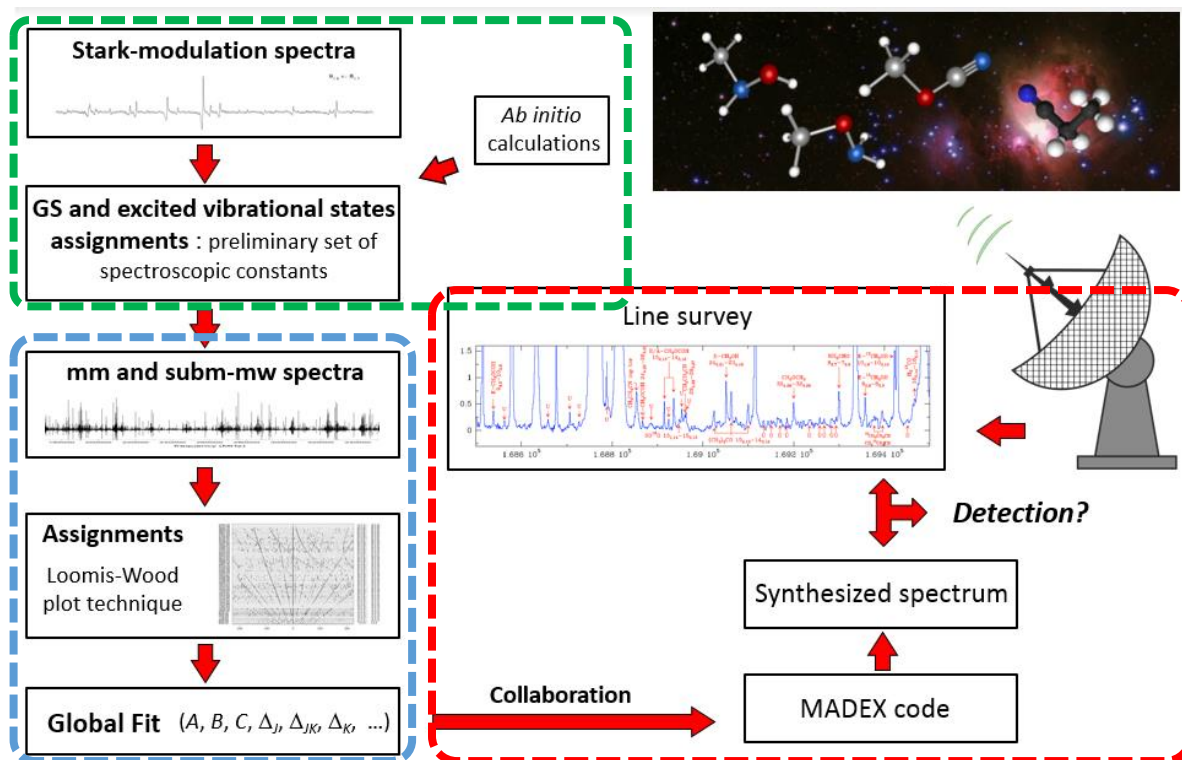


Image 6: ISM detection complete work scheme. Previous work by Stiefvater et al. is marked in green, the current work objectives in blue and future collaboration in red.

### + WORKING PLAN:

Bibliographic research was first carried out to ensure there was not high frequency data yet, familiarize with the technique and result interpretation. As previous research on the low frequency region was found (Stiefvater et al.<sup>32</sup>), we used this preliminary set of spectroscopical constants to facilitate the experimental work and line assignment.

After a commercial sample of the substance was acquired, we proceeded with the experimental part. The spectrum was assigned and analysed. Once a global fit is made, a future collaboration will allow to study the presence of this particular substance in the Interstellar Medium using this current work spectroscopic material.

## THEORETICAL BASIS

### + ENERGIES OF THE SEMI-RIGID ASYMMETRIC TOP

As both gauche and trans rotamers belong to the C<sub>1</sub> symmetry group, they are described as asymmetric rotors<sup>33</sup>. In this case, there is no internal component angular momentum: H does not commute with any component of angular momentum in a direction fixed in the rotator, and thus, only J and M are considered as accurate quantum numbers.

The molecular rotation is treated on account of a Cartesian axis system, which has its origin located at the centre of mass of the system. They are also oriented so that they coincide with the principal axes of inertia. The quantum mechanical Hamiltonian that describes an asymmetric rotor is defined as<sup>34</sup>:

$$\hat{H} = A \cdot P_A^2 + B \cdot P_B^2 + C \cdot P_C^2$$

*Equation 1: general form of the rotation Hamiltonian.*

The components of the angular momentum of rotation (P<sub>a</sub>, P<sub>b</sub> and P<sub>c</sub>) are now operators. The calculation of the energy levels is facilitated by rearrangement:

$$\begin{aligned}\hat{H} &= \frac{1}{2}(A + C) \cdot P^2 + \frac{1}{2}(A - C) \cdot \hat{H}(\kappa) \\ \hat{H}(\kappa) &= A \cdot P_A^2 + B \cdot P_B^2 + C \cdot P_C^2\end{aligned}$$

*Equation 2: rearranged Hamiltonian. Using Ray's asymmetry parameter.*

A good measure of the asymmetry of a molecule is Ray's asymmetry parameter ( $\kappa$ ), which is a relation of the rotational constants A, B and C of a molecule.

$$K = \frac{2B - A - C}{A - C}$$

*Equation 3: Ray's asymmetry parameter. It is a relation between the rotational constants in the main three axis.*

The highest asymmetry is achieved when K=0, whereas the prolate and oblate tops limit the value of K at -1 and +1 respectively. Most molecules possess moment of inertia relationships that lie somewhere between both limits.

The symmetry of the Hamiltonian operator does not allow direct solution of Schrödinger's equation. The common procedure is to expand the unknown eigenfunction in terms of a known orthogonal set of functions:

$$\psi_{J\tau} = \sum_{J,K,M} a_{JKM} \psi_{JKM} \quad \text{where} \quad \psi_{JKM} = \theta_{JKM} e^{iK\varphi} e^{iM\chi}$$

*Equation 4: expanded rotational Hamiltonian. Expressed as a weighted sum of orthogonal functions.*

Substituting equation (anterior) in the conventional  $\hat{H}\psi = E\psi$  Schrödinger's equation and multiplying by the conjugate of a member of the orthogonal set, we obtain the general formula:

$$\sum_n c_n \int \psi_m^* \hat{H} \psi_n d\tau = E \sum_n c_n \int \psi_m^* \psi_n d\tau$$

**Equation 5: Schrödinger's equation general formula.** Note the position of the Hamiltonian inside the integral, in contrast to the eigenvalue  $E$ , at the very beginning outside the integral.

The assumed set is orthogonal except when  $m=n$ . Since they are normalized, this quantity will be one whenever  $m=n$ . The previous formula will therefore be converted to the secular equation, as it represents a set of "I" linear equations containing "I" unknown coefficients with a nontrivial solution only if the determinant of the coefficient vanishes.

$$|(m|\hat{H}|n) - E\delta_{m,n}| = 0$$

**Equation 6: secular equation.** It represents a set of "I" linear equations with "I" unknown coefficients.

The final solution is given by the secular determinant, in which the  $\lambda$  values that make the determinant vanish, are the allowed energy levels for an asymmetric rotor<sup>35,36</sup>.

$$\sum_{K=-J}^{+J} (\hat{H}_{K'K} - \delta_{K'K}\lambda) a_{JKM} = 0 \quad \text{where } K' = -J \dots J$$

**Equation 7: setup of the secular determinant.** A very similar representation from equation 6.

As there are no off-diagonal matrix elements in  $J$ , they can be treated separately: we will have a secular determinant for each  $J$ , each one composed of  $2J+1$  rows and columns where  $K$  will take all integer values from  $J$  to  $-J$ .

This particular matrix has diagonal and off-diagonal elements and it is symmetrical about both diagonals. It is related to the fact that the basis vectors are degenerate in  $\pm K$  and thus can be separated in two blocks; one consisting of even  $K$  values, and the other of odd  $K$  values.

The diagonalization is carried out using Wang's matrix  $U_J$ , yielding the final eigenvalues:

$$U_J H U_J = \hat{H} \quad \text{where } U_J = 1/\sqrt{2} \begin{bmatrix} -1 & 0 & 0 & 0 & 1 \\ 0 & -1 & 0 & 1 & 0 \\ 0 & 0 & \sqrt{2} & 0 & 0 \\ 0 & 1 & 0 & 1 & 0 \\ 1 & 0 & 0 & 0 & 1 \end{bmatrix}$$

**Equation 8: Wang's diagonalizing matrix.** It can be further expanded as  $J$  values go higher.

The non-commuting properties of  $P_z$  and  $\hat{H}$  do not allow us to use  $K$  as a quantum number. However, each energy level is linked to a  $K$  value in the prolate limit ( $K_{-1}$ ) and another in the oblate limit ( $K_1$ ). This lets us represent the relation between the energy levels of a symmetric top with an asymmetric one.

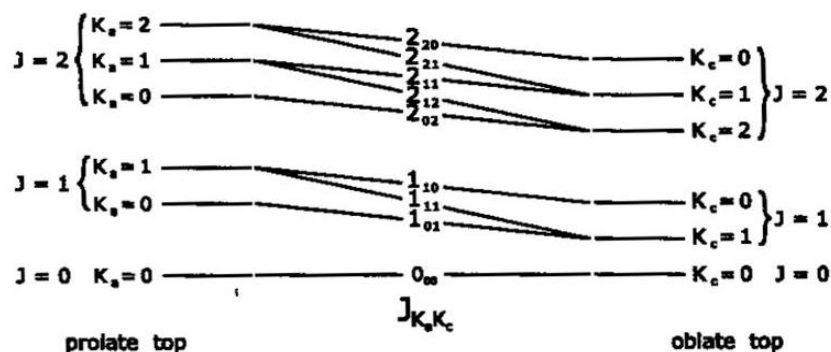


**Image 7: symmetric and asymmetric top energies correlation diagram**<sup>33</sup>. The straight-line representation is only approximate. The asymmetry splitting of the K levels decrease as K increases, and for a given K, it increases as J increases.

Energy levels are usually marked as  $J_{K_1, K_2}$  ( $K_1=K_A$  and  $K_2=K_C$ ) using King-Hainer-Cross notation<sup>34</sup>. In the older notation, a single  $\tau$  subscript can be used, making clear that  $\tau=K_1-K_2$ .

The conventional rigid rotor model is not completely appropriate for describing rotational transitions: molecules are not stiff since during rotation, centrifugal forces are interfering, modifying bond lengths and angles. At higher frequencies, distortions are more important and produce huge shifts in transitions' energies.

Its effects on spectra will depend on the angular momentum operators and the  $\tau$  constants of distortion defined by Kivelson and Willson and later corrected by Watson and Howard. A first order approximation is not enough for fully describing the distortion. Instead, using Watson's A reduction, we will describe up to the sextics distortion terms<sup>34</sup>:

$$\hat{H} = AJ_A^2 + BJ_B^2 + CJ_C^2 - \Delta_J J^4 - \Delta_{JK} J^2 J_A^2 - \Delta_K J_A^4 - \frac{1}{2} (\delta_J + \delta_K J_A^2 J_+^2 + J_-^2)_+ + \Phi_J J^6 + \Phi_{JK} J^4 J_A^2 + \Phi_{KJ} J^2 J_A^4 + \Phi_K J_A^6 + \frac{1}{2} (\varphi_J J^4 + \varphi_{JK} J^2 J_A^2 + \varphi_K J^4 J_+^2 + J_-^2)_+$$

**Equation 9: semi-rigid rotor Hamiltonian up to sextics distortion terms.** As in equation 7, the first three terms come from the rigid rotor Hamiltonian, whereas the rest account for centrifugal distortion.

The distortion terms included are:

- Quartics:  $\Delta_J, \Delta_{JK}, \Delta_K, \delta_J, \delta_K$ .
- Sextics:  $\Phi_J, \Phi_{JK}, \Phi_{KJ}, \Phi_K, \phi_J, \phi_{JK}, \phi_K$

## + SELECTION RULES AND LINE INTENSITY

The selection rules arise from the non-vanishing property of the dipole matrix elements<sup>33</sup>:

$$R_r = \int \psi_r'^* \mu \psi_r''^* d\tau$$

**Equation 10: transition dipole moment.** The gross selection rule for rotational spectroscopy is that molecules must have dipolar moment.

The first selection rule involves the J quantum number, as only  $\Delta J=0, \pm 1$  changes are allowed. We refer to these transitions as branches: P-Branch ( $\Delta J=-1$ ), Q-Branch ( $\Delta J=0$ ) or R-Branch ( $\Delta J=1$ ).

Another set of restrictions involving the "K" pseudoquantum numbers arise from the symmetry properties of the ellipsoid of inertia. The component of the electric moment along a space-fixed axis F, can be written as:

$$\mu_F = \sum_g \cos(Fg) \mu_g$$

**Equation 11: electric moment along axis F.** The cosine function defines the angles between the fixed F-axes and the rotating g-axes.

The substitution of equation 8 into 7 gives the true transition integral:

$$(J, K_{-1}, K_1 | \mu_F | J', K'_{-1}, K'_1) = \mu_g (J, K_{-1}, K_1 | \text{Cos}(Fg) | J', K'_{-1}, K'_1)$$

**Equation 12: transition integral.** The considered  $g$ -axis in each case will define different selection rules.

For this integral not to vanish, it must be unchanged for any operation which carries the system into a configuration indistinguishable from the original. The symmetry of the ellipsoid of inertia will be characterized by the Four-group operations<sup>34</sup>:

Symmetry	E	C <sub>2</sub> <sup>a</sup>	C <sub>2</sub> <sup>b</sup>	C <sub>2</sub> <sup>c</sup>
A	1	1	1	1
B <sub>a</sub>	1	1	-1	-1
B <sub>b</sub>	1	-1	1	-1
B <sub>c</sub>	1	-1	-1	1

**Table 1: Four-Group character table V (a,b,c).** Cos (Fa) transforms according to B<sub>a</sub>, Cos (Fb) to B<sub>b</sub> and Cos (Fc) to B<sub>c</sub>

Taking into account the transition integral in equation 14, it comes clear that for  $\mu_a$  only transitions A  $\leftrightarrow$  B<sub>a</sub> and B<sub>b</sub>  $\leftrightarrow$  B<sub>c</sub> are possible. For  $\mu_b$ , A  $\leftrightarrow$  B<sub>b</sub> and B<sub>a</sub>  $\leftrightarrow$  B<sub>c</sub>; or for  $\mu_c$ , A  $\leftrightarrow$  B<sub>c</sub> and B<sub>a</sub>  $\leftrightarrow$  B<sub>b</sub>.

The selections rules are stated in terms of the evenness or oddness of K<sub>-1</sub> and K<sub>1</sub>. The connection between the numbers K<sub>-1</sub> and K<sub>1</sub>, and the symmetry of the Four-Group is given by Mulliken, who used the expanded rotational eigenfunction in equation 4 and Wang symmetrizing transformation matrix<sup>34,36,37</sup>.

Dipole Moment	$\Delta K_{-1}$	$\Delta K_1$
$\mu_a$ (a-type transitions)	Even	Odd
$\mu_b$ (b-type transitions)	Odd	Odd
$\mu_c$ (c-type transitions)	Odd	Even

**Table 2: selection rules for the pseudoquantum numbers "K" in terms of evenness and oddness**

In order to evaluate intensities, we must obtain the matrix elements. The z component of the matrix element for a given transition will be expressed by:

$$\mu_z = \mu_a \int \cos(az) \psi_i \psi_j^* d\tau + \mu_b \int \cos(bz) \psi_i \psi_j^* d\tau + \mu_c \int \cos(cz) \psi_i \psi_j^* d\tau$$

**Equation 13: Z component of the matrix element for a given transition**

As seen in equation 9, the wave functions of an asymmetric rotor can be expanded in terms of those of a symmetric one, and thus, the matrix elements can be derived. The dipole elements for a symmetric top can be divided in various factors:

$$\mu_g = \mu \varphi_{JJ'} \varphi_{JKJ'K'} \varphi_{JMJM'}$$

**Equation 14: dipole matrix elements as function of direction-cosine matrix factors.** They are dependant of the quantum numbers marked in the subscript.

These dipole moments will be used in the next equation, which represents the proportionality between them and the transition strength:

$$(\mu_x)^2 S(x)_{JklJ'_{mn}}(K) = (2J + 1) \left| (\mu_x)_{JklJ'_{mn}} \right|^2$$

**Equation 15: relation between dipole moment and the intensity of a transition.** S is a tabulated quantity obtained as a function of initial and final state and of the asymmetry parameter K.

Taking into account the Maxwell-Boltzmann's distribution applied to rotation:

$$f_{rot} = \frac{(2J + 1)e^{-\frac{W(J,K,K')}{kT}}}{\sum_J (2J + 1)e^{-\frac{W(J,K,K')}{kT}}}$$

**Equation 16: Maxwell-Boltzmann's factor applied to rotation.** It is defined as the population ratio of an energy level in comparison to another (or various levels)

Assuming there are no other effects (nuclear spins), the highest intensity will be defined by the maximum absorption coefficient<sup>35</sup>. Mixing equations 11 and 12':

$$\gamma_{max} = \frac{8\pi h N f_v}{3c(kT)^2} \sqrt{\frac{\pi h ABC}{kT}} e^{-\frac{W(J,K,K')}{kT}} (2J + 1) |\mu_{ij}|^2 \frac{v^2}{\Delta v}$$

**Equation 17: maximum absorption coefficient.** Note the dependence with  $T$ .

In order to match the shape of astronomical interferometers' surveys and rotational spectra shapes, intensities are modified using the partition function. Neglecting the electronic and nuclear spin states, as at room temperature molecules are in their ground states, we are left with vibrational and rotational terms only.

If anharmonicities are neglected, the vibrational partition function can be expressed as:

$$Q_V = \prod_j (1 - e^{-hv_j/kT})$$

**Equation 18: vibrational partition function.** Where  $v$  represents the frequencies of the fundamental modes of vibration.

In case of the rotational partition function, an approximate formula is usually employed:

$$Q_R = \left( \frac{5.34 * 10^6}{\sigma} \right) * \left( \frac{T^3}{ABC} \right)$$

**Equation 19: rotational partition function.** Where  $\sigma$  is a measure of the degree of symmetry.

## **+ COMPUTATIONAL METHODS**

Although the present study has been completely experimental, computational methods have played an important role in it. The spectra was fully analysed using Pickett's SPFIT/SPCAT program suite<sup>38</sup>.

To prove that O.L Stiefvater<sup>32</sup> constants were accurate, an initial set of calculus was made using three different methods. First, a simple DFT (B3LYP/6-311G(d,p)) is used to optimize the structure in minimum time. Rotational constants and dipole moment were then improved with MP2/6-311++G(d,p) and B2PLYPD3/aug-cc-pVTZ methods.



## EXPERIMENTAL METHODOLOGY

### + FREQUENCY MODULATION MILLIMETER-WAVE SPECTROSCOPIES

The experiment was carried out using two different millimetre-wave spectrometer configurations in the GEM at the University of Valladolid<sup>26,39</sup>. A double pass configuration was used to cover a range from 75 to 112 GHz and 170-325 GHz, whereas in the single pass array the range from 120-170 GHz was swept.

The microwave source is a frequency modulated signal generator (Agilent E8257D) operating from 12 to 20 GHz, phased locked to a Rubidium standard. A series of amplifier multipliers (Virginia Diodes) multiply the frequency of the source by factors of 3,4,6,9, 12(as combination of 3\*4) and 18 (as combination of 3\*6).

Frequency	Configuration	Multiplier	Multiplier	Detector	Output	Input
75-110	Double Pass	6	WR 10.0	WR 10.0	5-20	16
120-170	Single Pass	9	WR 6.5	QOD	2-8	18
170-240	Double Pass	12	WR 9.0 + WR 4.3	WR 4.3	2.5-4	16
240-325	Double Pass	18	WR 9.0 + WR 2.8	WR 3.4	1	16

**Table 3: spectrometer configuration chart.** Operation parameters are conditioned by manufacturer specifications. All experiments were conducted under 1.8 V attenuation.

For both configurations, the detected signal is amplified and sent back to a brand new lock-in amplifier (SR810-DSP), where  $2f$  detection is applied, where  $f$  is the modulation frequency, to increase the sensitivity of the measurements. A 10.2 kHz modulation frequency is used for both detectors, whereas phase is automatically imposed by the new lock-in amplifier. Standard GPIB connects the generator and amplifier to the computer, being controlled by LabVIEW software. A set of metallic parabolic mirrors (Edmund Optics) are used to focus the input and output radiation.

A home-made rooftop mirror and a polarization grid (Millitech Inc.) allow us to double the optical path length of the Pyrex glass cell from 3.6 to 7.2 metres, resulting in the creation of the double pass configuration.

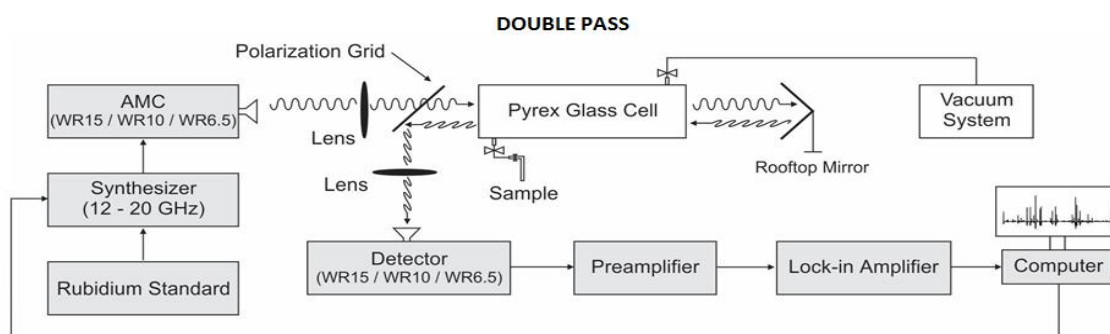


**Image 8: double pass spectrometer scheme.** Note that the input and output radiation enter the Pyrex chamber through the same end, and how the polarization grid reflects the output radiation towards the detection array.

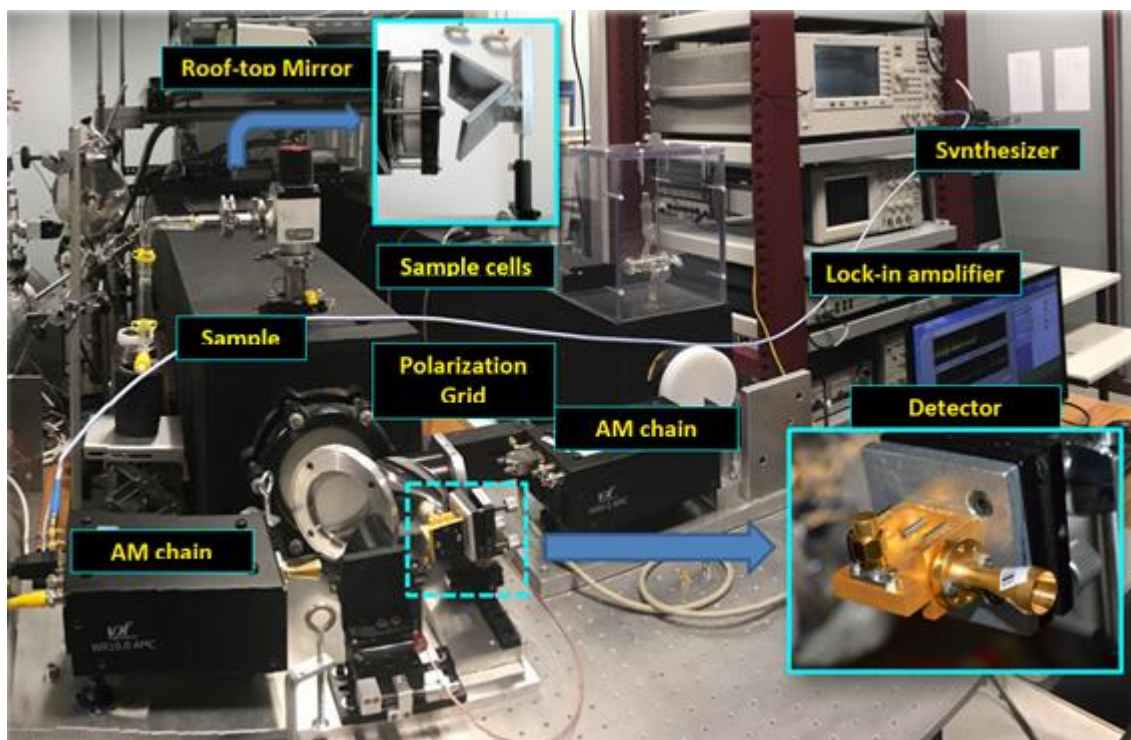


*Image 9: GEM's millimetre-wave spectrometer double pass configuration. Note on the right side of the picture the single pass apparatus without the polarization grid nor the rooftop mirror.*

In case we operate between 120-170 GHz, a single configuration apparatus involving a Quasi-Optical Detector (QOD) by VDI is used. The main difference is the absence of the mirror and the grid, resulting in an optical path of 300 cm.

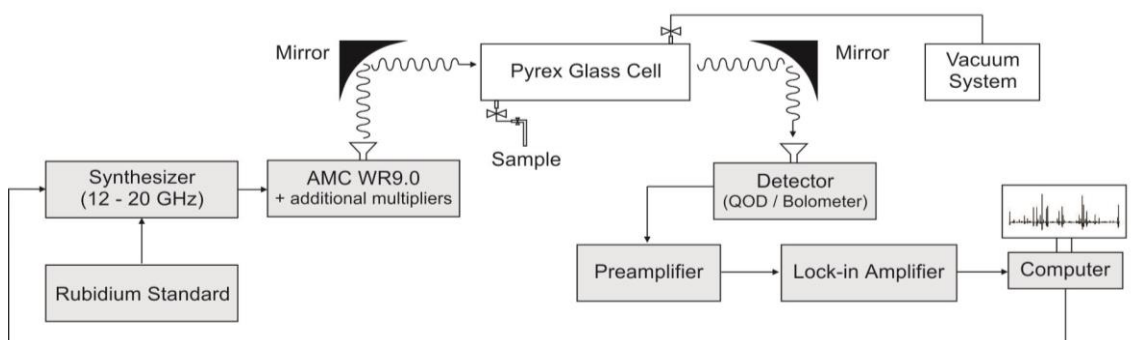


*Image 10: single pass configuration scheme. In this case, a QOD detector at the back end of the Pyrex glass sample cell is used.*

### **+ EXPERIMENTAL:**

Iso-butyraldehyde is a colourless liquid at room temperature with a fairly low boiling point (b.p. 63°C). Spectroscopic work was carried out on a commercial sample, which was used without further purification. The liquid was introduced into a flask, which was later connected to the vacuum pressurized Pyrex glass. The sample was previously cooled with liquid nitrogen to avoid the introduction of the oxidation by-products (iso-butyric acid; b.p. 155°C). Using the vacuum system, pressure inside the chamber is regulated at around 20  $\mu$ bar.

The spectrometer is set up depending on the region being studied and connected. Five line measurements (involving the most intense transitions) are performed to ensure the quality of the spectrum. The spectrum is finally recorded in 1 GHz sections in both directions, yielding a precision better than 30 kHz. The spectra are combined in one single spectrum, which is finally analysed using H.M.Pickett's package<sup>38</sup>.

Once the experimental procedure is finished, the Pyrex glass cell is emptied using high vacuum and the flask is disconnected.

## SPECTRA ANALYSIS AND RESULTS

### + PREVIOUS WORKS ON ISO-BUTYRALDEHYDE

Iso-butyraldehyde was first studied by Stiefvater et al. (1986)<sup>32</sup> using a K-Band DRM spectrometer and a Stark-Effect Modulated spectrometer (SEM) at dry ice temperature (200 K). Out of four possible rotameric structures, only two were found to be stable: gauche and trans.

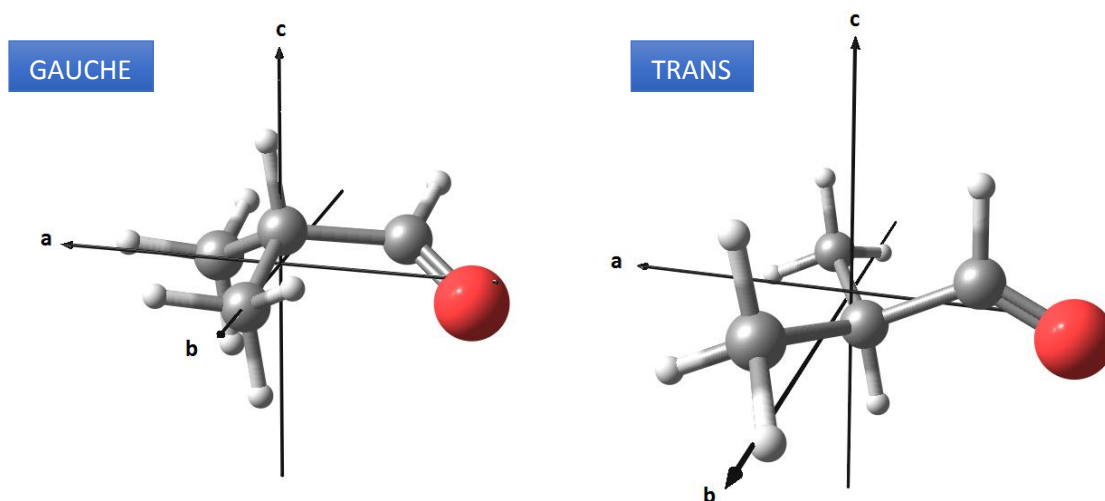


Image 11: gauche and trans conformers. Note the ac symmetry plane in the trans rotameric form.

The energy difference between both is 1030 cal/mol ( $360.25 \text{ cm}^{-1}$ ), so according to Maxwell-Boltzmann's distribution, ISM detection can be performed attending mainly to the gauche rotameric form.

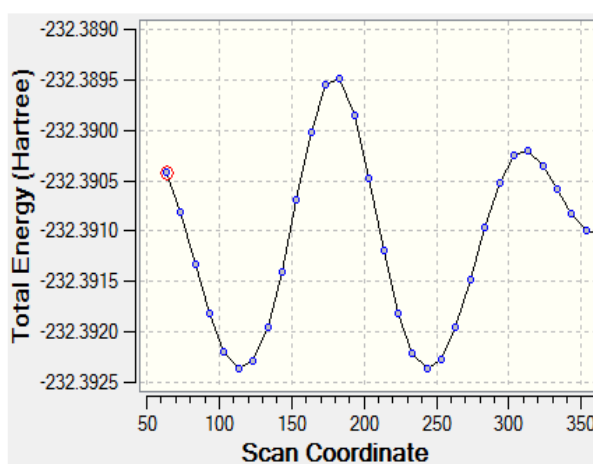
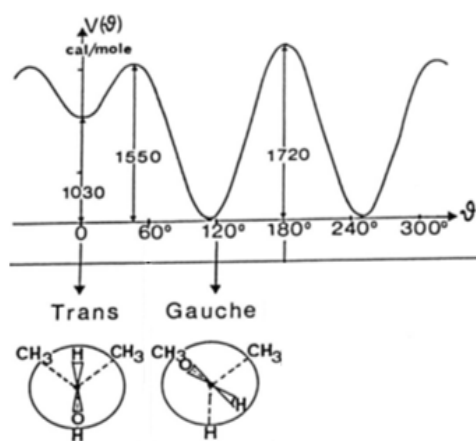


Image 12: O.L. Stiefvater and B3LYP/6-311G(d,p) predicted energy barriers. Both methods predict a similar energetic difference between the conformers.

Measures with a precision better than 76 kHz in the gauche conformer and 97 kHz for trans allowed to obtain up to quartic distortion terms.

Parameter	Gauche	Trans
A (MHz)	7494.62 ± 0.02	7707.84 ± 0.03
B (MHz)	4107.51 ± 0.02	3736.63 ± 0.02
C (MHz)	2980.70 ± 0.02	2815.08 ± 0.02
ΔJ (kHz)	1.9 ± 0.5	0.7 ± 0.4
ΔJK (kHz)	-0.3 ± 0.3	48.4 ± 0.7
ΔK (kHz)	11.2 ± 0.7	-19.0 ± 5.0
δJ (kHz)	0.28 ± 0.02	0.18 ± 0.02
δK (kHz)	3.6 ± 0.2	25.0 ± 0.5
μ <sub>A</sub>	2.43 ± 0.02	2.82 ± 0.02
μ <sub>B</sub>	0.80 ± 0.03	Zero by symmetry
μ <sub>C</sub>	0.83 ± 0.02	0.46 ± 0.03
μ <sub>TOTAL</sub>	2.69 ± 0.03	2.86 ± 0.03
K	-0.501	-0.623

Table 4: Stiefvater et al. (1986) iso-butyraldehyde rotational parameters. A new fit was made on the trans conformer due to data contradictions.

### + SPECTRAL RANGE SELECTION

Best resolution is achieved in frequencies where transitions are most intense. Using data from the previous article, a simulation of the spectrum is generated. Line intensities are modified by imposing a temperature of 100 K. In both species, the line with maximum intensity at ISM temperatures belongs to the 170-240 GHz range.

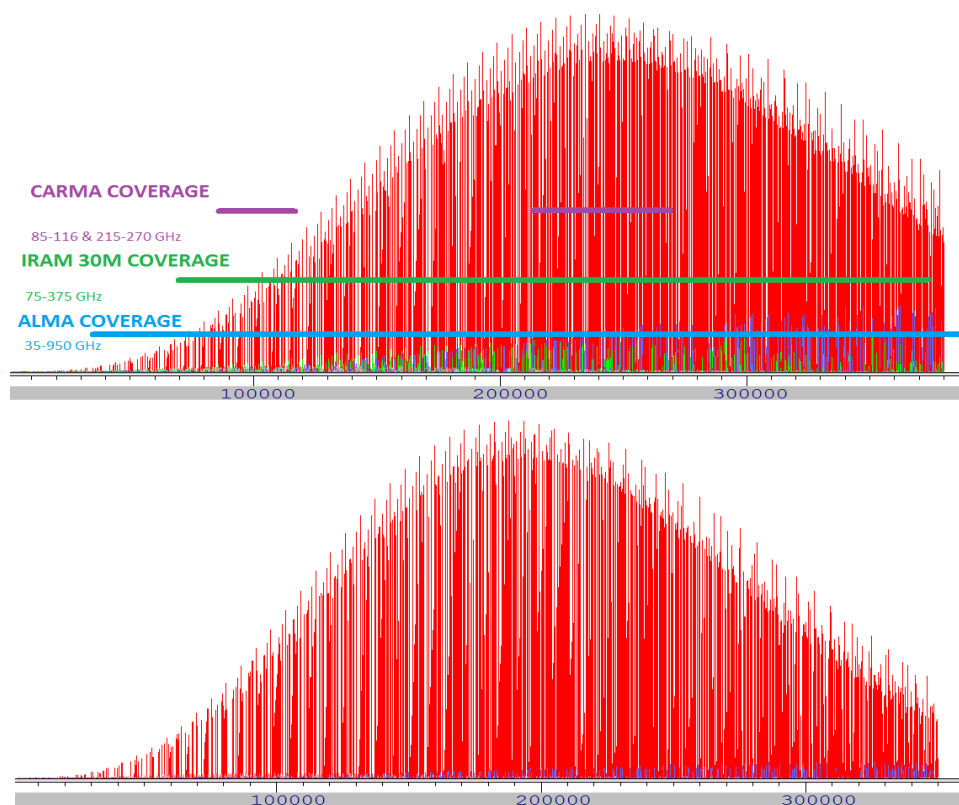


Image 13: intensity profile at 100K compared to some astronomical interferometers coverage. The gauche conformer in the upper part, has maximum expected intensity between 230-260 GHz, whereas the trans specie maximum in the lower part, lies between 170-200 GHz<sup>18,19</sup>.

The most intense line in the gauche form would be formed by the combination of transitions  $39_{0,39} \leftarrow 38_{0,38}$ ;  $39_{0,39} \leftarrow 38_{1,38}$ ;  $39_{1,39} \leftarrow 38_{0,38}$  and  $39_{1,39} \leftarrow 38_{1,38}$  at 234422.9325 Hz. In the trans conformation it is the  $33_{0,33} \leftarrow 32_{0,33}$  and  $33_{1,33} \leftarrow 32_{1,32}$  set at 187869.5016 Hz.

Note that low frequency parameters are not precise at higher frequencies since centrifugal and vibrational distortions take place. However, to make a first approach, instead of using computational methods, we can rely on this information.

It seems that the best range for study would lie somewhere between 170 and 240 GHz. To ensure that there is sufficient data, we extend our study up to 75-325 GHz, where most interferometers operate: CARMA, IRAM 30M, ALMA...

### + GAUCHE ROTAMER: RESULTS

Previous measurements by Stiefvater et al (1986) significantly facilitated the assignments at lower frequencies. It was proved that a, b and c-type transitions will be relevant in the gauche isomers; however, due to the bc symmetry plane only a and c-type transitions will be present in the trans isomer.

Some calculations were made using the Gaussian 16 package at B3LYP/6-311G(d,p), MP2-/6-311++(d,p) and B2PLYPD3/aug-cc-pVTZ levels to predict the rotational constants.

Level	A (MHz)	B (MHz)	C (MHz)	$\mu_A$	$\mu_B$	$\mu_C$	$\mu_{TOTAL}$
MP2	7439.24	4125.23	3007.61	2.408	0.757	0.978	2.707
B2PLYPD3	7497.13	4123.61	2997.15	2.544	0.774	0.971	2.831
B3LYP	7461.32	4092.43	2968.66	2.627	0.781	0.974	2.909
Stiefvater	7494.62	4107.51	2980.70	2.43	0.80	0.83	2.69

Table 5: rotational constant and dipole moment comparison for gauche rotamer. Note that the B2PLYP/aug-cc-pVTZ level seems to be most accurate.

It is quite clear that the B2PLYPD3/aug-cc-pVTZ is the most accurate. However, since we have previous experimental data, line assignment will not rely on computational calculus. A prediction using this information at high frequency is made to prove the need of further centrifugal distortion terms.

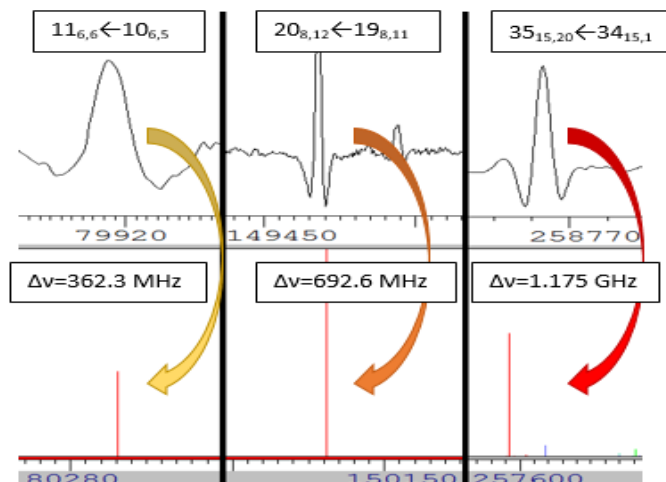


Image 14: prediction using up to quartic distortion terms by Stiefvater et al.<sup>32</sup> versus real spectra. At higher frequencies when centrifugal distortion is more important, line shift is greater.



R-branch a-type transitions were first assigned due to their high intensity. They form a very particular harmonic pattern, set up in groups centred at approximately  $(B+C)(J''+1)$  and spanning  $(B-C)(J''+1)$ . As they do not depend on A; B and C parameters get more precise as transitions are input.

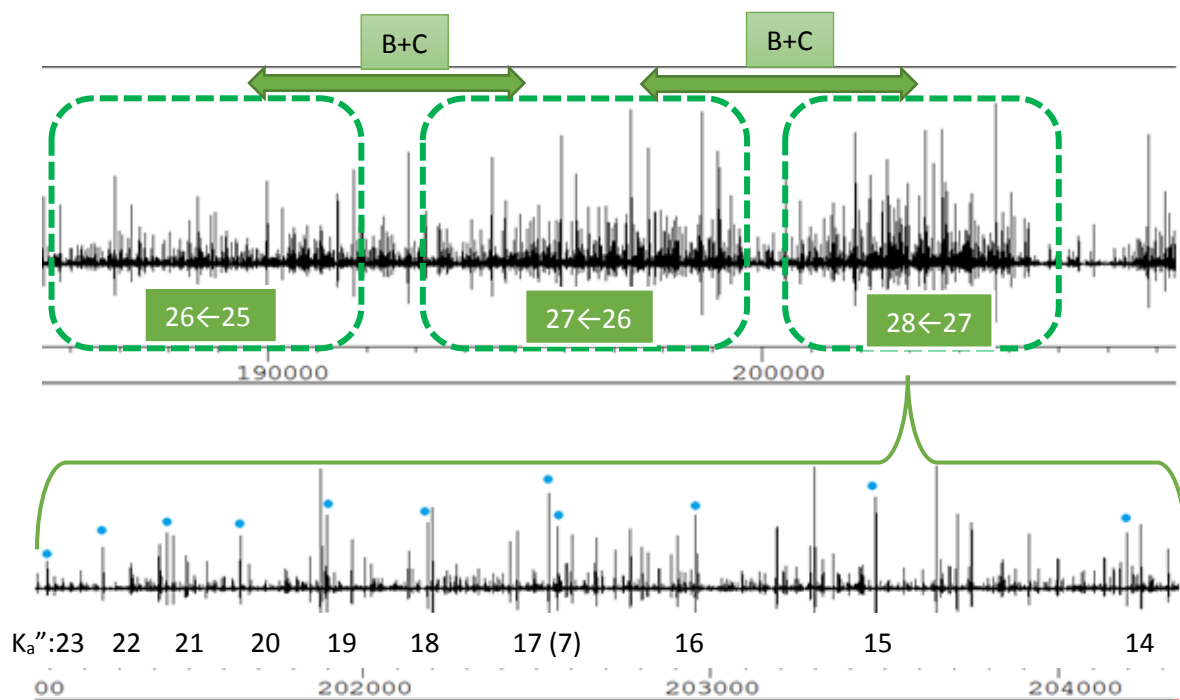


Image 15: a 22 GHz section of the room-temperature rotational spectrum of *i*-butylaldehyde. Groups of transitions involving  $J''=25, 26$  and  $27$  are displayed, showing a clear  $B+C$  distancing between them.

Image 16:  $J(28\leftarrow 27)$  section zoom. Higher  $K_a''$  are found at lower frequencies until they lose degeneracy, when the branch splits towards higher and lower frequencies (note the presence of  $K_a''=7$  between  $K_a''=16$  and  $K_a''=17$ )

Transitions involving low  $K_a$  numbers are not degenerate. As  $K_a$  values begin to rise, transitions tend to merge until one line finally contains two features with the same  $K_a$  but different  $K_c$ :  $(K_a, K_c)$  and  $(K_a, K_c+1)$ . Some lines cannot be taken into account on the global fit since they are not degenerate but closer than the 30 kHz spectral resolution.

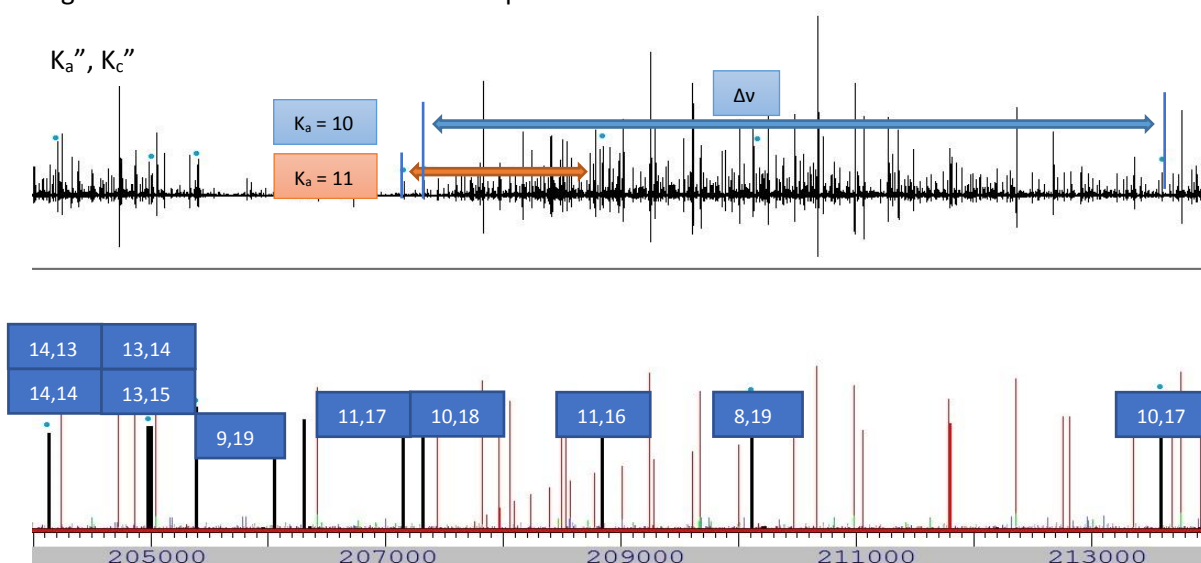
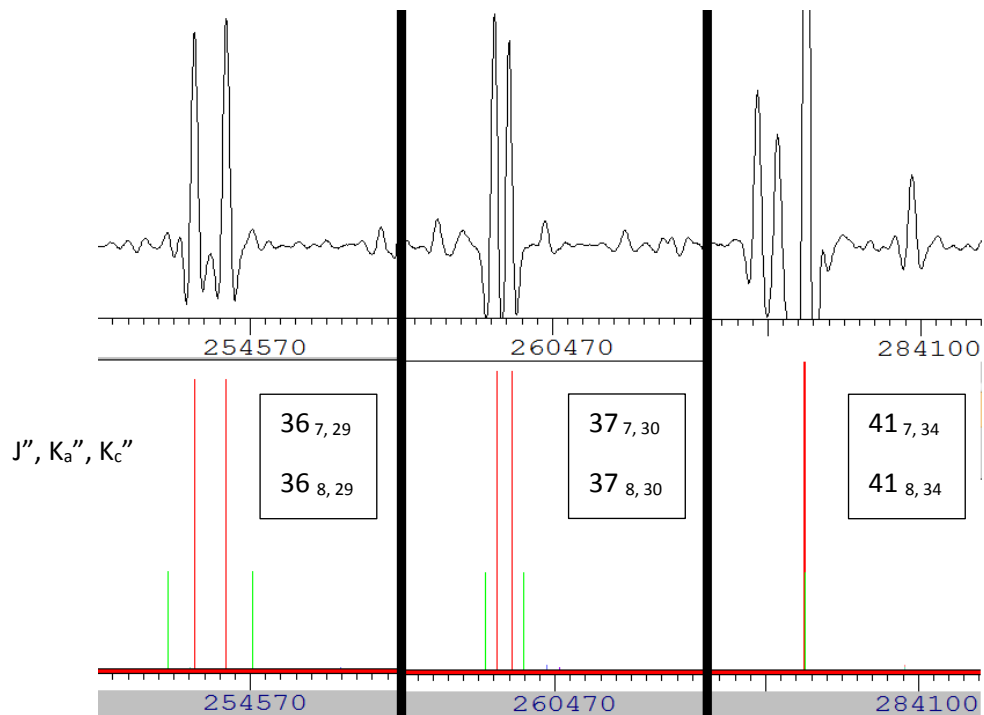


Image 17:  $J(28\leftarrow 27)$  lines selection degeneracy split. Note the higher shift in frequencies for  $K=10$ .

R-branch a-type transitions are also degenerate with R.b-type.  $J''_{K_a, K_c}$  levels produce b.R ( $\Delta K_a=1$ ;  $\Delta K_c=1$ ) transitions, whereas  $J''_{K_a+1, K_c}$  levels do so with  $\Delta K_a=-1$ ;  $\Delta K_c=1$ . Most of these lines were measured with a.R transitions, as when not degenerate line intensity is very poor.

Lines are found not degenerate at low frequencies and tend to merge into one line at higher ranges. As higher  $K_a''$  numbers are involved, blending takes place at higher energies.



*Image 18: b.R transitions blending with a.R type. Lines begin to merge as frequency rises.*

R-branch c-type transitions can be measured also as long as they are accompanied by more intense b-type lines.

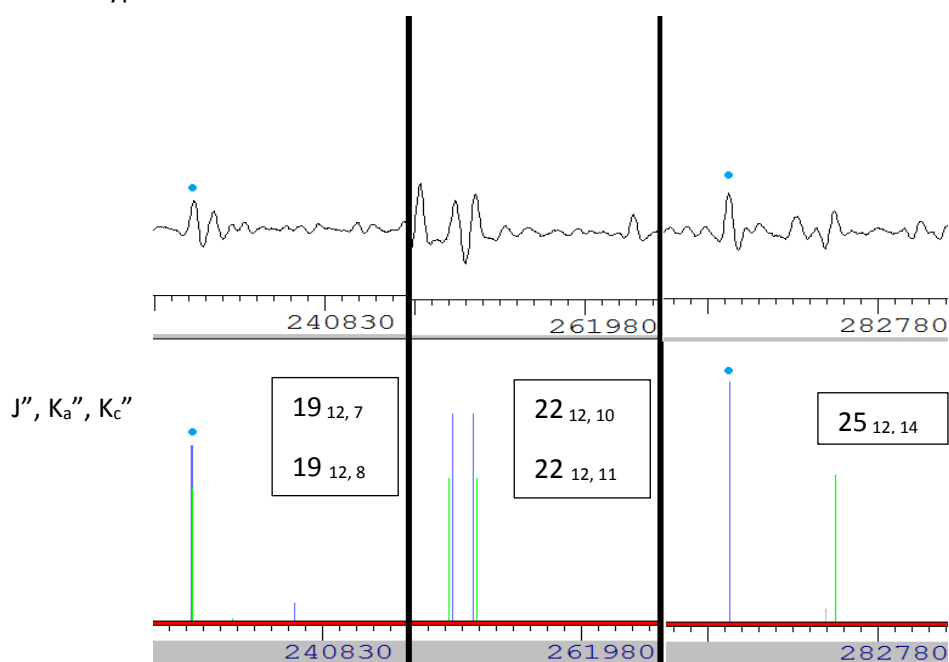


*Image 19: b.R and c.R-type transitions split. Note that b.R not degenerate lines are indistinguishable from the noise.*

In this case, the involved lower energy levels are  $J''_{K_a, K_c}$  and  $J''_{K_a, K_c+1}$ . The first one produces b.R ( $\Delta K_a=1; \Delta K_c=1$ ) transitions, the second  $\Delta K_a=1; \Delta K_c=-1$  and both of them c-type  $\Delta K_a=1; \Delta K_c=0$ . Lines diverge as frequency rises: at higher  $K_a''$ , transitions remain degenerate for longer ranges.

Q-branch a, b and c-type transitions are also included. However, due to their low intensity, they are studied when degenerate with other lines. Given the initial  $J''_{K_a, K_c}$  level, it is possible to study a-type  $\Delta K_a=2; \Delta K_c=-1$  and b-type  $\Delta K_a=1; \Delta K_c=-1$  transitions, and in the  $J''_{K_a+1, K_c}$  level, a-type  $\Delta K_a=0; \Delta K_c=-1$  and b-type  $\Delta K_a=1; \Delta K_c=-1$ . As frequency drops, degeneracy is lost. Higher  $K_a''$  values imply that this split will take place at higher frequencies.

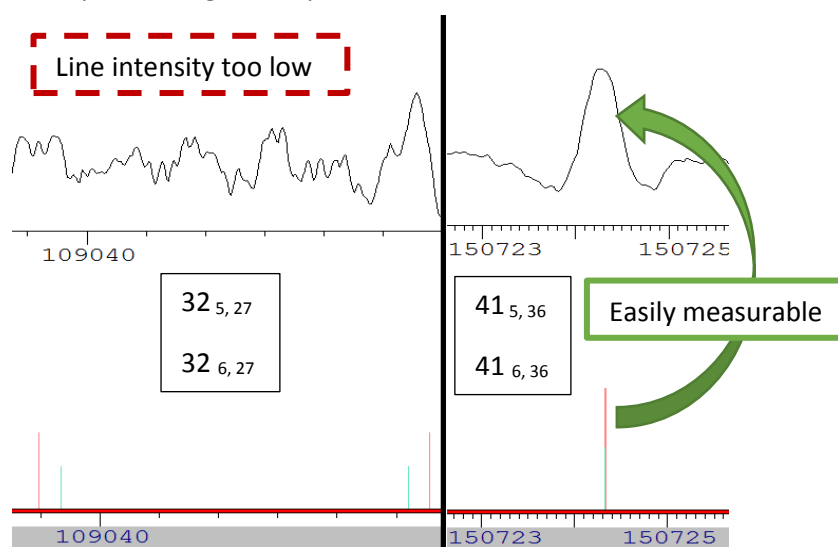


Image 20: a.Q and b.Q-type transitions degeneracy split. Note that in most cases, when these lines are not degenerate, their intensity is not high enough to be measured.

Only a few c-type transitions could be seen, and they were always accompanied by b.Q transitions. No pattern could be described in this case.

About 1900 lines corresponding to 3888 transitions were measured, and the ranges of the quantum numbers  $J''$  and  $K_a''$  were extended up to 79 and 44. The fits and prediction were made in terms of Watson's A-reduced Hamiltonian with the Pickett's SPFIT/SPCAT program suite<sup>38</sup>.

Constant	Unit	Value <sup>a</sup>
A	MHz	7494.613589 (162)
B	MHz	4107.511610 ( 68)
C	MHz	2980.699704 ( 71)
$\Delta_J$	kHz	1.960525 ( 51)
$\Delta_{JK}$	kHz	-0.298455 (160)
$\Delta_K$	kHz	11.39002 ( 44)
$\delta_J$	kHz	0.2790495 (163)
$\delta_K$	kHz	3.704685 (145)
$\Phi_J$	Hz	0.0054768 (125)
$\Phi_{JK}$	Hz	0.062851 ( 70)
$\Phi_K$	Hz	0.34070 ( 45)
$\Phi_{KJ}$	Hz	-0.399255 (243)
$\phi_J$	Hz	0.0001810 ( 38)
$\phi_{JK}$	Hz	0.048063 ( 50)
$\phi_K$	Hz	-0.093600 (199)

$\sigma_{\text{fit}}^{\text{b}}$	kHz	23
$\kappa$		-0.501
$J''_{\text{max}}$		79
$K''_{\text{max}}$		44

- a) The number in parenthesis are  $1\sigma$  uncertainties in units of the last decimal digit.  
 b) Root mean square deviation of the fit.

Table 6: ground state spectroscopic constants of gauche iso-butyraldehyde (Watson's A-Reduction)

The line intensity of the present spectrum will be modified for ISM search using the partition function. The rotational contribution is calculated with the present work constants, and the vibrational part is estimated at B2PLYPD3/aug-cc-pVTZ computational level and using J.R.Durig (1990)<sup>40</sup> data:

T /K	$Q_{\text{rot}}$	$Q_{\text{vib}}$ (IR gas)	$Q_{\text{tot}}$ (Exp)
9.38	507.7790	1.0000	507.7841
18.75	1432.7594	1.0032	147.3068
37.50	4048.2085	1.0601	4291.5771
75.00	11447.6189	1.3607	15577.3579
150.00	32395.4141	2.9026	55190.5621
225.00	59557.2200	7.0407	419326.4039
300.00	91764.5868	17.4012	1596818.0587

Mode	IR gas ( $\text{cm}^{-1}$ )
$\nu_1$	75
$\nu_2$	212
$\nu_3$	227
$\nu_4$	272
$\nu_5$	351
$\nu_6$	395
$\nu_7$	632
$\nu_8$	800
$\nu_9$	922
$\nu_{10}$	933
$\nu_{11}$	942
$\nu_{12}$	965

Table 7: partition function of the gauche conformer at various temperatures. The vibrational partition function was calculated using J.R. Durig's gas phase infrared analysis data.

Table 8: normal vibrational modes for the gauche conformer.

### + TRANS ROTAMER: RESULTS

In this case due to the bc symmetry plane, only a and c type transitions are possible. On account of the energetic difference between the cis and trans rotameric conformations, line intensity in the latter one is expected to be very low. Thus, only a.R-type transitions could be assigned.

Level	A (MHz)	B (MHz)	C (MHz)	$\mu_A$	$\mu_B$	$\mu_C$	$\mu_{TOTAL}$
MP2	7730.12	3713.45	2813.13	2.783	0	0.658	2.860
B2PLYPD3	7747.19	3734.07	2823.61	2.904	0	0.679	2.982
B3LYP	7680.41	3719.41	2807.57	2.986	0	0.689	3.065
Stiefvater	7707.84	3736.63	2815.8	2.82	0	0.46	2.86

Table 9: rotational constant and dipole moment comparison for trans rotamer. Both MP2 and B2PLYPD3 methods are quite accurate.

No clear pattern could be observed in this conformation. However, as in the previous conformer, transitions involving low values of the  $K_a$  number are degenerate. When  $K_a$  takes higher values, these lines begin to merge, finally blending into one single line, containing transitions between the fundamental states  $(J, K_a, K_c)$  and  $(J, K_a, K_c+1)$ .

Only 394 transitions up to  $K_a=5$  could be assigned. As this number got higher, huge shifts between the observed and predicted frequencies appeared. Including further centrifugal distortion correction terms was not appropriate since uncertainties became as high as the calculated parameter itself.

Loomis-Wood plots represent the deviation of the observed transitions from the original prediction, and they are a very reliable method to see if lines follow a clear pattern.

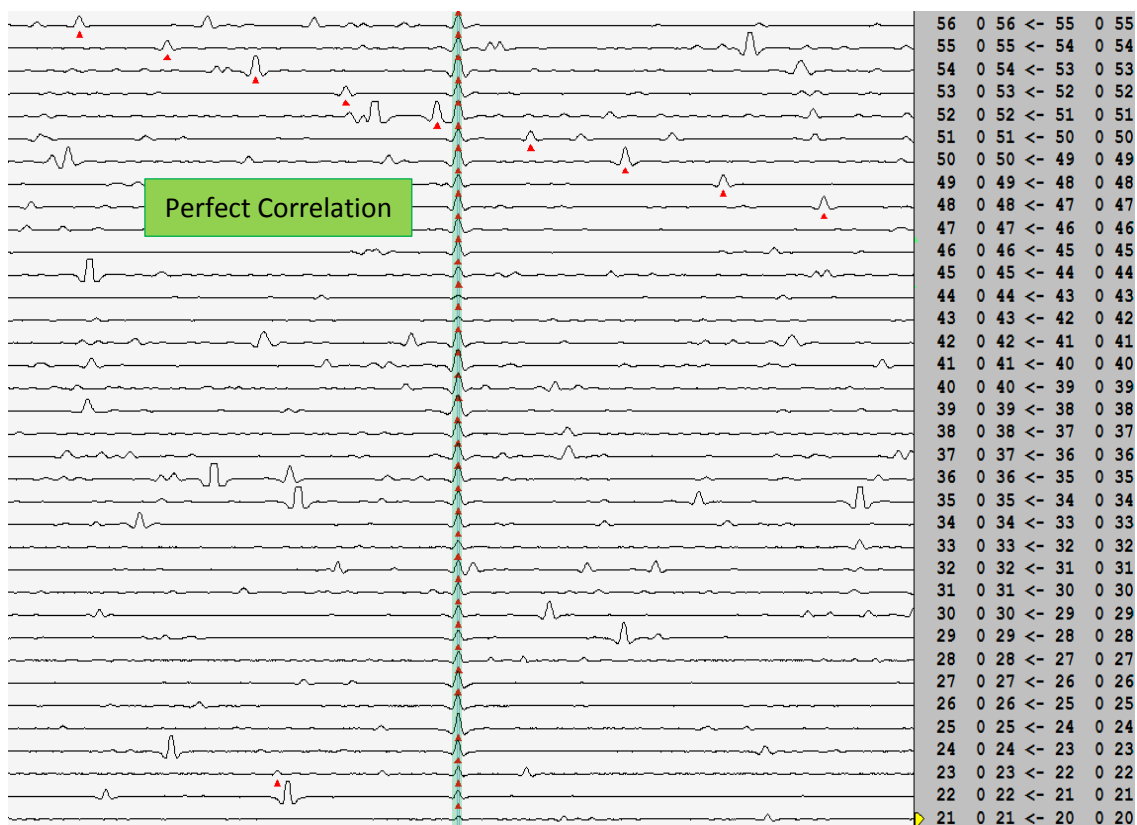


Image 21: Loomis-Wood plot for  $K_a=0$  in the trans rotamer. Assigned lines match perfectly the prediction.

The green line represents the prediction using the final fit data and the red triangles are the assigned frequencies for a given line. At the lowest  $K_a$  value possible ( $K_a=0$ ), there is a perfect matching. In the upper part, there is a crossing pattern that belongs to the series involving  $K_a=4$ .

Further plots were made involving  $K_a$  numbers up to 15. Only a few plots are displayed as they were found most representative.

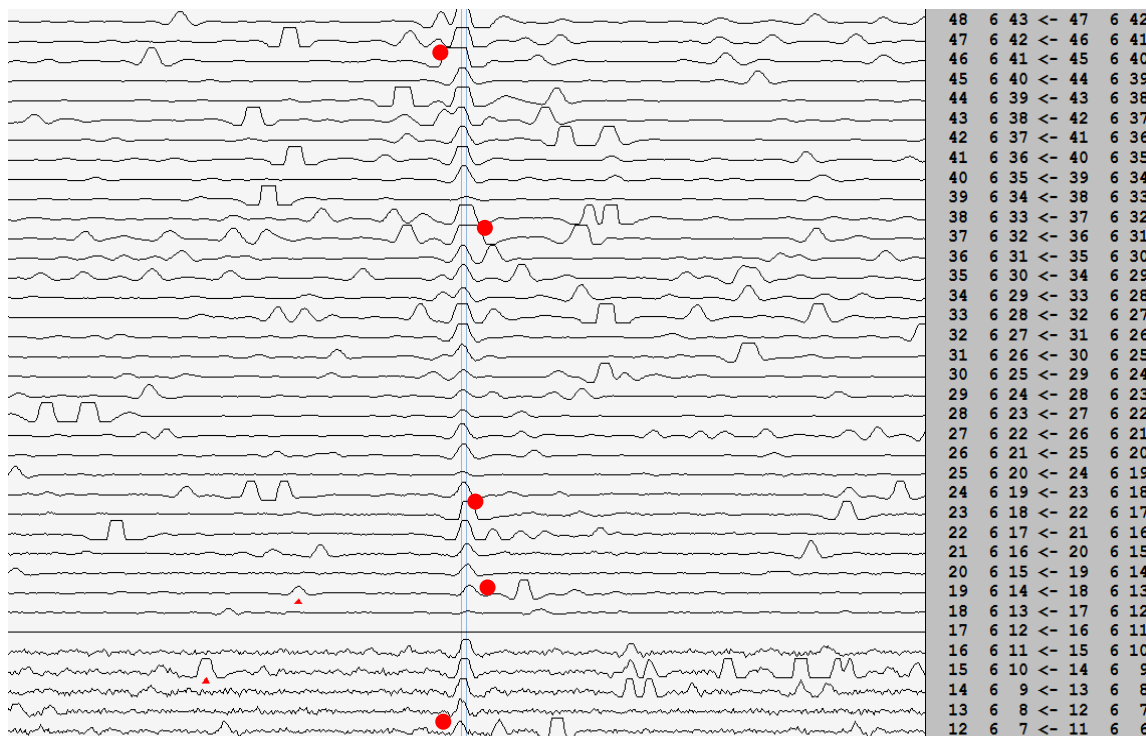


Image 22: LW plot for  $K_a=6$  in the *trans* rotamer. Red dots indicate lines too deviated.

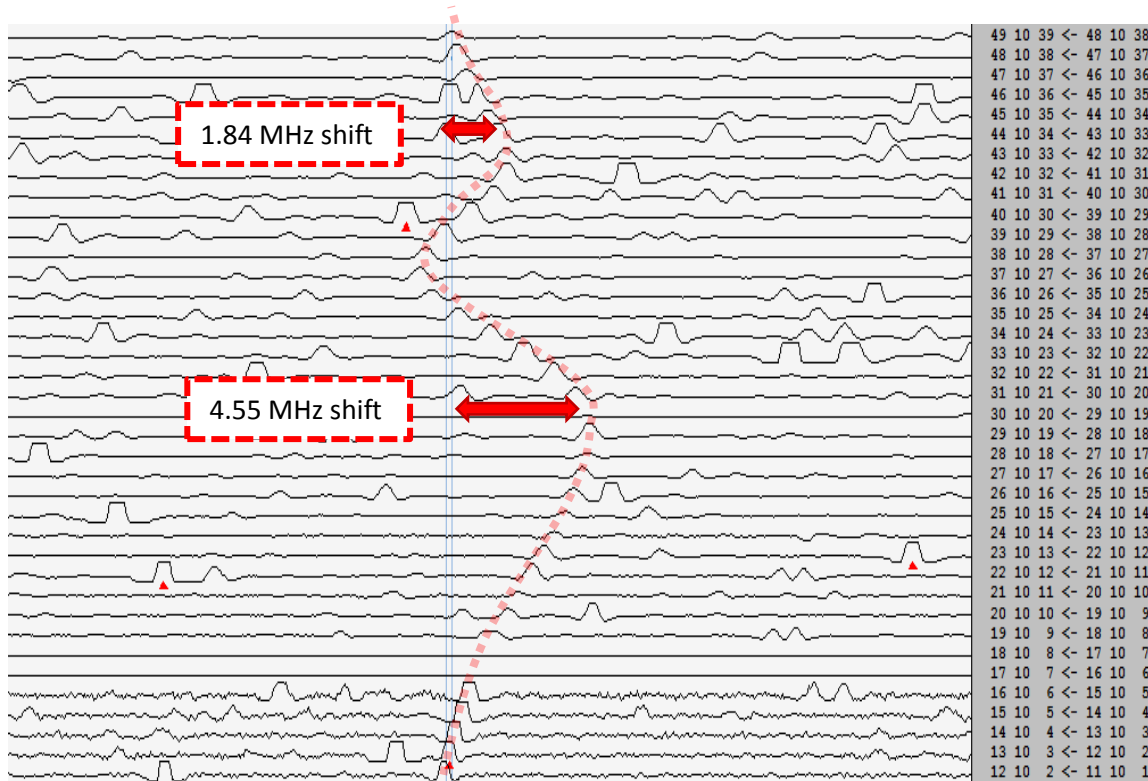


Image 23: LW plot for  $K_a=10$  in the *trans* rotamer. The blue line indicates the prediction and the red one, the real pattern.



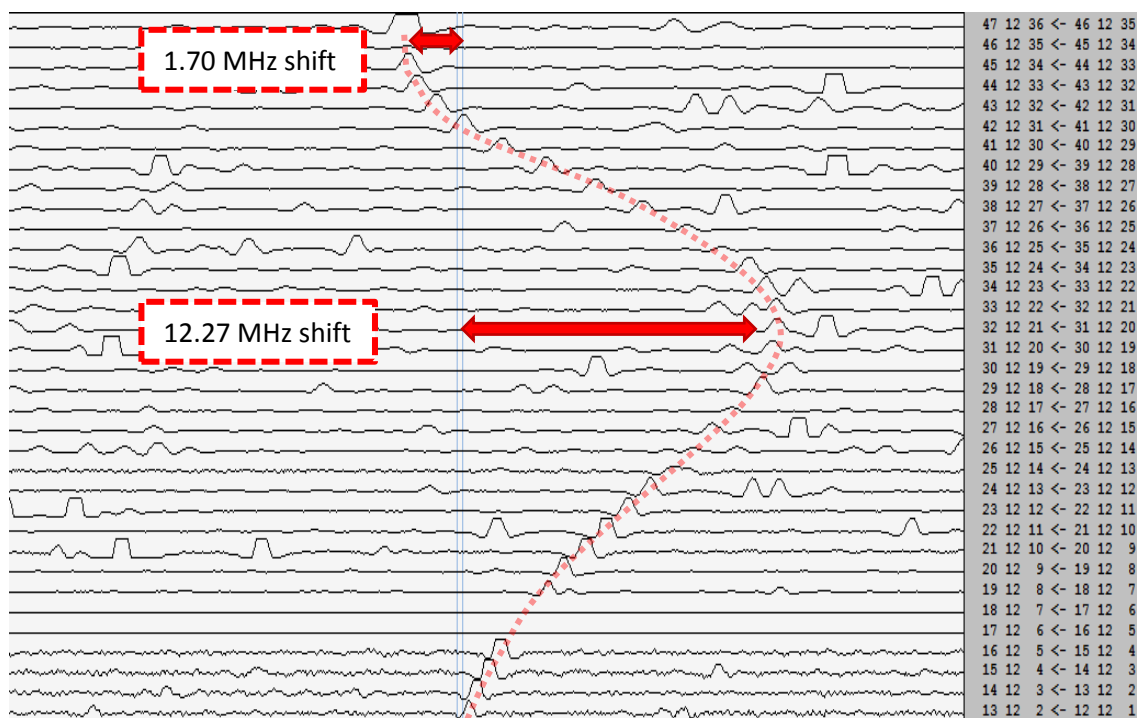


Image 24: LW plot for  $K_a=12$  in the trans rotamer. The blue line indicates the prediction and the red one, the real pattern.

At lower  $K_a$  numbers, only a few transitions are displaced or disappear, whereas at high  $K_a$  values, shifts are huge and no line can be assigned. It is possible that the excited first normal mode of vibration and the second mode in the fundamental state are interacting, thus producing this shift. At this point, various options arise:

- Continue with the analysis including as many distortion terms as we need.
- Make a complete study of the vibrational states and how they affect rotation.
- Stop at  $K_a=5$  the assignment.

The first option is clearly discarded since as we mentioned earlier, including further distortion terms make uncertainties rise enormously. Moreover, the reason of the energetic displacement is clearly not centrifugal distortion and the Hamiltonian operator would lack of physical meaning, though it could probably reproduce the spectrum.

The intensity of the lines produced by the trans conformer is quite low in comparison to those of the gauche rotamer. As we know from Maxwell-Boltzmann's population equation, the number of particles in a higher energy state (trans specie) compared to a more stable state (gauche) becomes lower as temperature decreases.

Taking into account that this experiment was performed at room temperature and that the intensity of some lines could not be distinguished from the noise in the spectrum. It seems quite clear that at much lower temperatures in the ISM, only a few lines will be visible.

There are little benefits in continuing with the analysis, and as Prof. Lucie Kolesniková suggested, the assignment ends at  $K_a=5$  and the terms included in the Hamiltonian will be only those who provide accurate results while maintaining their physical meaning.

Further investigation on the vibrationally excited states is being made with a computational calculus of the anharmonic vibration frequencies using the B2PLYPD3/aug-cc-pVTZ level.

The yielded global fit parameters are:

Constant	Unit	Value <sup>a</sup>
A	MHz	7707.8917 ( 42)
B	MHz	3736.6548 ( 11)
C	MHz	2815.08435 ( 13)
$\Delta_J$	kHz	0.8134 ( 14)
$\Delta_{JK}$	kHz	54.5344 ( 74)
$\Delta_K$	kHz	-46.44 ( 12)
$\delta_J$	kHz	0.24233 ( 72)
$\delta_K$	kHz	26.9932 ( 84)
$\Phi_{JK}$	Hz	0.01118 (100)
$\Phi_K$	Hz	43.450 (483)
$\Phi_{KJ}$	Hz	-4.102 ( 36)
$\sigma_{\text{fit}}^b$	kHz	19
$\kappa$		-0.623
$J''_{\text{max}}$		57
$K''_{\text{max}}$		10 (two c.R type); 5 (a.R type)

a) The number in parenthesis are  $1\sigma$  uncertainties in units of the last decimal digit.

b) Root mean square deviation of the fit.

*Table 10: ground state spectroscopic constants of trans iso-butyraldehyde (Watson's A-Reduction)*

The vibrational partition function in this case is calculated using the B2PLYPD3/aug-cc-pVTZ level with the harmonic approximation.

T /K	$Q_{\text{rot}}$	$Q_{\text{vib}}$	$Q_{\text{tot}}$
9.38	540.1055	1.0000	540.1216
18.75	1524.3672	1.0055	1532.7415
37.50	4308.2241	1.0803	4654.1502
75.00	12186.6007	1.4193	17296.3681
150.00	34487.1656	3.0340	104634.2330
225.00	63361.6091	7.3443	465345.1723
300.00	97507.9158	18.0473	1759757.9252

Mode	Calculated ( $\text{cm}^{-1}$ )	Mode	Calculated ( $\text{cm}^{-1}$ )
$\nu_1$	67.88	$\nu_7$	549.25
$\nu_2$	207.68	$\nu_8$	861.95
$\nu_3$	242.41	$\nu_9$	939.11
$\nu_4$	333.00	$\nu_{10}$	950.31
$\nu_5$	333.10	$\nu_{11}$	961.73
$\nu_6$	353.90		

*Table 11 : partition function of the trans conformer at various temperatures*

*Table 12: normal vibrational modes for the trans conformer.*

### **+ GAUCHE-TRANS ENERGETIC DIFFERENCE**

Through the analysis of line intensity, the link between the relative population of a given rotamer with the square dipolar moment seems quite evident. Let us use equation 17 employing five different transitions observable for both conformers that accomplish the following conditions:

- Transitions in the same frequency range: the intensity of the signal depends of the detector used, and thus only transitions measured with the same equipment can be compared.
- Non degenerate transitions: lines must correspond to only one transition; otherwise, the intensity profile could be heavily modified.

Using Stiefvater et al. (1986)<sup>32</sup> experimental dipolar moments, we calculate the energy difference between both species:

J	K <sub>a</sub>	K <sub>c</sub>	J''	K'' <sub>a</sub>	K'' <sub>c</sub>	Gauche Int.	Trans Int.	Int. Trans/ Int. Gauche
25	5	21	24	5	20	43834382.2	11494136.8	0.26221738
13	3	11	12	3	10	73240016	22655306.7	0.309329626
12	3	10	11	3	9	65056811	17993505.4	0.276581423
16	3	14	15	3	13	113610000	31599251.3	0.278137939
15	3	13	14	3	12	100000001	30381174.2	0.303811738

*Table 13: relative intensities of representative transitions. The stability of both species can be clearly seen by the relative intensity.*

The new energy difference between both gauche and trans conformers is 321.49 cm<sup>-1</sup> in comparison to the previous theoretical 360.25 cm<sup>-1</sup>. Our proposals to explain these differences are:

- The article does not explain whether the Zero Point Vibrational Energy has been taken into account or not. Moreover, only harmonic models are able to do so, which are not the best approach to the real molecular behaviour.
- Collisional cooling in low torsional barriers can produce shifts in the relative population.

Using Maxwell-Boltzmann's population equation, we can predict the number of particles in both states at different temperatures:

T (K)	Rel. Trans Pop. (%)
5	0.0000%
10	0.0000%
25	0.0000%
50	0.0096%
100	0.9801%
150	4.5798%
200	9.9000%
298.15	21.1967%

*Table 14: expected trans population at different temperatures. Most molecules are expected to be in the gauche conformation in the ISM.*

The low number of particles in the trans rotameric form ensures that only the gauche conformer will be relevant in ISM detection.

## CONCLUSIONS

The rotational spectrum of iso-butyraldehyde has been recorded from 75 to 325 GHz (excepting 110-120 GHz). 1921 lines corresponding to 3888 transitions were measured for the most stable conformation, as for the second rotamer, only 243 lines corresponding to 394 transitions could be observed.

As there is an experimental  $321.49 \text{ cm}^{-1}$  energy barrier between both conformers, efforts were focused on the gauche rotamer since it will be most important for ISM detection. Very precise measurements allowed us to yield up to the sextics distortion terms of the Hamiltonian in this rotamer, and up to the quartics and  $\Phi_{JK}$ ,  $\Phi_K$  and  $\Phi_{KJ}$  sextic terms in the trans conformation.

A wide variety of transitions (a,b and c-type in both Q and R branches) corresponding to the gauche conformation have been measured. The rotational parameters provided by Stiefvater et al.<sup>32</sup> have been further improved, allowing the recreation of the experimental spectrum for ISM search.

Since distortion terms were not precisely determined in the trans rotamer, using Loomis-Wood plots, a clear pattern of deviation was observed. Vibrational distortions are proposed as the possible cause of this shift. Further investigation through the anharmonic frequencies vibration calculus is being made.

The high precision data obtained in the current work will allow detection in the future. Additional work for characterization of the rotational spectrum involving excited vibrational states can be carried out in case of detection for line subtraction.

## BIBLIOGRAPHY

- [1] Shapiro, A. E. (2001). **A History of Colour: The Evolution of Theories of Lights and Colour**. Robert A. Crone. *Isis*, 92(1), 145. <https://doi.org/10.1086/385064>
- [2] Tennyson, J. (2019). **Astronomical Spectroscopy: An Introduction To The Atomic And Molecular Physics Of Astronomical Spectroscopy** (Advanced Textbooks in Physics) (3rd ed.). WSPC (EUROPE).
- [3] Hunt, Robert. (2011). **History of Spectroscopy - an essay**. 10.13140/RG.2.2.21410.84169.
- [4] Tatarewicz, J. N. (1987). **The Analysis of Starlight: One Hundred and Fifty Years of Astronomical Spectroscopy**. J. B. Hearnshaw. *Isis*, 78(4), 603–604. <https://doi.org/10.1086/354568>
- [5] Maxwell, J. C. (2013). **A Dynamical Theory of the Electromagnetic Field**. Rough Draft Printing.
- [6] Hollas, M. J. (2004). **Modern Spectroscopy** (4th ed.). Wiley.
- [7] Herschel, W., & Dreyer, J. L. E. (2013). **The Scientific Papers of Sir William Herschel 2 Volume Set: Including Early Papers Hitherto Unpublished** (Cambridge Library Collection - Astronomy) (1st ed.). Cambridge University Press.
- [8] Huggins, W. (1899). **An atlas of representative stellar spectra from 4870 to 3300: Together with a discussion of the evolutionary order of the stars, and the interpretation of their spectra**. W. Wesley and son [etc.].
- [9] Wilson, T. L. (2008). **Tools of Radio Astronomy** (Astronomy and Astrophysics Library) (5th ed.). Springer.
- [10] Swings, P., & Rosenfeld, L. (1937). **Considerations Regarding Interstellar Molecules**. *The Astrophysical Journal*, 86, 483. <https://doi.org/10.1086/143880>
- [11] McKellar, A. (1940). **The Excitation of Molecular Bands in Cometary Spectra**. *Publications of the Astronomical Society of the Pacific*, 52, 283. <https://doi.org/10.1086/125191>
- [12] Adams, W. S. (1941). **Some Results with the COUDÉ Spectrograph of the Mount Wilson Observatory**. *The Astrophysical Journal*, 93, 11. <https://doi.org/10.1086/144237>
- [13] Jenkins, F. A., & Wooldridge, D. E. (1938). **Mass Ratio of the Carbon Isotopes from the Spectrum of CN**. *Physical Review*, 53(2), 137–140. <https://doi.org/10.1103/physrev.53.137>
- [14] Cleeton, C. E., & Williams, N. H. (1934). **Electromagnetic Waves of 1.1 cm Wave-Length and the Absorption Spectrum of Ammonia**. *Physical Review*, 45(4), 234–237. <https://doi.org/10.1103/physrev.45.234>
- [15] Cheung, A. C., Rank, D. M., Townes, C. H., Thornton, D. D., & Welch, W. J. (1968). **Detection of NH<sub>3</sub> Molecules in the Interstellar Medium by Their Microwave Emission**. *Physical Review Letters*, 21(25), 1701–1705. <https://doi.org/10.1103/physrevlett.21.1701>

- [16] McGuire, B. A. (2018). **2018 Census of Interstellar, Circumstellar, Extragalactic, Protoplanetary Disk, and Exoplanetary Molecules**. The Astrophysical Journal Supplement Series, 239(2), 17. <https://doi.org/10.3847/1538-4365/aae5d2>
- [17] Kolesníková, L., Alonso, E. R., Mata, S., & Alonso, J. L. (2017). **Rotational Spectra in 29 Vibrationally Excited States of Interstellar Aminoacetonitrile**. The Astrophysical Journal Supplement Series, 229(2), 26. <https://doi.org/10.3847/1538-4365/aa5d13>
- [18] Smith, I. W. M., Cockell, C. S., & Leach, S. (2012). **Astrochemistry and Astrobiology** (Physical Chemistry in Action) (2013th ed.). Springer.
- [19] Cernicharo, J., Kisiel, Z., Tercero, B., Kolesníková, L., Medvedev, I. R., López, A., Fortman, S., Winnewisser, M., de Lucia, F. C., Alonso, J. L., & Guillemin, J. C. (2016). **A rigorous detection of interstellar CH<sub>3</sub>NCO: An important missing species in astrochemical networks**. Astronomy & Astrophysics, 587, L4. <https://doi.org/10.1051/0004-6361/201527531>
- [20] <https://www.iram-institute.org/>
- [21] <https://www.almaobservatory.org/en/about-alma/origins/>
- [22] Garrod, R. T., Weaver, S. L. W., & Herbst, E. (2008). **Complex Chemistry in Star - forming Regions: An Expanded Gas - Grain Warm - up Chemical Model**. The Astrophysical Journal, 682(1), 283 - 302. <https://doi.org/10.1086/588035>
- [23] Monje, R. R., Emprechtinger, M., Phillips, T. G., Lis, D. C., Goldsmith, P. F., Bergin, E. A., Bell, T. A., Neufeld, D. A., & Sonnentrucker, P. (2011). **HERSCHEL /HIFI observations of hydrogen fluoride toward Sagittarius B2 (M)**. The Astrophysical Journal, 734(1), L23. <https://doi.org/10.1088/2041-8205/734/1/L23>
- [24] Abplanalp, M. J., Góbi, S., Bergantini, A., Turner, A. M., & Kaiser, R. I. (2018). **On the Synthesis of Chocolate Flavonoids (Propanols, Butanals) in the Interstellar Medium**. ChemPhysChem, 19(5), 556–560. <https://doi.org/10.1002/cphc.201701350>
- [25] Alonso, E., Kolesníková, L., Peña, I., Shipman, S., Tercero, B., Cernicharo, J., & Alonso, J. (2015). **Waveguide CP-FTMW and millimetre wave spectra of s-cis- and s-trans-acrylic acid**. Journal of Molecular Spectroscopy, 316, 84–89. <https://doi.org/10.1016/j.jms.2015.08.002>
- [26] Daly, A. M., Bermúdez, C., López, A., Tercero, B., Pearson, J. C., Marcelino, N., Alonso, J. L., & Cernicharo, J. (2013). **Laboratory characterization and astrophysical detection of vibrationally excited states of ethyl cyanide**. The Astrophysical Journal, 768(1), 81. <https://doi.org/10.1088/0004-637x/768/1/81>
- [27] Daly, A. M., Bermúdez, C., Kolesníková, L., & Alonso, J. L. (2015). **Comprehensive analysis of prebiotic propenal up to 660 GHz**. The Astrophysical Journal Supplement Series, 218(2), 30. <https://doi.org/10.1088/0067-0049/218/2/30>
- [28] Jabri, A., Kolesníková, L., Alonso, E., León, I., Mata, S., & Alonso, J. (2020). **A laboratory rotational study of the interstellar propynal**. Journal of Molecular Spectroscopy, 372, 111333. <https://doi.org/10.1016/j.jms.2020.111333>
- [29] Cernicharo, J., Kisiel, Z., Tercero, B., Kolesníková, L., Medvedev, I. R., López, A., Fortman, S., Winnewisser, M., de Lucia, F. C., Alonso, J. L., & Guillemin, J. C. (2016). **A rigorous detection of interstellar CH<sub>3</sub>NCO: An important missing species in astrochemical networks**. Astronomy & Astrophysics, 587, L4. <https://doi.org/10.1051/0004-6361/201527531>



- [30] Belloche, A., Garrod, R. T., Muller, H. S. P., & Menten, K. M. (2014). **Detection of a branched alkyl molecule in the interstellar medium: iso-propyl cyanide.** *Science*, 345(6204), 1584–1587. <https://doi.org/10.1126/science.1256678>
- [31] Kolesníková, L., Alonso, E. R., Mata, S., Cernicharo, J., & Alonso, J. L. (2017). **A Comprehensive Rotational Study of Interstellar Iso-propyl Cyanide up to 480 GHz.** *The Astrophysical Journal Supplement Series*, 233(2), 24. <https://doi.org/10.3847/1538-4365/aa9614>
- [32] Stiefvater, O. L. (1986). **Preferred Rotameric Conformations of Isobutyraldehyde, Their Dipole Moments and Vibrationally Excited States by Microwave Spectroscopy.** *Zeitschrift Für Naturforschung A*, 41(3), 483–490. <https://doi.org/10.1515/zna-1986-0305>
- [33] Hollas, M. J. (2004). **Modern Spectroscopy** (4th ed.). Wiley.
- [34] Gordy, W., & Cook, R. L. (1984). **Techniques of Chemistry, Microwave Molecular Spectra** (Volume 18). Wiley-Interscience.
- [35] Townes, C. H., & Schawlow, A. L. (2013). **Microwave Spectroscopy** (Dover Books on Physics) (2nd ed.). Dover Publications.
- [36] Kroto, H. W. (2003). **Molecular Rotation Spectra** (Dover Phoenix Editions). Dover Publications.
- [37] Cooke, S. A., & Ohring, P. (2013). **Decoding Pure Rotational Molecular Spectra for Asymmetric Molecules.** *Journal of Spectroscopy*, 2013, 1–10. <https://doi.org/10.1155/2013/698392>
- [38] Pickett, H. M. (1991). **The fitting and prediction of vibration-rotation spectra with spin interactions.** *Journal of Molecular Spectroscopy*, 148(2), 371–377. [https://doi.org/10.1016/0022-2852\(91\)90393-o](https://doi.org/10.1016/0022-2852(91)90393-o)
- [39] Alonso, J., Lesarri, A., Leal, L., & Lopez, J. (1993). **The Millimeter-Wave Spectra of 1-Chloro-1-fluoroethylene and cis-1-Chloro-2-fluoroethylene.** *Journal of Molecular Spectroscopy*, 162(1), 4–19. <https://doi.org/10.1006/jmsp.1993.1265>
- [40] Durig, J., Guirgis, G., Brewer, W., & Little, T. (1991). **Vibrational spectra and structure, ab initio calculations, and conformational stability of 2-methylpropanal.** *Journal of Molecular Structure*, 248(1–2), 49–77. [https://doi.org/10.1016/0022-2860\(91\)85003-l](https://doi.org/10.1016/0022-2860(91)85003-l)

## IMAGES, TABLES AND EQUATIONS

### + LIST OF IMAGES:

<b>Image 1. Fraunhofer's Betelgeuse spectrum.</b> Note the black lines in the upper part signalling absorption zones <sup>3</sup> .....	3
<b>Image 2: laboratory and various astronomical interferometers coverage.</b> .....	4
<b>Image 3: excited vibrational states of aminoacetonitrile.</b> Up to 29 excited states and many 13-C satellites were detected in the millimetre region <sup>17</sup> . .....	4
<b>Image 4: atmospheric absorption graphic.</b> The operation of astronomical interferometers is submitted to the radiation absorption. ....	5
<b>Image 5: Orion KL selected spectra.</b> Note the presence of three unidentified lines, six different molecules, deuterium and 13-C isotopologues and two excited vibrational states.....	5
<b>Image 6: ISM detection complete work scheme.</b> Previous work by Stiefvater et al. is marked in green, the current work objectives in blue and future collaboration in red. ....	7
<b>Image 7: symmetric and asymmetric top energies correlation diagram<sup>33</sup>.</b> The straight-line representation is only approximate. The asymmetry splitting of the K levels decrease as K increases, and for a given K, it increases as J increases. ....	10
<b>Image 8: double pass spectrometer scheme.</b> Note that the input and output radiation enter the Pyrex chamber through the same end, and how the polarization grid reflects the output radiation towards the detection array.....	13
<b>Image 9: GEM's millimetre-wave spectrometer double pass configuration.</b> Note on the right side of the picture the single pass apparatus without the polarization grid nor the rooftop mirror. ....	14
<b>Image 10: single pass configuration scheme.</b> In this case, a QOD detector at the back end of the Pyrex glass sample cell is used.....	14
<b>Image 11: gauche and trans conformers.</b> Note the ac symmetry plane in the trans rotameric form.....	16
<b>Image 12: O.L. Stiefvater and B3LYP/6-311G(d,p) predicted energy barriers.</b> Both methods predict a similar energetic difference between the conformers.....	16
<b>Image 13: intensity profile at 100K compared to some astronomical interferometers coverage.</b> The gauche conformer in the upper part, has maximum expected intensity between 230-260 GHz, whereas the trans specie maximum in the lower part, lies between 170-200 GHz <sup>18,19</sup> . ....	17
<b>Image 14: prediction using up to quartic distortion terms by Stiefvater et al.<sup>30</sup> versus real spectra.</b> At higher frequencies when centrifugal distortion is more important, line shift is greater.....	18
<b>Image 15: a 22 GHz section of the room-temperature rotational spectrum of i-butyraldehyde.</b> Groups of transitions involving $J''=25, 26$ and $27$ are displayed, showing a clear B+C distancing between them.....	19
<b>Image 16: J (28←27) section zoom.</b> Higher $K_a''$ are found at lower frequencies until they lose degeneracy, when the branch splits towards higher and lower frequencies (note the presence of $K_a''=7$ between $K_a''=16$ and $K_a''=17$ ) .....	19
<b>Image 17: J (28←27) lines selection degeneracy split.</b> Note the higher shift in frequencies for $K=10$ .....	19
<b>Image 18: b.R transitions blending with a.R type.</b> Lines begin to merge as frequency rises....	20

<b>Image 19: b.R and c.R-type transitions split.</b> Note that b.R not degenerate lines are indistinguishable from the noise.....	20
<b>Image 20: a.Q and b.Q-type transitions degeneracy split.</b> Note that in most cases, when these lines are not degenerate, their intensity is not high enough to be measured. ....	21
<b>Image 21: Loomis-Wood plot for <math>K_a=0</math> in the trans rotamer.</b> Assigned lines match perfectly the prediction.....	23
<b>Image 22: LW plot for <math>K_a=6</math> in the trans rotamer.</b> Red dots indicate lines too deviated.....	24
<b>Image 23: LW plot for <math>K_a=10</math> in the trans rotamer.</b> The blue line indicates the prediction and the red one, the real pattern. ....	24
<b>Image 24: LW plot for <math>K_a=12</math> in the trans rotamer.</b> The blue line indicates the prediction and the red one, the real pattern. ....	25

**+ LIST OF EQUATIONS:**

<b>Equation 1: general form of the rotation Hamiltonian.</b> ....	8
<b>Equation 2: rearranged Hamiltonian.</b> Using Ray's asymmetry parameter.....	8
<b>Equation 3: Ray's asymmetry parameter.</b> It is a relation between the rotational constants in the main three axis.....	8
<b>Equation 4: expanded rotational Hamiltonian.</b> Expressed as a weighted sum of orthogonal functions.....	8
<b>Equation 5: Schrödinger's equation general formula.</b> Note the position of the Hamiltonian inside the integral, in contrast to the eigenvalue E, at the very beginning outside the integral..	9
<b>Equation 6: secular equation.</b> It represents a set of "I" linear equations with "I" unknown coefficients.....	9
<b>Equation 7: setup of the secular determinant.</b> A very similar representation from equation 6.	9
<b>Equation 8: Wang's diagonalizing matrix.</b> It can be further expanded as J values go higher. ....	9
<b>Equation 9: semi-rigid rotor Hamiltonian up to sextics distortion terms.</b> As in equation 7, the first three terms come from the rigid rotor Hamiltonian, whereas the rest account for centrifugal distortion.....	10
<b>Equation 10: transition dipole moment.</b> The gross selection rule for rotational spectroscopy is that molecules must have dipolar moment.....	10
<b>Equation 11: electric moment along axis F.</b> The cosine function defines the angles between the fixed F-axes and the rotating g-axes.....	10
<b>Equation 12: transition integral.</b> The considered g-axis in each case will define different selection rules. ....	11
<b>Equation 13: Z component of the matrix element for a given transition</b> .....	11
<b>Equation 14: dipole matrix elements as function of direction-cosine matrix factors.</b> They are dependant of the quantum numbers marked in the subscript. ....	11
<b>Equation 15: relation between dipole moment and the intensity of a transition.</b> S is a tabulated quantity obtained as a function of initial and final state and of the asymmetry parameter K.....	11
<b>Equation 16: Maxwell-Boltzmann's factor applied to rotation.</b> It is defined as the population ratio of an energy level in comparison to another (or various levels).....	12
<b>Equation 17: maximum absorption coefficient.</b> Note the dependence with T.....	12
<b>Equation 18: vibrational partition function.</b> Where $\nu$ represents the frequencies of the fundamental modes of vibration. ....	12
<b>Equation 19: rotational partition function.</b> Where $\sigma$ is a measure of the degree of symmetry. ....	12

**+ LIST OF TABLES:**

<b>Table 1: Four-Group character table V (a,b,c).</b> Cos (Fa) transforms according to $B_a$ , Cos (Fb) to $B_b$ and Cos (Fc) to $B_c$ .....	11
<b>Table 2: selection rules for the pseudoquantum numbers "K" in terms of evenness and oddness</b> .....	11
<b>Table 3: spectrometer configuration chart.</b> Operation parameters are conditioned by manufacturer specifications. All experiments were conducted under 1.8 V attenuation. ....	13
<b>Table 4: Stiefvater et al. (1986) iso-butyraldehyde rotational parameters.</b> A new fit was made on the trans conformer due to data contradictions. ....	17
<b>Table 5: rotational constant and dipole moment comparison for gauche rotamer.</b> Note that the B2PLYP/aug-cc-pVTZ level seems to be most accurate. ....	18
<b>Table 6: ground state spectroscopic constants of gauche iso-butyraldehyde (Watson's A-Reduction)</b> .....	22
<b>Table 7: partition function of the gauche conformer at various temperatures.</b> The vibrational partition function was calculated using J.R. Durig's gas phase infrared analysis data. ....	22
<b>Table 8: normal vibrational modes for the gauche conformer</b> .....	22
<b>Table 9: rotational constant and dipole moment comparison for trans rotamer.</b> Both MP2 and B2PLYPD3 methods are quite accurate.....	23
<b>Table 10: ground state spectroscopic constants of trans iso-butyraldehyde (Watson's A-Reduction)</b> .....	26
<b>Table 11 : partition function of the trans conformer at various temperatures</b> .....	26
<b>Table 12: normal vibrational modes for the trans conformer</b> .....	26
<b>Table 13: relative intensities of representative transitions.</b> The stability of both species can be clearly seen by the relative intensity. ....	27
<b>Table 14: expected trans population at different temperatures.</b> Most molecules are expected to be in the gauche conformation in the ISM. ....	27



Comprehensive analysis of Isobutyraldehyde: millimetre-wave spectroscopy as an approach to ISM detection

13	11	2	12	11	1	93392.593	0.01097	0.5	37	11	27	37	9	28	100762.373	0.03493	
13	11	3	12	11	2	93392.593	0.01101	0.5	15	2	13	14	2	12	100831.844	-0.02179	
13	10	3	12	10	2	93551.213	0.00172	0.5	14	10	4	13	10	3	100901.163	0.01747	0.5
13	10	4	12	10	3	93551.213	0.00464	0.5	14	10	5	13	10	4	100901.163	0.0339	0.5
13	9	5	12	9	4	93768.222	0.07508	0.5	32	7	25	32	7	26	101399.825	-0.01852	
13	9	4	12	9	3	93768.222	-0.05627	0.5	32	7	25	32	6	26	101406.049	-0.01897	
39	13	27	39	12	28	93854.547	-0.03377		35	15	21	35	14	22	101414.977	-0.0052	
13	8	6	12	8	5	94076.875	0.03144		32	8	25	32	7	26	101481.147	-0.01051	
13	8	5	12	8	4	94080.641	-0.01342		32	8	25	32	6	26	101487.363	-0.01898	
37	12	26	37	10	27	94159.954	-0.03036		14	8	7	13	8	6	101563.403	-0.00101	
10	3	7	9	2	7	94515.793	0.04745		14	8	6	13	8	5	101576.174	-0.01253	
13	7	7	12	7	6	94519.340	0.0082		26	3	23	26	3	24	101661.691	0.06227	0.3368
13	7	6	12	7	5	94589.748	0.01864		26	3	23	26	2	24	101661.691	0.05864	0.1632
14	2	12	13	3	11	94612.581	0.01666		26	4	23	26	3	24	101661.691	-0.06314	0.1632
34	10	25	34	8	26	94683.723	-0.01799		26	4	23	26	2	24	101661.691	-0.06677	0.3368
13	5	9	12	5	8	94731.775	-0.00892		14	5	10	13	5	9	101737.200	0.00446	
14	3	12	13	3	11	94768.365	0.02877		39	12	28	39	10	29	102030.668	0.02526	
29	6	23	29	6	24	94804.500	-0.02292		14	7	8	13	7	7	102093.718	-0.02065	
29	7	23	29	5	24	94872.360	-0.00336		16	1	15	15	1	14	102144.393	0.0367	
14	2	12	13	2	11	94950.096	-0.00224		14	7	7	13	7	6	102280.696	-0.00156	
13	6	8	12	6	7	94990.888	-0.0021		14	4	11	13	3	10	102484.607	-0.04255	
13	3	10	12	3	9	95008.772	0.01047		14	6	9	13	6	8	102493.466	0.0087	
14	3	12	13	2	11	95105.849	-0.02212		34	8	26	34	8	27	102881.248	0.01728	
32	14	19	32	13	20	95316.024	0.00021		34	8	26	34	7	27	102899.402	-0.01128	
10	4	6	9	3	6	95569.694	0.00502		34	9	26	34	8	27	103086.605	0.02729	
36	11	26	36	10	27	95579.006	0.04574		34	9	26	34	7	27	103104.720	-0.04036	
22	1	21	22	1	22	95713.017	0.02654	0.3449	11	4	7	10	3	7	103312.449	-0.02325	
22	1	21	22	0	22	95713.017	0.02651	0.1551	25	2	23	25	2	24	103316.663	0.0158	0.3414
22	2	21	22	0	22	95713.017	0.02322	0.3449	25	2	23	25	1	24	103316.663	0.01563	0.1586
22	2	21	22	1	22	95713.017	0.02326	0.1551	25	3	23	25	1	24	103316.663	0.00629	0.3414
13	6	7	12	6	6	95758.301	0.01136		25	3	23	25	2	24	103316.663	0.00646	0.1586
20	13	8	20	12	8	96028.224	0.06801	0.2081	17	0	17	16	1	16	103573.500	0.01604	0.047
20	13	7	20	12	8	96028.224	0.06388	0.2919	17	1	17	16	1	16	103573.500	0.01085	0.453
20	13	8	20	12	9	96028.224	-0.05328	0.2919	17	0	17	16	0	16	103573.500	0.00185	0.453
20	13	7	20	12	9	96028.224	-0.05741	0.2081	17	1	17	16	0	16	103573.500	-0.00334	0.047
41	14	28	41	13	29	96042.119	-0.03168		21	14	7	21	13	8	103930.550	0.00984	0.2905
36	11	26	36	9	27	96062.428	0.01928		21	14	8	21	13	8	103930.550	0.01037	0.2905
15	1	14	14	2	13	96185.031	0.03406		21	14	8	21	13	9	103930.550	-0.00674	0.2905
15	2	14	14	2	13	96187.562	0.03254		21	14	7	21	13	9	103930.550	-0.00726	0.2905
15	1	14	14	1	13	96191.283	0.01226		36	9	27	36	9	28	103952.009	0.00202	
15	2	14	14	1	13	96193.818	0.01536		36	9	27	36	8	28	104000.954	-0.01228	
19	13	7	19	12	8	96379.006	-0.00465		14	6	8	13	6	7	104049.795	0.01771	
31	7	24	31	7	25	96481.337	-0.03353		20	14	6	20	13	7	104250.260	0.00628	0.2882
31	7	24	31	6	25	96495.112	0.04464		20	14	7	20	13	8	104250.260	0.00226	0.2882
31	8	24	31	7	25	96648.997	-0.00719		20	14	6	20	13	8	104250.260	0.00215	0.2118
31	8	24	31	6	25	96662.751	0.05057		20	14	7	20	13	7	104250.260	0.00639	0.2118
18	13	6	18	12	7	96676.811	0.00891		31	6	25	31	6	26	104328.097	-0.03508	
17	13	5	17	12	6	96928.064	0.02856		31	7	25	31	5	26	104342.671	0.00243	
16	13	4	16	12	5	97138.394	-0.00211		36	10	27	36	9	28	104435.486	0.02995	
15	13	3	15	12	4	97312.952	-0.02304		36	10	28	36	10	29	104478.624	0.04411	
14	13	2	14	12	3	97456.310	-0.04672		36	10	27	36	8	28	104484.395	-0.01941	
28	5	23	28	5	24	97488.793	0.01531		24	1	23	24	1	24	104747.969	-0.00868	0.3448
28	6	23	28	4	24	97499.207	0.02803		24	2	23	24	0	24	104747.969	-0.00915	0.3448
16	0	16	15	1	15	97616.797	0.01149	0.0467	24	2	23	24	1	24	104747.969	-0.00914	0.1552
16	1	16	15	1	15	97616.797	-0.0027	0.4533	24	1	23	24	0	24	104747.969	-0.00868	0.1552
16	0	16	15	0	15	97616.797	-0.02703	0.4533	18	14	4	18	13	5	104757.699	-0.00292	0.2845
16	1	16	15	0	15	97616.797	-0.04122	0.0467	18	14	5	18	13	5	104757.699	-0.00292	0.2155
38	12	27	38	10	28	97732.988	-0.01008		18	14	4	18	13	6	104757.699	-0.00309	0.2155
33	8	25	33	8	26	97759.317	-0.00685		18	14	5	18	13	6	104757.699	-0.00309	0.2845
40	13	28	40	12	29	97879.729	0.01019		17	14	3	17	13	4	104955.211	-0.0097	0.2827
33	9	25	33	7	26	98206.859	-0.01354		17	14	4	17	13	4	104955.211	-0.0097	0.2173
13	5	8	12	5	7	98502.918	0.02162		17	14	3	17	13	5	104955.211	-0.00973	0.2173
35	9	26	35	9	27	98513.960	0.00915		17	14	4	17	13	5	104955.211	-0.00973	0.2827
37	10	27	37	10	28	98538.812	0.05854		15	4	12	14	4	11	105148.629	0.00507	
37	15	23	37	14	24	98573.766	-0.01676		11	3	8	10	2	8	105463.372	0.01067	
37	10	27	37	9	28	98784.866	0.00333		38	11	28	38	10	29	105546.921	0.01296	
24	2	22	24	2	23	98785.981	0.02589	0.3403	38	11	28	38	9	29	105669.819	0.02631	
24	2	22	24	1	23	98785.981	0.02543	0.1597	15	3	12	14	3	11	106084.159	0.00544	
24	3	22	24	1	23	98785.981	0.00156	0.3403	14	4	10	13	4	9	106181.146	0.01311	
24	3	22	24	2	23	98785.981	0.00202	0.1597	27	3	24	27	3	25	106214.777	0.03845	0.3373
14	4	11	13	4	10	98957.809	0.00289		27	3	24	27	2	25	106214.777	0.03705	0.1627
13	4	9	12	4	8	99378.058	0.01452		27	4	24	27	3	25	106214.777	-0.01246	0.1627
35	10	26	35	9	27	99442.768	0.00428		27	4	24	27	2	25	106214.777	-0.01386	0.3373
32	17	15	31	18	14	99454.049	-0.00536		33	7	26	33	7	27	106247.685	-0.0306	
42	14	29	42	13	30	99470.060	-0.01111		33	7	26	33	6	27	106250.486	-0.02091	
35	10	26	35	8	27	99543.906	-0.00148		33	8	26	33	7	27	106286.501	0.03139	
30	6	24	30	6	25	99586.849	0.01625		33	8	26	33	6	27	106289.273	0.01104	
30	6	24	30	5	25	99588.808	0.04245		16	2	14	15	3	13	106675.840	0.00547	
30	7	24	30	6	25	99616.553	0.00873		16	3	14	15	3	13	106706.383	0.0088	
30	7	24	30	5	25	99618.440	-0.03746		16	2	14	15	2	13	106745.659	0.01711	
9	5	5	8	4	5	99875.455	-0.02616		40	12	29	40	10	30	106756.477	0.03924	
23	1	22	23	1	23	100230.753	0.01048	0.3444	16								









Comprehensive analysis of Isobutyraldehyde: millimetre-wave spectroscopy as an approach to ISM detection

38	6	32	38	6	33	136926.208	-0.00918	0.3301	22	2	20	21	2	19	142405.348	-0.11098	0.4597
38	6	32	38	5	33	136926.208	-0.01109	0.1699	22	3	20	21	2	19	142405.348	-0.26346	0.0403
38	7	32	38	5	33	136926.208	-0.05441	0.3301	17	6	12	16	5	11	142511.540	-0.01234	
38	7	32	38	6	33	136926.208	-0.0525	0.1699	35	3	32	35	3	33	142525.942	-0.02111	0.3403
36	14	23	36	12	24	137043.726	0.04633	0.0224	35	4	32	35	2	33	142525.942	-0.02114	0.3403
19	13	6	18	13	5	137043.726	-0.00094	0.4888	35	4	32	35	3	33	142525.942	-0.02114	0.1597
19	13	7	18	13	6	137043.726	-0.00021	0.4888	35	3	32	35	2	33	142525.942	-0.02111	0.1597
19	12	8	18	12	7	137341.576	0.05838	0.5	28	19	9	28	18	10	142616.752	-0.01346	0.2888
19	12	7	18	12	6	137341.576	0.03438	0.5	28	19	9	28	18	11	142616.752	-0.01347	0.2112
19	6	14	18	6	13	137612.239	-0.02279		28	19	10	28	18	10	142616.752	-0.01346	0.2112
22	1	21	21	2	20	137866.599	0.03468	0.0439	28	19	10	28	18	11	142616.752	-0.01347	0.2888
22	2	21	21	2	20	137866.599	0.0314	0.0439	26	19	7	26	18	8	143168.745	0.02108	0.2144
22	1	21	21	1	20	137866.599	0.02598	0.4561	26	19	7	26	18	9	143168.745	0.02108	0.1604
22	2	21	21	1	20	137866.599	0.0227	0.0439	26	19	8	26	18	8	143168.745	0.02108	0.1604
10	9	2	9	8	1	138123.034	0.02967	0.5317	26	19	8	26	18	9	143168.745	0.02108	0.2144
10	9	2	9	8	1	138123.034	0.03011	0.4683	13	7	7	12	6	6	143168.745	-0.20404	0.2504
44	7	38	43	8	36	138134.578	-0.02889	0.5	13	7	6	12	6	6	143271.658	-0.01266	
44	6	38	43	7	36	138134.578	-0.04064	0.5	14	2	12	13	1	12	143388.841	-0.02442	
19	10	10	18	10	9	138259.361	0.03587		20	19	1	19	19	0	143396.708	0.03738	0.5
19	10	9	18	10	8	138270.015	0.03907		20	19	2	19	19	1	143396.708	0.03738	0.5
18	6	12	17	6	11	138293.333	-0.0349		25	19	6	25	18	7	143400.289	-0.01712	0.2843
33	7	26	32	8	24	138524.836	-0.05793		25	19	6	25	18	8	143400.289	-0.01712	0.2157
19	9	11	18	9	10	138967.526	0.00854		25	19	7	25	18	7	143400.289	-0.01712	0.2157
37	5	32	37	5	33	138997.431	0.00391	0.3338	25	19	7	25	18	8	143400.289	-0.01712	0.2843
37	5	32	37	4	33	138997.431	0.00375	0.1662	20	18	2	19	18	1	143501.275	0.01634	0.5
37	6	32	37	5	33	138997.431	-0.00075	0.1662	20	18	3	19	18	2	143501.275	0.01634	0.5
37	6	32	37	4	33	138997.431	-0.00091	0.3338	38	5	33	38	5	34	143568.659	-0.00277	0.3343
19	9	10	18	9	9	139104.229	0.02988		38	5	33	38	4	34	143568.659	-0.00283	0.1657
40	7	33	40	7	34	139264.330	0.08415	0.3269	38	6	33	38	5	34	143568.659	-0.00468	0.1657
40	7	33	40	6	34	139264.330	0.07644	0.1731	38	6	33	38	4	34	143568.659	-0.00474	0.3343
40	8	33	40	7	34	139264.330	-0.06563	0.1731	24	19	5	24	18	6	143605.568	-0.00409	0.2832
40	8	33	40	6	34	139264.330	-0.07334	0.3269	24	19	5	24	18	7	143605.568	-0.00409	0.2168
23	1	23	22	1	22	139301.161	0.04226	0.4526	24	19	6	24	18	6	143605.568	-0.00409	0.2168
23	0	23	22	0	22	139301.161	0.04223	0.4526	24	19	6	24	18	7	143605.568	-0.00409	0.2832
23	1	23	22	0	22	139301.161	0.04222	0.0474	13	7	7	12	6	7	143687.354	0.04116	
23	0	23	22	1	22	139301.161	0.04227	0.0474	20	16	4	19	16	3	143772.090	0.04096	
20	4	16	19	5	15	139419.188	0.01183		23	19	4	23	18	5	143786.813	0.04424	0.2818
35	19	17	35	18	17	139426.413	0.07067	0.1985	23	19	4	23	18	6	143786.813	0.04424	0.2182
35	19	16	35	18	17	139426.413	0.06677	0.3015	23	19	5	23	18	5	143786.813	0.04424	0.2182
35	19	17	35	18	18	139426.413	-0.00144	0.3015	23	19	5	23	18	6	143786.813	0.04424	0.2818
35	19	16	35	18	18	139426.413	-0.00535	0.1985	23	2	22	22	2	21	143818.880	0.01187	0.4559
33	2	31	33	2	32	139511.665	-0.00508	0.343	23	1	22	22	1	21	143818.880	0.00982	0.4559
33	3	31	33	1	32	139511.665	-0.00509	0.343	23	2	22	22	1	21	143818.880	0.00858	0.0441
33	3	31	33	2	32	139511.665	-0.00509	0.157	23	1	22	22	2	21	143818.880	0.0131	0.0441
33	2	31	33	1	32	139511.665	-0.00508	0.157	41	7	34	41	7	35	143908.739	-0.00183	0.3276
19	7	13	18	7	12	139633.103	0.01593		41	7	34	41	6	35	143908.739	-0.00504	0.1724
19	8	12	18	8	11	139703.736	-0.01495		41	8	34	41	6	35	143908.739	-0.07007	0.3276
20	5	16	19	5	15	139752.747	0.00844		41	8	34	41	7	35	143908.739	-0.06685	0.1724
15	5	10	14	4	10	139786.549	-0.00287		20	15	5	19	15	4	143950.310	-0.00306	0.5
46	25	22	45	26	19	139803.423	-0.00848	0.2696	20	15	6	19	15	5	143950.310	-0.00306	0.5
46	25	22	45	26	20	139803.423	-0.00848	0.2304	20	6	15	19	6	14	143993.506	-0.03728	
46	25	21	45	26	19	139803.423	-0.00849	0.2304	34	2	32	34	2	33	144032.127	-0.0109	0.3432
46	25	21	45	26	20	139803.423	-0.00849	0.2696	34	3	32	34	1	33	144032.127	-0.0109	0.3432
34	19	15	34	18	16	140032.480	0.03772	0.2994	34	3	32	34	2	33	144032.127	-0.0109	0.1568
34	19	16	34	18	16	140032.480	0.03892	0.2006	34	2	32	34	1	33	144032.127	-0.0109	0.1568
34	19	16	34	18	17	140032.480	0.0147	0.2994	20	14	6	19	14	5	144169.329	0.03041	0.5
34	19	15	34	18	17	140032.480	0.0135	0.2006	20	14	7	19	14	6	144169.329	0.0305	0.5
14	3	11	13	2	11	140033.743	0.03692		14	6	9	13	5	9	144222.069	0.01562	
20	4	16	19	4	15	140098.250	0.03215		20	13	7	19	13	6	144443.284	-0.01836	0.5
33	19	14	33	18	15	140580.961	0.02433	0.2974	20	13	8	19	13	7	144443.284	-0.01512	0.5
33	19	15	33	18	16	140580.961	0.01691	0.2974	19	7	12	18	7	11	144462.084	-0.01989	
33	19	14	33	18	16	140580.961	0.01656	0.2026	20	12	9	19	12	8	144794.064	0.03179	0.5
33	19	15	33	18	15	140580.961	0.02468	0.2026	20	12	8	19	12	7	144794.064	-0.05827	0.5
19	8	11	18	8	10	140848.959	0.0308		46	10	36	46	10	37	145204.185	0.09209	0.6339
36	4	32	36	4	33	140854.991	-0.01127	0.3371	46	10	36	46	9	37	145204.185	-0.19541	0.3661
36	5	32	36	4	33	140854.991	-0.01168	0.1629	46	11	36	46	9	37	145208.234	-0.00984	
36	5	32	36	3	33	140854.991	-0.01169	0.3371	24	0	24	23	0	23	145253.298	0.00348	0.4525
36	4	32	36	3	33	140854.991	-0.01128	0.1629	24	0	24	23	1	23	145253.298	0.0035	0.0475
32	1	31	32	1	32	140875.982	-0.03558	0.3462	24	1	24	23	0	23	145253.298	0.00348	0.0475
32	2	31	32	0	32	140875.982	-0.03558	0.3462	24	1	24	23	1	23	145253.298	0.00349	0.4525
32	2	31	32	1	32	140875.982	-0.03558	0.1538	20	11	10	19	11	9	145255.965	0.04941	
32	1	31	32	0	32	140875.982	-0.03558	0.1538	20	11	9	19	11	8	145257.809	0.0104	
20	5	15	19	6	14	140910.890	-0.01664		11	9	3	10	8	2	145279.349	0.01997	0.2292
19	5	14	18	5	13	140978.434	-0.00136		11	9	2	10	8	2	145279.349	0.01563	0.2708
21	3	18	20	4	17	141042.532	-0.02288		11	9	3	10	8	3	145279.349	-0.02076	0.2708
21	4	18	20	4	17	141052.249	-0.03929		11	9	2	10	8	3	145279.349	-0.02511	0.2292
21	3	18	20	3	17	141064.863	-0.01537		15	4	11	14	3	11	145298.747	0.00546	
31	19	12	31	18	13	141524.471	-0.00707	0.294	41	20	22	40	21	19	145316.158	0.04277	0.53



Comprehensive analysis of Isobutyraldehyde: millimetre-wave spectroscopy as an approach to ISM detection

40	21	20	40	20	21	153656.126	0.00999	0.3036	30	21	9	30	20	10	158280.238	-0.01397	0.2874
40	21	19	40	20	21	153656.126	0.00699	0.1964	30	21	9	30	20	11	158280.238	-0.01397	0.2126
24	2	22	23	3	21	154303.485	0.06543	0.0413	30	21	10	30	20	10	158280.238	-0.01397	0.2126
24	3	22	23	3	21	154303.485	0.04156	0.4587	30	21	10	30	20	11	158280.238	-0.01397	0.2874
24	2	22	23	2	21	154303.485	0.00485	0.4587	17	6	11	16	5	11	158344.451	-0.01558	
24	3	22	23	2	21	154303.485	-0.01902	0.0413	21	8	13	20	8	12	158395.908	-0.03108	
39	21	19	39	20	19	154330.111	0.00878	0.1983	22	16	6	21	16	5	158431.607	0.02588	0.5
39	21	18	39	20	19	154330.111	0.00781	0.3017	22	16	7	21	16	6	158431.607	0.02588	0.5
39	21	19	39	20	20	154330.111	-0.00911	0.3017	21	6	15	20	6	14	158565.187	0.01301	
39	21	18	39	20	20	154330.111	-0.01009	0.1983	22	15	8	21	15	7	158670.655	0.03312	0.5
21	9	13	20	9	12	154419.276	-0.03858		22	15	7	21	15	6	158670.655	0.03307	0.5
39	4	35	39	3	36	154485.987	0.00614	0.1619	24	4	21	23	4	20	158873.805	0.0357	
39	4	35	39	4	36	154485.987	0.00614	0.3381	24	3	21	23	3	20	158874.796	-0.00213	
39	5	35	39	3	36	154485.987	0.00612	0.3381	22	14	9	21	14	8	158965.477	-0.00734	0.5
39	5	35	39	4	36	154485.987	0.00612	0.1619	22	14	8	21	14	7	158965.477	-0.00912	0.5
21	8	14	20	8	13	154827.208	0.01248		27	21	6	27	20	7	158991.466	-0.03352	0.2838
38	21	18	38	20	18	154946.703	0.02014	0.2001	27	21	6	27	20	8	158991.466	-0.03352	0.2162
38	21	17	38	20	18	154946.703	0.01984	0.2999	27	21	7	27	20	7	158991.466	-0.03352	0.2162
38	21	18	38	20	19	154946.703	0.01411	0.2999	27	21	7	27	20	8	158991.466	-0.03352	0.2838
38	21	17	38	20	19	154946.703	0.0138	0.2001	26	21	5	26	20	6	159181.419	-0.04108	0.2827
21	9	12	20	9	11	155093.235	0.01823		26	21	5	26	20	7	159181.419	-0.04108	0.2173
15	7	9	14	6	8	155157.180	-0.01805		26	21	6	26	20	6	159181.419	-0.04108	0.2173
42	6	36	42	5	37	155309.913	-0.03466	0.1675	26	21	6	26	20	7	159181.419	-0.04108	0.2827
42	6	36	42	6	37	155309.913	-0.03461	0.3325	22	13	10	21	13	9	159336.642	0.00478	0.5
42	7	36	42	6	37	155309.913	-0.03594	0.1675	22	13	9	21	13	8	159336.642	-0.04263	0.5
42	7	36	42	5	37	155309.913	-0.036	0.3325	44	22	22	44	21	23	159560.054	0.09204	0.5
45	8	37	45	8	38	155453.936	0.02781	0.2645	44	22	23	44	21	24	159560.054	-0.08155	0.5
45	8	37	45	7	38	155453.936	0.02567	0.1409	22	12	10	21	12	9	159816.783	-0.03492	
45	9	37	45	8	38	155453.936	-0.01294	0.1409	43	6	37	43	5	38	159889.860	-0.00602	0.1671
45	9	37	45	7	38	155453.936	-0.01509	0.2645	43	6	37	43	6	38	159889.860	-0.006	0.3329
55	15	41	55	13	42	155453.936	-0.03222	0.1892	43	7	37	43	6	38	159889.860	-0.00655	0.1671
37	21	17	37	20	17	155510.438	0.03553	0.2019	43	7	37	43	5	38	159889.860	-0.00657	0.3329
37	21	16	37	20	17	155510.438	0.03544	0.2981	46	8	38	46	8	39	160103.047	0.02742	0.6541
37	21	17	37	20	18	155510.438	0.03358	0.2981	46	8	38	46	7	39	160103.047	0.02652	0.3459
37	21	16	37	20	18	155510.438	0.03349	0.2019	22	7	16	21	7	15	160175.526	-0.01845	
25	1	24	24	2	23	155721.534	0.03809	0.0445	25	2	23	24	3	22	160252.158	-0.00626	0.0414
25	2	24	24	2	23	155721.534	0.03792	0.4555	25	3	23	24	3	22	160252.158	-0.0156	0.4586
25	1	24	24	1	23	155721.534	0.03763	0.4555	25	2	23	24	2	22	160252.158	-0.03013	0.4586
25	2	24	24	1	23	155721.534	0.03746	0.0445	25	3	23	24	2	22	160252.158	-0.03947	0.0414
55	23	33	55	22	33	155752.925	-0.01503		12	10	3	11	9	2	160257.394	-0.0222	0.2301
15	7	8	14	6	8	155892.491	0.00506		12	10	2	11	9	2	160257.394	-0.02265	0.2699
36	21	15	36	20	16	156025.432	0.03837	0.2965	12	10	3	11	9	3	160257.394	-0.02654	0.2699
36	21	16	36	20	16	156025.432	0.03884	0.2035	12	10	2	11	9	3	160257.394	-0.02699	0.2301
36	21	15	36	20	17	156025.432	0.03776	0.2035	43	22	22	43	21	22	160360.650	0.03747	0.1945
36	21	16	36	20	17	156025.432	0.03779	0.2965	43	22	21	43	21	22	160360.650	0.03308	0.3055
22	6	17	21	6	16	156288.785	-0.04126		43	22	22	43	21	23	160360.650	-0.03234	0.3055
35	21	14	35	20	15	156495.342	-0.05292	0.2947	43	22	21	43	21	23	160360.650	-0.03673	0.1945
35	21	15	35	20	15	156495.342	-0.05291	0.2053	22	11	12	21	11	11	160451.801	-0.00341	
35	21	14	35	20	16	156495.342	-0.0531	0.2053	22	11	11	21	11	10	160466.972	-0.0079	
35	21	15	35	20	16	156495.342	-0.05309	0.2947	39	3	36	39	2	37	160637.638	-0.00968	0.159
34	21	13	34	20	14	156923.787	-0.02422	0.293	39	3	36	39	3	37	160637.638	-0.00968	0.341
34	21	14	34	20	14	156923.787	-0.02422	0.207	39	4	36	39	2	37	160637.638	-0.00968	0.341
34	21	13	34	20	15	156923.787	-0.02427	0.207	39	4	36	39	3	37	160637.638	-0.00968	0.159
34	21	14	34	20	15	156923.787	-0.02427	0.293	11	11	0	10	10	0	160909.003	-0.04029	0.261
22	5	17	21	5	16	157092.403	0.00048		11	11	1	10	10	0	160909.003	-0.04029	0.239
41	5	36	41	4	37	157255.384	-0.00922	0.1645	11	11	0	10	10	1	160909.003	-0.04029	0.239
41	5	36	41	5	37	157255.384	-0.00921	0.3355	11	11	1	10	10	1	160909.003	-0.04029	0.261
41	6	36	41	4	37	157255.384	-0.00934	0.3355	16	6	11	15	5	11	161013.146	0.02662	
41	6	36	41	5	37	157255.384	-0.00934	0.1645	22	10	13	21	10	12	161286.976	0.02734	
33	21	12	33	20	13	157313.744	-0.00831	0.2916	17	5	12	16	4	12	161419.245	0.00076	
33	21	12	33	20	14	157313.744	-0.00832	0.2084	22	10	12	21	10	11	161460.253	0.02894	
33	21	13	33	20	13	157313.744	-0.00831	0.2084	21	7	14	20	7	13	161505.424	0.01412	
33	21	13	33	20	14	157313.744	-0.00832	0.2916	26	1	25	25	2	24	161671.754	0.03427	0.0448
23	4	19	22	5	18	157554.860	0.01289		26	2	25	25	2	24	161671.754	0.03421	0.4552
47	9	38	47	9	39	157584.843	0.12636	0.3233	26	1	25	25	1	24	161671.754	0.0341	0.4552
47	9	38	47	8	39	157584.843	0.11873	0.1767	26	2	25	25	1	24	161671.754	0.03404	0.0448
47	10	38	47	9	39	157584.843	-0.00225	0.1767	41	22	19	41	21	20	161772.546	0.02358	0.302
47	10	38	47	8	39	157584.843	-0.00988	0.3233	41	22	20	41	21	21	161772.546	0.01519	0.302
23	5	19	22	5	18	157588.732	0.023		41	22	19	41	21	21	161772.546	0.01471	0.198
37	2	35	37	1	36	157590.686	0.01412	0.1566	41	22	20	41	21	20	161772.546	0.02407	0.198
37	2	35	37	2	36	157590.686	0.01412	0.3434	22	9	14	21	9	13	162146.342	0.02524	
37	3	35	37	1	36	157590.686	0.01412	0.3434	22	8	15	21	8	14	162161.100	0.04293	
37	3	35	37	2	36	157590.686	0.01412	0.1566	23	6	18	22	6	17	162290.503	0.01783	
23	4	19	22	4	18	157629.046	0.01484		23	5	18	22	5	17	162723.725	0.04216	
32	21	11	32	20	12	157668.038	-0.04124	0.2902	22	9	13	21	9	12	163477.092	-0.02386	
32	21	11	32	20	13	157668.038	-0.04125	0.2098	24	4	20	23	5	19	163501.323	-0.04343	
32	21	12	32	20	12	157668.038	-0.04124	0.2098	24	5	20	23	5	19	163516.524	-0.02347	
32	21	12	32	20	13	157668.038	-0.04125										

Comprehensive analysis of Isobutyraldehyde: millimetre-wave spectroscopy as an approach to ISM detection

69	43	27	68	44	25	164809.009	-0.65957	0.0027	38	23	16	38	22	17	171880.534	-0.01535	0.2937
35	22	13	35	21	14	164809.009	-0.04187	0.2887	24	23	2	23	23	1	172016.561	-0.01127	0.5
35	22	13	35	21	15	164809.009	-0.04187	0.2055	24	23	1	23	23	0	172016.561	-0.01127	0.5
35	22	14	35	21	14	164809.009	-0.04187	0.2055	24	22	3	23	22	2	172117.829	-0.00933	0.5
35	22	14	35	21	15	164809.009	-0.04187	0.2887	24	22	2	23	22	1	172117.829	-0.00933	0.5
23	22	1	22	22	0	164863.513	0.00648	0.5	27	2	25	26	2	24	172148.263	-0.03252	0.4579
23	22	2	22	22	1	164863.513	0.00648	0.5	27	3	25	26	2	24	172148.263	-0.03392	0.0421
23	21	2	22	21	1	164965.422	0.02133	0.5	27	2	25	26	3	24	172148.263	-0.0289	0.0421
23	21	3	22	21	2	164965.422	0.02133	0.5	27	3	25	26	3	24	172148.263	-0.0303	0.4579
23	20	3	22	20	2	165082.586	-0.00379	0.5	18	7	11	17	6	11	172158.585	0.04373	
23	20	4	22	20	3	165082.586	-0.00379	0.5	23	9	14	22	9	13	172220.805	-0.01548	
80	4	76	79	5	74	165162.904	-0.59083	0.0033	24	21	3	23	21	2	172233.499	0.02242	0.5
80	5	76	79	6	74	165162.904	-0.59083	0.0033	24	21	4	23	21	3	172233.499	0.02242	0.5
40	3	37	40	2	38	165162.904	-0.01539	0.1578	24	20	4	23	20	3	172366.593	0.00961	0.5
40	3	37	40	3	38	165162.904	-0.01539	0.339	24	20	5	23	20	4	172366.593	0.00961	0.5
40	4	37	40	2	38	165162.904	-0.01539	0.339	24	19	6	23	19	5	172521.092	-0.04479	0.5
40	4	37	40	3	38	165162.904	-0.01539	0.1578	24	19	5	23	19	4	172521.092	-0.04479	0.5
34	22	12	34	21	13	165176.244	-0.02735	0.2907	24	18	7	23	18	6	172702.350	0.01613	0.5
34	22	12	34	21	14	165176.244	-0.02735	0.2093	24	18	6	23	18	5	172702.350	0.01613	0.5
34	22	13	34	21	13	165176.244	-0.02735	0.2093	24	7	18	23	7	17	172780.160	0.00081	
34	22	13	34	21	14	165176.244	-0.02735	0.2907	24	17	8	23	17	7	172917.096	-0.0025	0.5
23	19	4	22	19	3	165218.545	0.00544	0.5	24	17	7	23	17	6	172917.096	-0.0025	0.5
23	19	5	22	19	4	165218.545	0.00544	0.5	24	16	8	23	16	7	173174.884	0.01295	0.5
23	18	5	22	18	4	165377.775	0.00951	0.5	24	16	9	23	16	8	173174.884	0.01298	0.5
23	18	6	22	18	5	165377.775	0.00951	0.5	18	5	13	17	4	13	173463.987	0.00733	
33	22	11	33	21	12	165511.092	-0.03385	0.2893	24	15	10	23	15	9	173488.898	0.00679	0.5
33	22	11	33	21	13	165511.092	-0.03385	0.2107	24	15	9	23	15	8	173488.898	0.00583	0.5
33	22	12	33	21	12	165511.092	-0.03385	0.2107	28	1	27	27	1	26	173569.783	0.02259	0.4549
33	22	12	33	21	13	165511.092	-0.03385	0.2893	28	1	27	27	2	26	173569.783	0.02261	0.0451
23	17	6	22	17	5	165566.260	0.00227	0.5	28	2	27	27	1	26	173569.783	0.02258	0.0451
23	17	7	22	17	6	165566.260	0.00227	0.5	28	2	27	27	2	26	173569.783	0.0226	0.4549
23	16	7	22	16	6	165792.120	-0.02297	0.5	49	24	26	49	23	26	173573.129	0.05229	0.1905
23	16	8	22	16	7	165792.120	-0.02296	0.5	49	24	25	49	23	26	173573.129	0.04387	0.3095
23	15	9	22	15	8	166066.734	0.00042	0.5	49	24	26	49	23	27	173573.129	-0.06705	0.3095
23	15	8	22	15	7	166066.734	0.00018	0.5	49	24	25	49	23	27	173573.129	-0.07547	0.1905
26	2	24	25	3	23	166200.467	-0.02057	0.0418	46	6	40	46	6	41	173600.621	-0.05381	0.3342
26	3	24	25	3	23	166200.467	-0.02419	0.4582	46	7	40	46	5	41	173600.621	-0.05385	0.3342
26	2	24	25	2	23	166200.467	-0.0299	0.4582	46	7	40	46	6	41	173600.621	-0.05385	0.1658
26	3	24	25	2	23	166200.467	-0.03353	0.0418	46	6	40	46	5	41	173600.621	-0.05381	0.1658
23	14	10	22	14	9	166406.306	-0.02264	0.5	15	9	6	14	8	7	173711.099	-0.0013	
23	14	9	22	14	8	166406.306	-0.02954	0.5	24	14	10	23	14	9	173878.455	0.007	0.5
23	13	11	22	13	10	166835.479	0.07568	0.5	24	14	11	23	14	10	173878.455	0.0317	0.5
23	13	10	22	13	9	166835.479	-0.08402	0.5	25	6	20	24	6	19	174170.054	-0.02619	
23	12	12	22	12	11	167392.149	0.02646		25	5	20	24	5	19	174281.786	-0.01598	
23	12	11	22	12	10	167394.951	-0.0322		24	13	12	23	13	11	174372.960	0.22277	0.5
13	10	4	12	9	3	167405.351	-0.00285	0.2267	24	13	11	23	13	10	174372.960	-0.27739	0.5
13	10	3	12	9	3	167405.351	-0.00621	0.2733	24	6	18	23	6	17	174423.892	0.01149	
13	10	4	12	9	4	167405.351	-0.03276	0.2733	14	10	5	13	9	4	174538.333	0.12708	0.2217
13	10	3	12	9	4	167405.351	-0.03612	0.2267	14	10	4	13	9	4	174538.333	0.1073	0.2783
22	8	14	21	8	13	167488.935	0.00502		14	10	5	13	9	5	174538.333	-0.03419	0.2783
27	2	26	26	2	25	167621.183	0.02696	0.4551	14	10	4	13	9	5	174538.333	-0.05397	0.2217
27	1	26	26	1	25	167621.183	0.02692	0.4551	29	0	29	28	0	28	175001.670	-0.02086	0.4523
27	2	26	26	1	25	167621.183	0.0269	0.0449	29	0	29	28	1	28	175001.670	-0.02086	0.0477
27	1	26	26	2	25	167621.183	0.02699	0.0449	29	1	29	28	0	28	175001.670	-0.02086	0.0477
12	11	1	11	10	1	168072.619	-0.01974	0.2648	29	1	29	28	1	28	175001.670	-0.02086	0.4523
12	11	1	11	10	2	168072.619	-0.01978	0.2352	24	12	13	23	12	12	175017.079	-0.01281	
12	11	2	11	10	1	168072.619	-0.01973	0.2352	24	12	12	23	12	11	175024.956	-0.00135	
12	11	2	11	10	2	168072.619	-0.01977	0.2648	13	11	3	12	10	2	175231.466	-0.00774	0.2312
23	11	13	22	11	12	168130.721	0.01303		13	11	2	12	10	2	175231.466	-0.00778	0.2688
23	11	12	22	11	11	168169.569	0.00289		13	11	2	12	10	3	175231.466	-0.00823	0.2312
24	6	19	23	6	18	168243.022	0.00732		13	11	3	12	10	3	175231.466	-0.00818	0.2688
24	5	19	23	5	18	168466.766	0.0144		26	5	22	25	5	21	175374.193	0.00135	
45	6	39	45	6	40	169034.793	0.02304	0.3339	26	4	22	25	4	21	175377.960	-0.01572	
45	7	39	45	5	40	169034.793	0.02294	0.3339	45	5	40	45	5	41	175456.466	-0.01505	0.3368
45	7	39	45	6	40	169034.793	0.02294	0.1661	45	6	40	45	4	41	175456.466	-0.01505	0.3368
45	6	39	45	5	40	169034.793	0.02303	0.1661	45	6	40	45	5	41	175456.466	-0.01505	0.1632
22	7	15	21	7	14	169049.902	-0.03219		45	5	40	45	4	41	175456.466	-0.01505	0.1632
28	0	28	27	0	27	169053.779	-0.00913	0.4523	23	7	16	22	7	15	175775.548	-0.0047	
28	0	28	27	1	27	169053.779	-0.00913	0.0477	24	11	14	23	11	13	175865.457	-0.02847	
28	1	28	27	0	27	169053.779	-0.00913	0.0477	12	12	1	11	11	0	175879.031	0.0013	0.2388
28	1	28	27	1	27	169053.779	-0.00913	0.4523	12	12	1	11	11	1	175879.031	0.0013	0.2612
23	6	17	22	6	16	169198.212	0.03414		12	12	0	11	11	0	175879.031	0.0013	0.2612
23	8	16	22	8	15	169276.318	-0.03647		12	12	0	11	11	1	175879.031	0.0013	0.2388
48	8	40	48	8	41	169370.237	-0.02103	0.3284	24	11	13	23	11	12	175958.886	-0.03498	
48	8	40	48	7	41	169370.237	-0.02118	0.1716	24	8	17	23	8	16	176146.485	-0.00038	
48	9	40	48	8	41	169370.237	-0.02429	0.1716	48	7	41	48	7	42	176165.639	-0.03823	0.3314
48	9	40	48	7	41	169370.237	-0.02445	0.3284	48	8	41	48	7	42	176165.639	-0.03838	0.1686
23	10	13	22	10	12	169442.324	0.0208		48	8	41	48	6	42	176165.639	-0.03839	0.3314
25																	

Comprehensive analysis of Isobutyraldehyde: millimetre-wave spectroscopy as an approach to ISM detection

28	3	26	27	3	25	178095.463	-0.03009	0.4576	51	8	43	51	7	44	183207.843	-0.0004	0.1701
47	6	41	47	6	42	178162.730	-0.00604	0.3346	48	25	23	48	24	24	183377.216	0.02854	0.3041
47	7	41	47	5	42	178162.730	-0.00606	0.3346	48	25	24	48	24	25	183377.216	0.02568	0.3041
47	7	41	47	6	42	178162.730	-0.00606	0.1654	48	25	23	48	24	25	183377.216	0.0255	0.1959
47	6	41	47	5	42	178162.730	-0.00604	0.1654	48	25	24	48	24	24	183377.216	0.02872	0.1959
19	7	12	18	6	12	178327.309	0.03068		18	3	15	17	2	15	183503.753	0.00177	
42	24	18	42	23	19	178387.253	0.01159	0.2972	25	11	15	24	11	14	183652.252	-0.01697	
42	24	19	42	23	19	178387.253	0.01159	0.2028	25	11	14	24	11	13	183863.744	-0.02826	
42	24	18	42	23	20	178387.253	0.01151	0.2028	29	2	27	28	3	26	184041.989	-0.02294	0.0426
42	24	19	42	23	20	178387.253	0.01151	0.2972	29	3	27	28	3	26	184041.989	-0.02314	0.4574
50	8	42	50	8	43	178602.710	0.01433	0.3295	29	2	27	28	2	26	184041.989	-0.02347	0.4574
50	8	42	50	7	43	178602.710	0.0143	0.1705	29	3	27	28	2	26	184041.989	-0.02368	0.0426
50	9	42	50	8	43	178602.710	0.01374	0.1705	47	5	42	47	5	43	184541.691	-0.04952	0.3374
50	9	42	50	7	43	178602.710	0.01371	0.3295	47	6	42	47	4	43	184541.691	-0.04952	0.3374
43	3	40	43	3	41	178734.014	0.01227	0.3419	47	6	42	47	5	43	184541.691	-0.04952	0.1626
43	4	40	43	2	41	178734.014	0.01227	0.3419	47	5	42	47	4	43	184541.691	-0.04952	0.1626
43	4	40	43	3	41	178734.014	0.01227	0.1581	25	10	16	24	10	15	184629.159	-0.03772	
43	3	40	43	2	41	178734.014	0.01227	0.1581	43	2	41	43	2	42	184699.724	-0.01845	0.3442
25	7	19	24	7	18	178860.467	0.01089		43	3	41	43	1	42	184699.724	-0.01845	0.3442
41	24	17	41	23	18	178884.911	-0.01114	0.296	43	3	41	43	2	42	184699.724	-0.01845	0.1558
41	24	18	41	23	18	178884.911	-0.01114	0.204	43	2	41	43	1	42	184699.724	-0.01845	0.1558
41	24	18	41	23	19	178884.911	-0.01117	0.296	25	9	17	24	9	16	184724.690	-0.0041	
41	24	17	41	23	19	178884.911	-0.01117	0.204	24	8	16	23	8	15	184729.970	-0.00391	
25	24	1	24	24	0	179168.212	-0.02755	0.5	26	7	20	25	7	19	184852.089	-0.01243	
25	24	2	24	24	1	179168.212	-0.02755	0.5	50	7	43	50	7	44	185324.158	0.01083	0.3327
25	23	3	24	23	2	179268.971	-0.01741	0.5	50	8	43	50	6	44	185324.158	0.0108	0.3327
25	23	2	24	23	1	179268.971	-0.01741	0.5	50	8	43	50	7	44	185324.158	0.0108	0.1673
25	22	4	24	22	3	179383.290	0.00609	0.5	50	7	43	50	6	44	185324.158	0.01083	0.1673
25	22	3	24	22	2	179383.290	0.00609	0.5	26	6	20	25	6	19	185375.908	-0.01402	
25	21	4	24	21	3	179513.896	-0.01081	0.5	30	1	29	29	1	28	185464.298	-0.01645	0.4546
25	21	5	24	21	4	179513.896	-0.01081	0.5	30	1	29	29	2	28	185464.298	-0.01645	0.0454
29	1	28	28	1	27	179517.502	0.00857	0.4547	30	2	29	29	1	28	185464.298	-0.01645	0.0454
29	1	28	28	2	27	179517.502	0.00857	0.0453	30	2	29	29	2	28	185464.298	-0.01645	0.4546
29	2	28	28	1	27	179517.502	0.00856	0.0453	27	6	22	26	6	21	185999.567	-0.01311	
29	2	28	28	2	27	179517.502	0.00857	0.4547	27	5	22	26	5	21	186025.305	-0.02764	
25	20	5	24	20	4	179664.369	-0.01885	0.5	25	10	15	24	10	14	186143.284	-0.02672	
25	20	6	24	20	5	179664.369	-0.01885	0.5	26	25	1	25	25	0	186318.399	-0.03398	0.5
18	6	13	17	5	13	179693.714	0.03103		26	25	2	25	25	1	186318.399	-0.03398	0.5
39	24	15	39	23	16	179768.401	-0.03372	0.2927	26	24	2	25	24	1	186418.756	-0.01126	0.5
39	24	15	39	23	17	179768.401	-0.03373	0.2073	26	24	3	25	24	2	186418.756	-0.01126	0.5
39	24	16	39	23	16	179768.401	-0.03372	0.2073	26	23	4	25	23	3	186531.898	-0.00336	0.5
39	24	16	39	23	17	179768.401	-0.03373	0.2927	26	23	3	25	23	2	186531.898	-0.00336	0.5
25	6	19	24	6	18	179814.321	-0.02812		26	22	5	25	22	4	186660.354	0.00488	0.5
25	19	7	24	19	6	179839.302	0.02377	0.5	26	22	4	25	22	3	186660.354	0.00488	0.5
25	19	6	24	19	5	179839.302	0.02377	0.5	26	21	5	25	21	4	186807.261	-0.0035	0.5
25	18	8	24	18	7	180044.542	-0.00207	0.5	26	21	6	25	21	5	186807.261	-0.0035	0.5
25	18	7	24	18	6	180044.542	-0.00207	0.5	31	0	31	30	0	30	186894.625	0.0233	0.4522
26	6	21	25	6	20	180086.275	0.0067		31	0	31	30	1	30	186894.625	0.0233	0.0478
26	5	21	25	5	20	180140.516	-0.01992		31	1	31	30	0	30	186894.625	0.0233	0.0478
18	4	14	17	3	14	180168.672	0.04114		31	1	31	30	1	30	186894.625	0.0233	0.4522
42	2	40	42	2	41	180182.004	-0.0158	0.3442	26	20	6	25	20	5	186976.680	0.0147	0.5
42	3	40	42	1	41	180182.004	-0.0158	0.3442	26	20	7	25	20	6	186976.680	0.0147	0.5
42	3	40	42	2	41	180182.004	-0.0158	0.1558	25	7	18	24	7	17	187053.928	-0.0102	
42	2	40	42	1	41	180182.004	-0.0158	0.1558	26	19	8	25	19	7	187173.755	0.01349	0.5
26	6	21	25	5	20	180188.119	-0.01629		26	19	7	25	19	6	187173.755	0.01349	0.5
25	17	9	24	17	8	180288.170	0.00298	0.5	26	18	9	25	18	8	187405.371	0.0479	0.5
25	17	8	24	17	7	180288.170	0.00298	0.5	26	18	8	25	18	7	187405.371	0.0479	0.5
25	16	9	24	16	8	180581.107	0.01072	0.5	26	17	10	25	17	9	187680.590	-0.00801	0.5
25	16	10	24	16	9	180581.107	0.01085	0.5	26	17	9	25	17	8	187680.590	-0.00803	0.5
16	9	7	15	8	7	180684.539	0.01913		17	9	9	16	8	9	187710.521	0.03131	
16	9	8	15	8	8	180730.772	0.00079		26	16	10	25	16	9	188012.270	0.01546	0.5
49	7	42	49	7	43	180747.332	-0.01983	0.3325	26	16	11	25	16	10	188012.270	0.01597	0.5
49	8	42	49	6	43	180747.332	-0.01989	0.3325	26	15	12	25	15	11	188418.419	0.008	0.5
49	8	42	49	7	43	180747.332	-0.01989	0.1675	26	15	11	25	15	10	188418.419	-0.00475	0.5
49	7	42	49	6	43	180747.332	-0.01983	0.1675	29	4	26	28	4	25	188587.216	0.00522	0.4602
25	15	11	24	15	10	180938.831	0.01269	0.5	29	3	26	28	3	25	188587.216	-0.00708	0.4602
25	15	10	24	15	9	180938.831	0.00906	0.5	29	3	26	28	4	25	188587.216	0.01342	0.0398
30	0	30	29	0	29	180948.634	-0.00559	0.4523	29	4	26	28	3	25	188587.216	-0.01528	0.0398
30	0	30	29	1	29	180948.634	-0.00559	0.0477	26	14	12	25	14	11	188926.165	-0.14087	0.5
30	1	30	29	0	29	180948.634	-0.00559	0.0477	26	14	13	25	14	12	188926.165	0.11431	0.5
30	1	30	29	1	29	180948.634	-0.00559	0.4523	48	5	43	48	5	44	189081.285	-0.01021	0.3379
27	5	23	26	5	22	181305.551	0.02482		48	6	43	48	4	44	189081.285	-0.01021	0.3379
24	9	15	23	9	14	181307.080	0.12515	0.4634	48	6	43	48	5	44	189081.285	-0.01021	0.1621
27	4	23	26	4	22	181307.080	-0.10857	0.5366	48	5	43	48	4	44	189081.285	-0.01021	0.1621
25	14	11	24	14	10	181384.159	-0.04169	0.5	26	8	19	25	8	18	189167.925	0.00056	
25	14	12	24	14	11	181384.159	0.04038	0.5	15	11	4	14	10	4	189521.062	0.03777	0.2769
25	13	13	24	13	12	181951.992	0.0464		15	11	5	14	10	5	189521.062	0.0203	0.2769
28	4	25	27	4	24	182644.357	0.03458	0.4606	15	11	4	14	10	5	189521.062	0.01799	0.2231
28	3	25															







Comprehensive analysis of Isobutyraldehyde: millimetre-wave spectroscopy as an approach to ISM detection

28	20	8	27	20	7	201647.436	0.01728	0.5	33	3	31	32	2	30	207820.004	-0.00707	0.0434
28	20	9	27	20	8	201647.436	0.01728	0.5	33	3	31	32	3	30	207820.004	-0.00706	0.4566
46	27	19	46	26	20	201678.279	0.03462	0.2951	29	27	3	28	27	2	207858.969	-0.0554	0.5
46	27	19	46	26	21	201678.279	0.03462	0.2049	29	27	2	28	27	1	207858.969	-0.0554	0.5
46	27	20	46	26	20	201678.279	0.03462	0.2049	27	9	18	26	9	17	207962.066	-0.00153	
46	27	20	46	26	21	201678.279	0.03462	0.2951	29	26	3	28	26	2	207969.557	-0.03655	0.5
32	2	30	31	2	29	201876.826	-0.00995	0.4568	29	26	4	28	26	3	207969.557	-0.03655	0.5
32	2	30	31	3	29	201876.826	-0.00992	0.0432	29	7	22	28	7	21	208050.105	0.00548	
32	3	30	31	2	29	201876.826	-0.00996	0.0432	29	25	4	28	25	3	208093.023	0.01514	0.5
32	3	30	31	3	29	201876.826	-0.00993	0.4568	29	25	5	28	25	4	208093.023	0.01514	0.5
28	19	10	27	19	9	201894.904	-0.01174	0.5	29	24	5	28	24	4	208231.598	0.00107	0.5
28	19	9	27	19	8	201894.904	-0.01174	0.5	29	24	6	28	24	5	208231.598	0.00107	0.5
20	4	16	19	3	16	202091.633	-0.0271		29	23	7	28	23	6	208388.252	0.02028	0.5
28	18	11	27	18	10	202186.565	0.00368	0.5	29	23	6	28	23	5	208388.252	0.02028	0.5
28	18	10	27	18	9	202186.565	0.00367	0.5	30	6	24	29	7	23	208468.977	-0.00825	
28	17	12	27	17	11	202534.483	-0.00761	0.5	30	7	24	29	7	23	208498.693	-0.00494	
28	17	11	27	17	10	202534.483	-0.00787	0.5	30	6	24	29	6	23	208532.445	0.01458	
29	6	23	28	7	22	202538.280	0.03165		20	9	12	19	8	12	208569.010	0.02261	
28	7	21	27	7	20	202559.450	-0.01498		58	9	49	58	9	50	208591.762	0.02409	0.3301
29	7	23	28	7	22	202601.686	-0.007		58	10	49	58	8	50	208591.762	0.02408	0.3301
29	6	23	28	6	22	202671.329	-0.00557		58	10	49	58	9	50	208591.762	0.02408	0.1699
29	7	23	28	6	22	202734.782	0.00318		58	9	49	58	8	50	208591.762	0.02409	0.1699
18	10	8	17	9	9	202797.519	-0.05364		29	21	8	28	21	7	208770.938	0.00441	0.5
28	16	12	27	16	11	202955.736	-0.02515	0.5	29	21	9	28	21	8	208770.938	0.00441	0.5
28	16	13	27	16	12	202955.736	-0.01861	0.5	28	11	17	27	11	16	208838.347	-0.00896	
33	1	32	32	1	31	203298.935	-0.0067	0.4543	51	4	47	51	4	48	208856.364	0.0078	0.3405
33	1	32	32	2	31	203298.935	-0.0067	0.0457	51	5	47	51	3	48	208856.364	0.0078	0.3405
33	2	32	32	1	31	203298.935	-0.0067	0.0457	51	5	47	51	4	48	208856.364	0.0078	0.1595
33	2	32	32	2	31	203298.935	-0.0067	0.4543	51	4	47	51	3	48	208856.364	0.0078	0.1595
28	15	14	27	15	13	203475.325	0.06502	0.5	29	20	9	28	20	8	209007.347	-0.0089	0.5
28	15	13	27	15	12	203475.325	-0.06444	0.5	29	20	10	28	20	9	209007.347	-0.0089	0.5
54	7	47	54	7	48	203590.145	0.00092	0.3338	21	5	16	20	4	16	209008.722	0.02479	
54	8	47	54	6	48	203590.145	0.00092	0.3338	20	9	11	19	8	12	209105.681	-0.00137	
54	8	47	54	7	48	203590.145	0.00092	0.1662	34	1	33	33	1	32	209241.747	-0.00529	0.4542
54	7	47	54	6	48	203590.145	0.00092	0.1662	34	1	33	33	2	32	209241.747	-0.00529	0.0458
17	11	7	16	10	6	203743.836	0.24412	0.2143	34	2	33	33	1	32	209241.747	-0.00529	0.0458
17	11	6	16	10	6	203743.836	0.18834	0.2857	34	2	33	33	2	32	209241.747	-0.00529	0.4542
17	11	7	16	10	7	203743.836	-0.16411	0.2857	29	19	11	28	19	10	209283.363	-0.01492	0.5
17	11	6	16	10	7	203743.836	-0.21988	0.2143	29	19	10	28	19	9	209283.363	-0.01493	0.5
30	5	25	29	6	24	203748.188	-0.00042		29	18	12	28	18	11	209609.159	-0.00912	0.5
30	6	25	29	6	24	203750.115	-0.00575		29	18	11	28	18	10	209609.159	-0.00916	0.5
30	5	25	29	5	24	203752.563	-0.0202		31	6	26	30	6	25	209672.170	0.00078	
30	6	25	29	5	24	203754.483	-0.03351		31	5	26	30	5	25	209673.243	-0.01951	
56	28	28	56	27	29	204077.463	-0.02183	0.3069	19	10	9	18	9	9	209683.515	0.02309	
56	28	29	56	27	30	204077.463	-0.02434	0.3069	19	10	10	18	9	10	209752.427	-0.01574	
56	28	28	56	27	30	204077.463	-0.02451	0.1931	29	17	13	28	17	12	209998.668	-0.00813	0.5
56	28	29	56	27	29	204077.463	-0.02165	0.1931	29	17	12	28	17	11	209998.668	-0.0091	0.5
28	14	15	27	14	14	204130.850	0.00873		54	6	48	54	6	49	210013.556	-0.00307	0.3367
28	14	14	27	14	13	204132.864	-0.04297		54	7	48	54	5	49	210013.556	-0.00307	0.3367
27	10	17	26	10	16	204238.552	-0.0109		54	7	48	54	6	49	210013.556	-0.00307	0.1633
50	4	46	50	4	47	204331.443	0.01465	0.3406	54	6	48	54	5	49	210013.556	-0.00307	0.1633
50	5	46	50	3	47	204331.443	0.01465	0.3406	21	8	14	20	7	14	210046.579	-0.01441	
50	5	46	50	4	47	204331.443	0.01465	0.1594	28	8	20	27	8	19	210116.922	0.00118	
50	4	46	50	3	47	204331.443	0.01465	0.1594	21	6	16	20	5	16	210349.229	-0.00553	
16	12	4	15	11	4	204496.799	0.02095	0.5491	50	3	47	50	3	48	210381.050	0.02429	0.3428
16	12	5	15	11	4	204496.799	0.02121	0.4509	50	4	47	50	2	48	210381.050	0.02429	0.3428
34	0	34	33	0	33	204726.265	0.01879	0.4521	50	4	47	50	3	48	210381.050	0.02429	0.1572
34	0	34	33	1	33	204726.265	0.01879	0.0479	50	3	47	50	2	48	210381.050	0.02429	0.1572
34	1	34	33	0	33	204726.265	0.01879	0.0479	29	16	13	28	16	12	210471.713	-0.01104	0.5
34	1	34	33	1	33	204726.265	0.01879	0.4521	29	16	14	28	16	13	210471.713	0.01022	0.5
27	8	19	26	8	18	204868.751	-0.01641		35	0	35	34	0	34	210667.922	-0.01802	0.4521
28	13	15	27	13	14	205003.724	-0.02641		35	0	35	34	1	34	210667.922	-0.01802	0.0479
31	5	27	30	4	26	205043.494	-0.08595	0.0375	35	1	35	34	0	34	210667.922	-0.01802	0.0479
31	4	27	30	4	26	205043.494	-0.04748	0.4625	35	1	35	34	1	34	210667.922	-0.01802	0.4521
31	5	27	30	5	26	205043.494	0.00723	0.4625	57	8	49	57	8	50	210719.345	0.01634	0.3324
31	4	27	30	5	26	205043.494	0.04571	0.0375	57	9	49	57	7	50	210719.345	0.01634	0.3324
15	13	2	14	12	2	205167.464	-0.00488	0.2667	57	9	49	57	8	50	210719.345	0.01634	0.1676
15	13	2	14	12	3	205167.464	-0.00489	0.2333	57	8	49	57	7	50	210719.345	0.01634	0.1676
15	13	3	14	12	2	205167.464	-0.00488	0.2333	32	4	28	31	4	27	210979.524	-0.02283	0.924
15	13	3	14	12	3	205167.464	-0.00489	0.2667	32	5	28	31	4	27	210979.524	-0.03859	0.076
28	9	20	27	9	19	205387.969	0.01735		17	12	5	16	11	5	211626.157	0.02752	0.2788
22	8	14	21	7	14	205777.657	-0.04347		17	12	6	16	11	6	211626.157	0.01676	0.2788
14	14	1	13	13	0	205807.778	0.00492	0.2398	17	12	5	16	11	6	211626.157	0.01528	0.2212
14	14	1	13	13	1	205807.778	0.00492	0.2602	17	12	6	16	11	5	211626.157	0.02899	0.2212
14	14	0	13	13	0	205807.778	0.00492	0.2602	53	5	48	53	5	49	211754.483	0.01994	0.3389
14	14	0	13	13	1	205807.778	0.00492	0.2398	53	6	48	53	4	49	211754.483	0.01994	0.3389
28	12	17	27	12	16	206053.907	0.016		53	6	48	53	5	49	211754.483	0.01994	0.1611
28	12	16	27	12	15	206304.905	0.01011		53	5	48	53	4	49	211754.483	0.01994	0.1611
32	4	29	31	4	28</												

Comprehensive analysis of Isobutyraldehyde: millimetre-wave spectroscopy as an approach to ISM detection

29	13	16	28	13	15	212821.242	0.02892			53	4	49	53	4	50	217904.152	-0.00651	0.3409
15	14	2	14	13	1	212970.016	0.03297	0.2371		53	5	49	53	3	50	217904.152	-0.00651	0.3409
15	14	2	14	13	2	212970.016	0.03297	0.2629		53	5	49	53	4	50	217904.152	-0.00651	0.1591
15	14	1	14	13	1	212970.016	0.03297	0.2629		53	4	49	53	3	50	217904.152	-0.00651	0.1591
15	14	1	14	13	2	212970.016	0.03297	0.2371		30	9	22	29	9	21	217999.189	-0.00747	
21	5	17	20	4	17	212979.625	-0.03214			30	16	14	29	16	13	218019.873	-0.05458	0.5
23	8	15	22	7	15	213111.414	-0.0053			30	16	15	29	16	14	218019.873	0.01078	0.5
28	10	18	27	10	17	213594.564	0.02375			34	4	31	33	4	30	218295.136	0.01832	0.4587
30	7	23	29	7	22	213686.721	0.02837			34	3	31	33	3	30	218295.136	0.0182	0.4587
34	2	32	33	2	31	213762.245	0.02522	0.4564		34	4	31	33	3	30	218295.136	0.01813	0.0413
34	2	32	33	3	31	213762.245	0.02522	0.0436		34	3	31	33	4	30	218295.136	0.0184	0.0413
34	3	32	33	2	31	213762.245	0.02521	0.0436		22	8	15	21	7	15	218641.155	0.03009	
34	3	32	33	3	31	213762.245	0.02522	0.4564		30	15	15	29	15	14	218680.595	-0.01909	
22	6	16	21	5	16	213908.486	0.02694			56	6	50	56	6	51	219093.302	-0.0114	0.3373
29	12	18	28	12	17	213930.256	0.02591			56	7	50	56	5	51	219093.302	-0.0114	0.3373
31	6	25	30	7	24	214383.759	0.00158			56	7	50	56	6	51	219093.302	-0.0114	0.1627
31	7	25	30	7	24	214397.431	-0.02214			56	6	50	56	5	51	219093.302	-0.0114	0.1627
31	6	25	30	6	24	214413.490	0.02128			31	7	24	30	7	23	219421.371	0.00244	
31	7	25	30	6	24	214427.188	0.02258			17	13	5	16	12	4	219466.423	0.01338	0.2264
29	12	17	28	12	16	214450.558	0.01491			17	13	4	16	12	5	219466.423	0.01309	0.2264
29	10	20	28	10	19	214478.781	0.00199			17	13	5	16	12	5	219466.423	0.01312	0.2736
55	6	49	55	6	50	214554.373	0.0233	0.3368		17	13	4	16	12	4	219466.423	0.01335	0.2736
55	7	49	55	5	50	214554.373	0.0233	0.3368		30	14	17	29	14	16	219520.324	-0.05042	
55	7	49	55	6	50	214554.373	0.0233	0.1632		30	14	16	29	14	15	219533.875	-0.0496	
55	6	49	55	5	50	214554.373	0.0233	0.1632		31	8	24	30	7	23	219588.986	-0.01572	
29	11	19	28	11	18	214891.084	-0.04209			59	30	29	59	29	30	219627.777	-0.02507	0.305
53	29	24	53	28	25	214917.139	-0.0219	0.2996		59	30	29	59	29	31	219627.777	-0.02531	0.195
53	29	24	53	28	26	214917.139	-0.0219	0.2004		59	30	30	59	29	31	219627.777	-0.02529	0.305
53	29	25	53	28	25	214917.139	-0.0219	0.2004		59	30	30	59	29	30	219627.777	-0.02506	0.195
53	29	25	53	28	26	214917.139	-0.0219	0.2996		35	2	33	34	2	32	219703.416	0.00069	0.4562
29	8	21	28	8	20	215093.699	-0.00813			35	2	33	34	3	32	219703.416	0.00069	0.0438
30	27	4	29	27	3	215112.408	-0.04016	0.5		35	3	33	34	2	32	219703.416	0.00069	0.0438
30	27	3	29	27	2	215112.408	-0.04016	0.5		35	3	33	34	3	32	219703.416	0.00069	0.4562
22	9	14	21	8	13	215172.743	0.01657			30	8	22	29	8	21	220111.644	-0.02896	
35	1	34	34	1	33	215183.501	0.02955	0.4541		16	14	3	15	13	2	220129.062	-0.02527	0.2342
35	1	34	34	2	33	215183.501	0.02955	0.0459		16	14	3	15	13	3	220129.062	-0.02527	0.2658
35	2	34	34	1	33	215183.501	0.02955	0.0459		16	14	2	15	13	2	220129.062	-0.02527	0.2658
35	2	34	34	2	33	215183.501	0.02955	0.4541		16	14	2	15	13	3	220129.062	-0.02527	0.2342
30	26	4	29	26	3	215234.576	-0.01807	0.5		62	10	52	62	10	53	220143.683	0.00855	0.3288
30	26	5	29	26	4	215234.576	-0.01807	0.5		62	11	52	62	9	53	220143.683	0.00854	0.3288
58	8	50	58	8	51	215288.610	-0.00791	0.3329		62	11	52	62	10	53	220143.683	0.00854	0.1712
58	9	50	58	7	51	215288.610	-0.00791	0.3329		62	10	52	62	9	53	220143.683	0.00855	0.1712
58	9	50	58	8	51	215288.610	-0.00791	0.1671		22	5	17	21	4	17	220209.884	-0.01777	
58	8	50	58	7	51	215288.610	-0.00791	0.1671		32	6	26	31	7	25	220293.515	0.04394	
30	25	5	29	25	4	215371.009	-0.02485	0.5		32	7	26	31	7	25	220299.659	-0.03668	
30	25	6	29	25	5	215371.009	-0.02485	0.5		32	6	26	31	6	25	220307.138	-0.02892	
30	24	6	29	24	5	215524.380	0.01257	0.5		32	7	26	31	6	25	220313.382	-0.00962	
30	24	7	29	24	6	215524.380	0.01257	0.5		58	30	28	58	29	29	220359.116	0.01338	0.3036
28	9	19	27	9	18	215558.469	-0.02337			58	30	29	58	29	29	220359.116	0.01338	0.1964
30	23	8	29	23	7	215697.826	0.02162	0.5		58	30	28	58	29	30	220359.116	0.01329	0.1964
30	23	7	29	23	6	215697.826	0.02162	0.5		58	30	29	58	29	30	220359.116	0.0133	0.3036
30	22	9	29	22	8	215895.380	0.01694	0.5		30	13	18	29	13	17	220597.294	-0.00177	
30	22	8	29	22	7	215895.380	0.01694	0.5		30	13	17	29	13	16	220734.170	-0.0442	
30	21	9	29	21	8	216122.126	-0.01464	0.5		15	15	1	14	14	0	220765.906	-0.00247	0.2395
30	21	10	29	21	9	216122.126	-0.01464	0.5		15	15	1	14	14	1	220765.906	-0.00247	0.2605
54	5	49	54	5	50	216285.010	-0.02191	0.3389		15	15	0	14	14	0	220765.906	-0.00247	0.2605
54	6	49	54	4	50	216285.010	-0.02191	0.3389		15	15	0	14	14	1	220765.906	-0.00247	0.2395
54	6	49	54	5	50	216285.010	-0.02191	0.1611		51	2	49	51	2	50	220839.884	0.00545	0.3447
54	5	49	54	4	50	216285.010	-0.02191	0.1611		51	3	49	51	1	50	220839.884	0.00545	0.3447
50	2	48	50	2	49	216322.327	0.0124	0.3446		51	3	49	51	2	50	220839.884	0.00545	0.1553
50	3	48	50	1	49	216322.327	0.0124	0.3446		51	2	49	51	1	50	220839.884	0.00545	0.1553
50	3	48	50	2	49	216322.327	0.0124	0.1554		22	6	17	21	5	17	220921.197	-0.01797	
50	2	48	50	1	49	216322.327	0.0124	0.1554		57	30	27	57	29	28	221047.354	0.02247	0.3025
30	20	10	29	20	9	216384.721	0.01836	0.5		57	30	28	57	29	28	221047.354	0.02247	0.1975
30	20	11	29	20	10	216384.721	0.01836	0.5		57	30	27	57	29	29	221047.354	0.02244	0.1975
20	10	10	19	9	10	216488.159	-0.03349			57	30	28	57	29	29	221047.354	0.02244	0.3025
36	0	36	35	0	35	216608.469	-0.01817	0.452		36	1	35	35	1	34	221124.071	0.00529	0.454
36	0	36	35	1	35	216608.469	-0.01817	0.048		36	1	35	35	2	34	221124.071	0.00529	0.046
36	1	36	35	0	35	216608.469	-0.01817	0.048		36	2	35	35	1	34	221124.071	0.00529	0.046
36	1	36	35	1	35	216608.469	-0.01817	0.452		36	2	35	35	2	34	221124.071	0.00529	0.454
20	10	11	19	9	11	216664.799	-0.01436			30	10	21	29	10	20	221382.268	-0.0321	
30	19	12	29	19	11	216691.636	-0.0416	0.5		58	7	51	58	7	52	221804.235	0.01205	0.3353
30	19	11	29	19	10	216691.636	-0.04161	0.5		58	8	51	58	6	52	221804.235	0.01205	0.3353
20	10	10	19	9	11	216709.576	-0.02961			58	8	51	58	7	52	221804.235	0.01205	0.1647
21	9	12	20	8	13	216876.962	-0.03849			58	7	51	58	6	52	221804.235	0.01205	0.1647
33	4	29	32	4	28	216915.643	-0.0087	0.4616		30	12	19	29	12	18	221819.124	-0.05024	
33	5	29	32	4														

Comprehensive analysis of Isobutyraldehyde: millimetre-wave spectroscopy as an approach to ISM detection

31	25	6	30	25	5	222659.659	0.03336	0.5	37	2	36	36	1	35	227063.521	0.01858	0.0461
31	25	7	30	25	6	222659.659	0.03336	0.5	30	11	19	29	11	18	227184.288	0.01108	
29	10	19	28	10	18	222707.336	0.00391		17	14	4	16	13	3	227283.267	0.03288	0.2305
31	24	7	30	24	6	222828.804	0.02151	0.5	17	14	4	16	13	4	227283.267	0.03288	0.2695
31	24	8	30	24	7	222828.804	0.02151	0.5	17	14	3	16	13	3	227283.267	0.03288	0.2695
30	12	18	29	12	17	222837.959	-0.01361		17	14	3	16	13	4	227283.267	0.03287	0.2305
34	4	30	33	5	29	222851.665	0.02761	0.0387	31	14	18	30	14	17	227293.404	-0.01383	
34	5	30	33	5	29	222851.665	0.02503	0.4613	31	14	17	30	14	16	227325.697	-0.01281	
34	4	30	33	4	29	222851.665	0.0212	0.4613	24	9	15	23	8	15	227369.317	0.00044	
34	5	30	33	4	29	222851.665	0.01862	0.0387	34	6	29	33	5	28	227449.165	-0.1246	0.036
30	9	22	29	8	21	222879.129	0.00936		34	5	29	33	5	28	227449.165	-0.05967	0.464
22	9	14	21	8	14	222985.551	0.0272		34	6	29	33	6	28	227449.165	0.02925	0.464
31	23	9	30	23	8	223020.298	0.02299	0.5	34	5	29	33	6	28	227449.165	0.09419	0.036
31	23	8	30	23	7	223020.298	0.02299	0.5	23	8	16	22	7	16	227741.929	-0.00618	
21	10	11	20	9	11	223121.846	-0.01626		16	15	2	15	14	1	227927.440	0.01083	0.2368
31	22	10	30	22	9	223238.593	-0.0031	0.5	16	15	2	15	14	2	227927.440	0.01083	0.2632
31	22	9	30	22	8	223238.593	-0.0031	0.5	16	15	1	15	14	1	227927.440	0.01083	0.2632
31	21	10	30	21	9	223489.480	0.01344	0.5	16	15	1	15	14	2	227927.440	0.01083	0.2368
31	21	11	30	21	10	223489.480	0.01344	0.5	31	10	22	30	10	21	228024.662	-0.00728	
22	4	18	21	3	18	223520.763	0.03538		30	9	21	29	9	20	228035.623	0.0009	
21	10	12	20	9	12	223540.369	0.00432		58	6	52	58	6	53	228166.301	0.03144	0.3376
22	5	18	21	4	18	223585.211	0.032		58	7	52	58	5	53	228166.301	0.03144	0.3376
57	6	51	57	6	52	223630.586	0.00574	0.3373	58	7	52	58	6	53	228166.301	0.03144	0.1624
57	7	51	57	5	52	223630.586	0.00574	0.3373	58	6	52	58	5	53	228166.301	0.03144	0.1624
57	7	51	57	6	52	223630.586	0.00574	0.1627	31	13	19	30	13	18	228484.094	0.0297	
57	6	51	57	5	52	223630.586	0.00574	0.1627	38	0	38	37	0	37	228486.056	0.04118	0.452
21	10	11	20	9	12	223658.600	0.04192		38	0	38	37	1	37	228486.056	0.04118	0.048
31	20	11	30	20	10	223780.292	0.00404	0.5	38	1	38	37	0	37	228486.056	0.04118	0.048
31	20	12	30	20	11	223780.292	0.00404	0.5	38	1	38	37	1	37	228486.056	0.04118	0.452
31	9	23	30	9	22	224063.639	0.01028		31	13	18	30	13	17	228775.556	0.00459	
31	19	13	30	19	12	224120.846	0.01105	0.5	35	4	31	34	5	30	228787.347	0.00289	0.039
31	19	12	30	19	11	224120.846	0.01103	0.5	35	5	31	34	5	30	228787.347	0.00185	0.461
35	3	32	34	3	31	224234.664	0.01184	0.4586	35	4	31	34	4	30	228787.347	0.0003	0.461
35	4	32	34	3	31	224234.664	0.01181	0.0414	35	5	31	34	4	30	228787.347	-0.00074	0.039
35	4	32	34	4	31	224234.664	0.01188	0.4586	23	7	17	22	6	17	228814.533	-0.02087	
35	3	32	34	4	31	224234.664	0.01191	0.0414	32	28	4	31	28	3	229513.106	-0.03354	0.5
60	8	52	60	8	53	224416.429	0.01381	0.3335	32	28	5	31	28	4	229513.106	-0.03354	0.5
60	9	52	60	7	53	224416.429	0.01381	0.3335	32	27	6	31	27	5	229645.982	-0.04028	0.5
60	9	52	60	8	53	224416.429	0.01381	0.1665	32	27	5	31	27	4	229645.982	-0.04028	0.5
60	8	52	60	7	53	224416.429	0.01381	0.1665	31	12	20	30	12	19	229681.593	0.01412	
31	18	14	30	18	13	224524.319	-0.02674	0.5	32	26	6	31	26	5	229793.865	0.03443	0.5
31	18	13	30	18	12	224524.319	-0.02724	0.5	32	26	7	31	26	6	229793.865	0.03443	0.5
20	11	10	19	10	9	224836.058	0.01388		53	2	51	53	2	52	229875.276	0.04601	0.3447
20	11	9	19	10	9	224838.753	0.01176		53	3	51	53	1	52	229875.276	0.04601	0.3447
20	11	10	19	10	10	224851.885	0.05988		53	3	51	53	2	52	229875.276	0.04601	0.1553
31	17	15	30	17	14	225009.307	-0.00685	0.5	53	2	51	53	1	52	229875.276	0.04601	0.1553
31	17	14	30	17	13	225009.307	-0.01758	0.5	31	11	21	30	11	20	229927.570	-0.01023	
32	7	25	31	8	24	225050.509	-0.026		32	25	7	31	25	6	229959.186	0.00065	0.5
32	8	25	31	8	24	225131.852	0.00357		32	25	8	31	25	7	229959.186	0.00065	0.5
32	7	25	31	7	24	225218.167	-0.00108		32	9	24	31	9	23	230029.686	-0.00155	
31	8	23	30	8	22	225323.189	0.02594		32	24	8	31	24	7	230145.333	0.03213	0.5
52	2	50	52	2	51	225357.536	0.02389	0.3446	32	24	9	31	24	8	230145.333	0.03213	0.5
52	3	50	52	1	51	225357.536	0.02389	0.3446	36	3	33	35	3	32	230173.321	0.00423	0.4581
52	3	50	52	2	51	225357.536	0.02389	0.1554	36	4	33	35	3	32	230173.321	0.00422	0.0419
52	2	50	52	1	51	225357.536	0.02389	0.1554	36	4	33	35	4	32	230173.321	0.00425	0.4581
22	9	13	21	8	14	225526.946	0.02538		36	3	33	35	4	32	230173.321	0.00426	0.0419
31	16	15	30	16	14	225602.682	-0.11877	0.5	32	23	10	31	23	9	230356.151	-0.01914	0.5
31	16	16	30	16	15	225602.682	0.07196	0.5	32	23	9	31	23	8	230356.151	-0.01914	0.5
36	2	34	35	2	33	225643.557	0.00036	0.4561	22	10	13	21	9	13	230408.012	0.01395	
36	2	34	35	3	33	225643.557	0.00036	0.0439	32	22	11	31	22	10	230596.823	0.01052	0.5
36	3	34	35	2	33	225643.557	0.00036	0.0439	32	22	10	31	22	9	230596.823	0.01052	0.5
36	3	34	35	3	33	225643.557	0.00036	0.4561	23	9	15	22	8	15	230636.676	0.00701	
19	12	8	18	11	7	225827.673	0.11974	0.2132	22	10	12	21	9	13	230699.448	-0.01195	
19	12	7	18	11	7	225827.673	0.08851	0.2868	32	8	24	31	8	23	230741.963	-0.01059	
19	12	8	18	11	8	225827.673	-0.10491	0.2868	32	21	11	31	21	10	230873.647	0.00629	0.5
19	12	7	18	11	8	225827.673	-0.13614	0.2132	32	21	12	31	21	11	230873.647	0.00629	0.5
19	12	8	18	11	7	225827.673	0.1206	0.2131	60	7	53	60	7	54	230896.214	0.02459	0.3359
19	12	7	18	11	7	225827.673	0.08937	0.2869	60	8	53	60	6	54	230896.214	0.02459	0.3359
19	12	8	18	11	8	225827.673	-0.10405	0.2869	60	8	53	60	7	54	230896.214	0.02459	0.1641
19	12	7	18	11	8	225827.673	-0.13528	0.2131	60	7	53	60	6	54	230896.214	0.02459	0.1641
23	6	17	22	5	17	226014.244	0.00997		33	7	26	32	8	25	230972.353	0.01963	
33	6	27	32	7	26	226202.979	-0.00552		33	8	26	32	8	25	231011.088	-0.00023	
33	7	27	32	7	26	226205.792	0.01583		33	7	26	32	7	25	231053.632	-0.01562	
33	6	27	32	6	26	226209.207	-0.00092		33	8	26	32	7	25	231092.376	-0.0268	
31	15	17	30	15	16	226344.727	0.01088		23	5	18	22	4	18	231190.754	0.00515	
31	15	16	30	15	15	226347.455	-0.03272		32	20	12	31	20	11	231194.980	-0.01251	0.5
59	7	52	59	7	53	226351.263	-0.05286	0.3355	32	20	13	31	20	12	231194.980	-0.01251	0.5
59	8	52	59	6	53	226351.263	-0.05286	0.3355	30	10	20	29	10	19	231197.553	-0.0014	
59	8	52	59	7	53	226351.263	-0.05286	0.1645	56	4	52	56	4	53	23147		

Comprehensive analysis of Isobutyraldehyde: millimetre-wave spectroscopy as an approach to ISM detection

34	7	28	33	7	27	232115.409	-0.00014			35	7	29	34	7	28	238028.082	0.01744		
32	17	16	31	17	15	232559.367	-0.01509	0.5		32	9	23	31	9	22	238063.391	-0.00667		
32	17	15	31	17	14	232559.367	-0.04794	0.5		63	8	55	63	8	56	238084.735	0.0237	0.3344	
25	8	17	24	7	17	232656.489	-0.04434			63	9	55	63	7	56	238084.735	0.0237	0.3344	
59	6	53	59	6	54	232700.507	0.01726	0.3378		63	9	55	63	8	56	238084.735	0.0237	0.1656	
59	7	53	59	5	54	232700.507	0.01726	0.3378		63	8	55	63	7	56	238084.735	0.0237	0.1656	
59	7	53	59	6	54	232700.507	0.01726	0.1622		33	21	12	32	21	11	238275.414	-0.0159	0.5	
59	6	53	59	5	54	232700.507	0.01726	0.1622		33	21	13	32	21	12	238275.414	-0.0159	0.5	
55	3	52	55	3	53	232977.030	0.01677	0.3432		22	11	11	21	10	11	238600.178	0.02169		
55	4	52	55	2	53	232977.030	0.01677	0.3432		33	20	13	32	20	12	238629.763	0.00554	0.5	
55	4	52	55	3	53	232977.030	0.01677	0.1568		33	20	14	32	20	13	238629.763	0.00555	0.5	
55	3	52	55	2	53	232977.030	0.01677	0.1568		22	11	12	21	10	12	238694.899	-0.0345		
38	1	37	37	1	36	233001.748	0.00095	0.4539		24	9	16	23	8	16	238718.226	0.03905		
38	1	37	37	2	36	233001.748	0.00095	0.0461		31	10	21	30	10	20	238817.860	-0.00638		
38	2	37	37	1	36	233001.748	0.00095	0.0461		59	5	54	59	5	55	238922.660	-0.00464	0.3397	
38	2	37	37	2	36	233001.748	0.00095	0.4539		59	6	54	59	4	55	238922.660	-0.00464	0.3397	
25	9	16	24	8	16	233174.612	0.0345			59	6	54	59	5	55	238922.660	-0.00464	0.1603	
31	9	22	30	9	21	233191.094	-0.02118			59	5	54	59	4	55	238922.660	-0.00464	0.1603	
32	16	16	31	16	15	233222.837	-0.32162	0.5		39	1	38	38	1	37	238938.752	-0.01686	0.4538	
32	16	17	31	16	16	233222.837	0.20848	0.5		39	1	38	38	2	37	238938.752	-0.01686	0.0462	
35	6	30	34	5	29	233376.978	-0.07145	0.0364		39	2	38	38	1	37	238938.752	-0.01686	0.0462	
35	5	30	34	5	29	233376.978	-0.04427	0.4636		39	2	38	38	2	37	238938.752	-0.01686	0.4538	
35	6	30	34	6	29	233376.978	-0.00651	0.4636		33	19	14	32	19	13	239046.183	-0.01497	0.5	
35	5	30	34	6	29	233376.978	0.02067	0.0364		33	19	15	32	19	14	239046.183	-0.01472	0.5	
62	8	54	62	8	55	233531.420	-0.03172	0.3341		36	5	31	35	6	30	239305.384	0.04612	0.0368	
62	9	54	62	7	55	233531.420	-0.03172	0.3341		36	6	31	35	6	30	239305.384	0.03483	0.4632	
62	9	54	62	8	55	233531.420	-0.03172	0.1659		36	5	31	35	5	30	239305.384	0.01894	0.4632	
62	8	54	62	7	55	233531.420	-0.03172	0.1659		36	6	31	35	5	30	239305.384	0.00764	0.0368	
19	13	7	18	12	7	233720.512	-0.01675			33	18	15	32	18	14	239542.017	-0.04315	0.5	
32	15	18	31	15	17	234056.574	-0.03738			33	18	16	32	18	15	239542.017	-0.03776	0.5	
32	15	17	31	15	16	234063.569	-0.02966			62	7	55	62	7	56	239979.795	-0.0611	0.3363	
23	4	19	22	3	19	234152.083	-0.05404			62	8	55	62	6	56	239979.795	-0.0611	0.3363	
39	0	39	38	0	38	234422.927	-0.00482	0.452		62	8	55	62	7	56	239979.795	-0.0611	0.1637	
39	0	39	38	1	38	234422.927	-0.00482	0.048		62	7	55	62	6	56	239979.795	-0.0611	0.1637	
39	1	39	38	0	38	234422.927	-0.00482	0.048		33	17	17	32	17	16	240142.083	0.03065	0.5	
39	1	39	38	1	38	234422.927	-0.00482	0.452		33	17	16	32	17	15	240142.083	-0.06511	0.5	
32	10	23	31	10	22	234428.175	0.03703			40	0	40	39	0	39	240358.560	-0.01841	0.452	
18	14	5	17	13	4	234430.337	0.01517	0.2278		40	0	40	39	1	39	240358.560	-0.01841	0.048	
18	14	5	17	13	5	234430.337	0.01514	0.2722		40	1	40	39	0	39	240358.560	-0.01841	0.048	
18	14	4	17	13	4	234430.337	0.01516	0.2722		40	1	40	39	1	39	240358.560	-0.01841	0.452	
18	14	4	17	13	5	234430.337	0.01513	0.2278		37	5	33	36	5	32	240657.334	0.01942	0.4604	
36	4	32	35	4	31	234722.593	-0.02043	0.4606		37	4	33	36	4	32	240657.334	0.01917	0.4604	
36	5	32	35	4	31	234722.593	-0.02084	0.0394		37	5	33	36	4	32	240657.334	0.019	0.0396	
36	4	32	35	5	31	234722.593	-0.01939	0.0394		37	4	33	36	5	32	240657.334	0.01958	0.0396	
36	5	32	35	5	31	234722.593	-0.0198	0.4606		20	13	7	19	12	7	240822.289	0.0066	0.2845	
17	15	3	16	14	2	235086.157	0.01073	0.234		20	13	8	19	12	8	240822.289	-0.02049	0.2845	
17	15	3	16	14	3	235086.157	0.01073	0.266		20	13	7	19	12	8	240822.289	-0.02463	0.2155	
17	15	2	16	14	2	235086.157	0.01073	0.266		20	13	8	19	12	7	240822.289	0.01073	0.2155	
17	15	2	16	14	3	235086.157	0.01073	0.234		38	3	35	37	3	34	242047.814	0.03767	0.458	
32	14	19	31	14	18	235121.887	-0.01494			38	3	35	37	4	34	242047.814	0.03767	0.042	
32	14	18	31	14	17	235195.372	-0.03999			38	4	35	37	3	34	242047.814	0.03767	0.042	
61	7	54	61	7	55	235438.961	-0.02921	0.3361		38	4	35	37	4	34	242047.814	0.03767	0.458	
61	8	54	61	6	55	235438.961	-0.02921	0.3361		18	15	4	17	14	3	242240.510	0.03073	0.2313	
61	8	54	61	7	55	235438.961	-0.02921	0.1639		18	15	4	17	14	4	242240.510	0.03073	0.2687	
61	7	54	61	6	55	235438.961	-0.02921	0.1639		18	15	3	17	14	3	242240.510	0.03073	0.2687	
23	10	13	22	9	13	235454.083	0.02532			18	15	3	17	14	4	242240.510	0.03073	0.2313	
33	8	25	32	9	24	235527.354	0.00846			18	15	3	17	14	3	242240.510	0.03106	0.2684	
16	16	0	15	15	1	235719.463	-0.00805	0.2399		18	15	3	17	14	4	242240.510	0.03106	0.2316	
16	16	1	15	15	0	235719.463	-0.00805	0.2399		18	15	4	17	14	3	242240.510	0.03106	0.2316	
16	16	1	15	15	1	235719.463	-0.00805	0.2601		18	15	4	17	14	4	242240.510	0.03106	0.2684	
16	16	0	15	15	0	235719.463	-0.00805	0.2601		35	7	28	34	7	27	242788.941	-0.01869		
33	9	25	32	9	24	235936.137	-0.00293			17	16	1	16	15	2	242880.203	-0.00903	0.2372	
37	3	34	36	3	33	236111.025	-0.0185	0.4578		17	16	2	16	15	1	242880.203	-0.00903	0.2372	
37	3	34	36	4	33	236111.025	-0.01849	0.0422		17	16	2	16	15	2	242880.203	-0.00903	0.2628	
37	4	34	36	3	33	236111.025	-0.01851	0.0422		17	16	1	16	15	1	242880.203	-0.00903	0.2628	
37	4	34	36	4	33	236111.025	-0.0185	0.4578		33	9	24	32	9	23	242979.304	0.02198		
33	8	25	32	8	24	236322.969	-0.00341			34	29	5	33	29	4	243914.925	-0.05042	0.5	
32	13	20	31	13	19	236406.154	-0.0058			34	29	6	33	29	5	243914.925	-0.05042	0.5	
31	11	20	30	11	19	236661.511	-0.01412			36	7	30	35	7	29	243943.310	0.14403	0.5	
33	28	5	32	28	4	236781.272	-0.04175	0.5		36	6	30	35	6	29	243943.310	-0.16316	0.5	
33	28	6	32	28	5	236781.272	-0.04175	0.5		33	11	23	32	11	22	244026.514	-0.00749		
34	8	27	33	8	26	236892.869	-0.00437			34	28	6	33	28	5	244058.434	-0.01032	0.5	
34	7	27	33	7	26	236913.448	0.00285			34	28	7	33	28	6	244058.434	-0.01032	0.5	
33	27	7	32	27	6	236926.764	-0.05601	0.5		33	13	21	32	13	20	244337.481	-0.00558		
33	27	6	32	27															

Comprehensive analysis of Isobutyraldehyde: millimetre-wave spectroscopy as an approach to ISM detection

34	21	13	33	21	12	245695.682	0.03162	0.5	62	6	57	62	4	58	252495.577	0.02761	0.34
34	21	14	33	21	13	245695.682	0.03162	0.5	62	6	57	62	5	58	252495.577	0.02761	0.16
32	11	21	31	11	20	245875.469	-0.01127		62	5	57	62	4	58	252495.577	0.02761	0.16
34	20	14	33	20	13	246085.563	-0.0291	0.5	39	4	35	38	4	34	252524.603	0.00534	0.4597
34	20	15	33	20	14	246085.563	-0.02907	0.5	39	4	35	38	5	34	252524.603	0.0054	0.0403
41	0	41	40	0	40	246292.892	-0.02815	0.452	39	5	35	38	4	34	252524.603	0.00531	0.0403
41	0	41	40	1	40	246292.892	-0.02815	0.048	39	5	35	38	5	34	252524.603	0.00538	0.4597
41	1	41	40	0	40	246292.892	-0.02815	0.048	34	12	23	33	12	22	252554.817	0.00735	
41	1	41	40	1	40	246292.892	-0.02815	0.452	35	10	26	34	10	25	252638.100	0.01519	
34	19	16	33	19	15	246544.871	-0.00987	0.5	35	22	14	34	22	13	252767.941	-0.01124	0.5
34	19	15	33	19	14	246544.871	-0.01072	0.5	35	22	13	34	22	12	252767.941	-0.01124	0.5
38	4	34	37	4	33	246591.347	0.00464	0.04	35	21	14	34	21	13	253135.148	-0.02388	0.5
38	5	34	37	4	33	246591.347	0.00458	0.04	35	21	15	34	21	14	253135.148	-0.02387	0.5
38	4	34	37	5	33	246591.347	0.00481	0.04	35	9	26	34	9	25	253447.777	-0.02259	
38	5	34	37	5	33	246591.347	0.00474	0.46	36	9	28	35	9	27	253533.993	0.00872	
34	10	25	33	10	24	246686.774	-0.01775		35	20	15	34	20	14	253563.561	-0.026	0.5
34	18	17	33	18	16	247093.368	0.00707	0.5	35	20	16	34	20	15	253563.561	-0.02587	0.5
34	18	16	33	18	15	247093.368	-0.00838	0.5	36	8	28	35	8	27	253586.171	0.00265	
35	9	27	34	9	26	247673.712	-0.00284		23	12	12	22	11	12	253846.603	-0.03714	
34	17	18	33	17	17	247759.830	0.0996	0.5	30	4	37	39	3	36	253918.035	-0.00078	0.4575
34	17	17	33	17	16	247759.830	-0.16704	0.5	40	3	37	39	4	36	253918.035	-0.00078	0.0425
35	8	27	34	8	26	247777.901	-0.0171		40	4	37	39	3	36	253918.035	-0.00078	0.0425
21	13	9	20	12	8	247901.712	0.07539	0.2116	40	4	37	39	4	36	253918.035	-0.00078	0.4575
21	13	8	20	12	8	247901.712	0.05829	0.2884	35	19	16	34	19	15	254069.387	-0.02927	0.5
21	13	9	20	12	9	247901.712	-0.0459	0.2884	35	19	17	34	19	16	254069.387	-0.02657	0.5
21	13	8	20	12	9	247901.712	-0.06301	0.2116	34	13	21	33	13	20	254286.794	0.00943	
39	3	36	38	3	35	247983.472	0.01559	0.4576	33	11	22	32	11	21	254432.913	0.03324	
39	3	36	38	4	35	247983.472	0.01559	0.0424	37	8	30	36	8	29	254566.340	0.01918	
39	4	36	38	3	35	247983.472	0.01559	0.0424	37	7	30	36	7	29	254568.423	-0.00488	
39	4	36	38	4	35	247983.472	0.01559	0.4576	71	11	60	71	11	61	254629.946	-0.00175	0.3295
34	9	25	33	9	24	248101.487	0.00776		71	12	60	71	10	61	254629.946	-0.00175	0.3295
34	16	19	33	16	18	248586.906	-0.01687		71	12	60	71	11	61	254629.946	-0.00175	0.1705
34	16	18	33	16	17	248590.468	-0.03239		71	11	60	71	10	61	254629.946	-0.00175	0.1705
36	8	29	35	8	28	248670.450	0.00274		35	18	18	34	18	17	254675.440	-0.0243	0.5
36	7	29	35	7	28	248674.995	-0.02166		35	18	17	34	18	16	254675.440	-0.0722	0.5
20	14	7	19	13	6	248693.596	0.04042	0.2208	22	13	10	21	12	9	254953.817	0.21914	0.2076
20	14	6	19	13	6	248693.596	0.04031	0.2792	22	13	9	21	12	9	254953.817	0.15463	0.2924
20	14	7	19	13	7	248693.596	0.03952	0.2792	22	13	10	21	12	10	254953.817	-0.21055	0.2924
20	14	6	19	13	7	248693.596	0.03941	0.2208	22	13	9	21	12	10	254953.817	-0.27506	0.2076
27	9	18	26	8	18	249375.730	0.00875		41	2	39	40	2	38	255327.024	-0.01355	0.4555
19	15	5	18	14	4	249388.620	-0.03303	0.2286	41	2	39	40	3	38	255327.024	-0.01355	0.0445
19	15	5	18	14	5	249388.620	-0.03304	0.2714	41	3	39	40	2	38	255327.024	-0.01355	0.0445
19	15	4	18	14	4	249388.620	-0.03303	0.2714	41	3	39	40	3	38	255327.024	-0.01355	0.4555
19	15	4	18	14	5	249388.620	-0.03304	0.2286	35	17	19	34	17	18	255415.186	0.05006	
40	2	38	39	2	37	249392.764	0.00018	0.4556	38	7	32	37	6	31	255778.616	-0.08411	0.0351
40	2	38	39	3	37	249392.764	0.00018	0.0444	38	6	32	37	6	31	255778.616	-0.04079	0.4649
40	3	38	39	2	37	249392.764	0.00018	0.0444	38	7	32	37	7	31	255778.616	0.0174	0.4649
40	3	38	39	3	37	249392.764	0.00018	0.4556	38	6	32	37	7	31	255778.616	0.06072	0.0351
34	15	20	33	15	19	249634.953	-0.04861		21	14	8	20	13	7	255804.036	0.00266	0.2175
34	15	19	33	15	18	249673.914	-0.0493		21	14	7	20	13	7	255804.036	0.00214	0.2825
37	6	31	36	7	30	249860.226	0.15834	0.0346	21	14	8	20	13	8	255804.036	-0.00147	0.2825
37	7	31	36	7	30	249860.226	0.05683	0.4654	21	14	7	20	13	8	255804.036	-0.002	0.2175
37	6	31	36	6	30	249860.226	-0.07753	0.4654	34	10	24	33	10	23	256273.136	0.0083	
37	7	31	36	6	30	249860.226	-0.17904	0.0346	35	16	20	34	16	19	256338.184	-0.0169	
18	16	2	17	15	3	250038.395	0.0162	0.2347	35	16	19	34	16	18	256346.880	-0.04292	
18	16	3	17	15	2	250038.395	0.0162	0.2347	26	9	18	25	8	18	256392.246	0.00814	
18	16	3	17	15	3	250038.395	0.0162	0.2653	20	15	6	19	14	5	256528.699	0.0154	0.2256
18	16	2	17	15	2	250038.395	0.0162	0.2653	20	15	6	19	14	6	256528.699	0.01538	0.2744
33	12	21	32	12	20	250138.724	0.04139		20	15	5	19	14	5	256528.699	0.0154	0.2744
17	17	1	16	16	0	250668.163	0.01461	0.2395	20	15	5	19	14	6	256528.699	0.01538	0.2256
17	17	1	16	16	1	250668.163	0.01461	0.2605	42	1	41	41	1	40	256742.179	0.0096	0.4535
17	17	0	16	16	0	250668.163	0.01461	0.2605	42	1	41	41	2	40	256742.179	0.0096	0.0465
17	17	0	16	16	1	250668.163	0.01461	0.2395	42	2	41	41	1	40	256742.179	0.0096	0.0465
34	11	24	33	11	23	250675.170	-0.00235		42	2	41	41	2	40	256742.179	0.0096	0.4535
41	1	40	40	1	39	250808.996	-0.01565	0.4536	35	11	25	34	11	24	257078.516	0.01538	
41	1	40	40	2	39	250808.996	-0.01565	0.0464	39	5	34	38	5	33	257091.014	0.0032	0.462
41	2	40	40	1	39	250808.996	-0.01565	0.0464	39	6	34	38	5	33	257091.014	0.00243	0.038
41	2	40	40	2	39	250808.996	-0.01565	0.4536	39	5	34	38	6	33	257091.014	0.00511	0.038
34	14	21	33	14	20	250936.323	-0.03373		39	6	34	38	6	33	257091.014	0.00434	0.462
35	30	6	34	30	5	251046.848	-0.04398	0.5	19	16	3	18	15	4	257192.602	-0.00783	0.2321
35	30	5	34	30	4	251046.848	-0.04398	0.5	19	16	4	18	15	3	257192.602	-0.00783	0.2321
38	6	33	37	5	32	251162.559	-0.02051	0.0377	19	16	4	18	15	4	257192.602	-0.00783	0.2679
38	5	33	37	6	32	251162.559	-0.01394	0.0377	19	16	3	18	15	3	257192.602	-0.00783	0.2679
38	6	33	37	6	32	251162.559	-0.01585	0.4623	27	8	19	26	7	19	257335.611	-0.01291	
38	5	33	37	5	32	251162.559	-0.0186	0.4623	35	15	21	34	15	20	257506.575	-0.00242	
35	29	6	34	29	5	251188.530	-0.0332	0.5	35	15	20	34	15	19	257592.914	-0.03561	
35	29	7	34	29	6	251188.530	-0.0332	0.5	26	8	19	25	7	19	257618.258	0.01098	
33	10	23	32	10	22	251207.891	0.01873		18	17	2	17	16	1	257828.025	0.0007	0.2375
34</																	

Comprehensive analysis of Isobutyraldehyde: millimetre-wave spectroscopy as an approach to ISM detection

36	27	9	35	27	8	258829.324	0.02036	0.5	37	30	7	36	30	6	265595.489	-0.04099	0.5
35	14	22	34	14	21	258900.918	-0.01221		18	18	1	17	17	0	265611.589	-0.03979	0.2396
36	9	27	35	9	26	258972.059	0.01837		18	18	1	17	17	1	265611.589	-0.03979	0.2604
36	26	10	35	26	9	259039.637	0.03753	0.5	18	18	0	17	17	0	265611.589	-0.03979	0.2604
36	26	11	35	26	10	259039.637	0.03753	0.5	18	18	0	17	17	1	265611.589	-0.03979	0.2396
36	25	11	35	25	10	259275.621	0.01851	0.5	36	15	21	35	15	20	265615.985	-0.03721	
36	25	12	35	25	11	259275.621	0.01851	0.5	37	29	8	36	29	7	265762.384	0.01198	0.5
37	8	29	36	9	28	259374.299	0.04911		37	29	9	36	29	8	265762.384	0.01198	0.5
37	9	29	36	9	28	259397.589	0.00702		42	3	39	41	3	38	265783.688	-0.00738	0.457
37	8	29	36	8	28	259423.214	0.00502		42	3	39	41	4	38	265783.688	-0.00738	0.043
36	24	12	35	24	11	259542.165	0.01495	0.5	42	4	39	41	3	38	265783.688	-0.00738	0.043
36	24	13	35	24	12	259542.165	0.01495	0.5	42	4	39	41	4	38	265783.688	-0.00738	0.457
35	14	21	34	14	20	259561.204	-0.01339		36	10	26	35	10	25	265857.820	-0.00588	
34	12	22	33	12	21	259731.684	0.02733		37	28	9	36	28	8	265946.683	0.00434	0.5
35	12	24	34	12	23	259754.693	0.016		37	28	10	36	28	9	265946.683	0.00434	0.5
36	23	14	35	23	13	259845.271	-0.04961	0.5	27	9	19	26	8	19	265978.160	-0.02212	
36	23	13	35	23	12	259845.271	-0.04961	0.5	37	27	11	36	27	10	266151.377	0.04204	0.5
41	3	38	40	3	37	259851.478	0.01412	0.4776	37	27	10	36	27	9	266151.377	0.04204	0.5
41	4	38	40	3	37	259851.478	0.01412	0.0448	27	7	20	26	6	20	266303.901	0.00339	
41	4	38	40	4	37	259851.478	0.01412	0.4776	39	7	32	38	8	31	266369.575	0.56509	0.0331
35	13	23	34	13	22	260054.242	0.00905		39	8	32	38	8	31	266369.575	0.22308	0.4669
28	9	19	27	8	19	260065.453	0.00654		39	7	32	38	7	31	266369.575	-0.20869	0.4669
36	22	15	35	22	14	260192.872	-0.00669	0.5	39	8	32	38	7	31	266369.575	-0.55069	0.0331
36	22	14	35	22	13	260192.872	-0.00669	0.5	37	26	11	36	26	10	266379.878	0.03378	0.5
38	8	31	37	8	30	260466.189	0.00412		37	26	12	36	26	11	266379.878	0.03378	0.5
38	7	31	37	7	30	260467.141	-0.00374		37	25	12	36	25	11	266636.523	0.01695	0.5
25	1	24	24	0	24	260469.515	0.04106	0.5	37	25	13	36	25	12	266636.523	0.01695	0.5
25	2	24	24	1	24	260469.515	0.04089	0.5	36	12	25	35	12	24	266682.109	0.03711	
28	10	18	27	9	18	260522.532	-0.04678		36	14	23	35	14	22	266871.607	0.01625	
36	21	15	35	21	14	260594.903	-0.02319	0.5	37	24	13	36	24	12	266926.663	-0.0053	0.5
36	21	16	35	21	15	260594.903	-0.02317	0.5	37	24	14	36	24	13	266926.663	-0.0053	0.5
24	12	13	23	11	13	260733.039	0.01523		43	2	41	42	2	40	267191.714	0.01489	0.4552
35	10	25	34	10	24	261042.889	0.01318		43	2	41	42	3	40	267191.714	0.01489	0.0448
36	20	16	35	20	15	261064.901	-0.02727	0.5	43	3	41	42	2	40	267191.714	0.01489	0.0448
36	20	17	35	20	16	261064.901	-0.02684	0.5	43	3	41	42	3	40	267191.714	0.01489	0.4552
42	2	40	41	2	39	261260.039	0.01239	0.4553	37	23	15	36	23	14	267257.063	-0.01344	0.5
42	2	40	41	3	39	261260.039	0.01239	0.0447	37	23	14	36	23	13	267257.063	-0.01344	0.5
42	3	40	41	2	39	261260.039	0.01239	0.0447	27	10	18	26	9	18	267300.938	-0.03916	
42	3	40	41	3	39	261260.039	0.01239	0.4553	27	11	17	26	10	16	267321.473	0.03408	
36	19	17	35	19	16	261621.344	-0.02411	0.5	25	12	14	24	11	14	267562.007	-0.02553	
36	19	18	35	19	17	261621.344	-0.01591	0.5	40	7	34	39	6	33	267618.172	-0.00275	0.036
39	7	33	38	6	32	261698.082	-0.00457	0.0355	40	6	34	39	6	33	267618.172	0.00496	0.464
39	6	33	38	6	32	261698.082	0.01377	0.4645	40	7	34	39	7	33	267618.172	0.01559	0.464
39	7	33	38	7	32	261698.082	0.03875	0.4645	40	6	34	39	7	33	267618.172	0.0233	0.036
39	6	33	38	7	32	261698.082	0.05709	0.0355	64	4	60	64	4	61	267634.267	-0.00071	0.3421
23	13	10	22	12	10	261972.412	0.00418		64	5	60	64	3	61	267634.267	-0.00071	0.3421
23	13	11	22	12	11	261973.583	-0.00473		64	5	60	64	4	61	267634.267	-0.00071	0.1579
25	9	16	24	8	17	262006.043	0.00872		64	4	60	64	3	61	267634.267	-0.00071	0.1579
34	11	23	33	11	22	262076.391	0.0338		37	22	16	36	22	15	267636.366	-0.0169	0.5
36	18	19	35	18	18	262290.547	0.02066	0.5	37	22	15	36	22	14	267636.366	-0.0169	0.5
36	18	18	35	18	17	262290.547	-0.11293	0.5	29	10	19	28	9	19	267671.425	0.00643	
43	1	42	42	1	41	262673.988	0.01266	0.4535	36	13	24	35	13	23	267725.683	0.01568	
43	1	42	42	2	41	262673.988	0.01266	0.0465	26	3	23	25	2	23	267862.182	0.05256	0.5
43	2	42	42	1	41	262673.988	0.01266	0.0465	26	4	23	25	3	23	267862.182	-0.06352	0.5
43	2	42	42	2	41	262673.988	0.01266	0.4535	71	9	62	71	9	63	267966.743	-0.05081	0.334
50	18	32	49	19	31	262717.973	-0.04912		71	10	62	71	8	63	267966.743	-0.05081	0.334
22	14	8	21	13	8	262896.006	-0.02096	0.2855	71	10	62	71	9	63	267966.743	-0.05081	0.166
22	14	9	21	13	9	262896.006	-0.03576	0.2855	71	9	62	71	8	63	267966.743	-0.05081	0.166
22	14	8	21	13	9	262896.006	-0.03806	0.2145	37	21	16	36	21	15	268075.882	-0.03779	0.5
22	14	9	21	13	8	262896.006	-0.01866	0.2145	37	21	17	36	21	16	268075.882	-0.03773	0.5
40	5	35	39	6	34	263019.098	0.00643	0.0383	36	14	22	35	14	21	268117.654	0.00759	
40	6	35	39	6	34	263019.098	0.00611	0.4617	27	8	20	26	7	20	268146.365	-0.01386	
40	5	35	39	5	34	263019.098	0.00565	0.4617	74	11	63	74	11	64	268363.529	0.00415	0.3307
40	6	35	39	5	34	263019.098	0.00533	0.0383	74	12	63	74	10	64	268363.529	0.00415	0.3307
36	17	20	35	17	19	263111.323	-0.00924		74	12	63	74	11	64	268363.529	0.00415	0.1693
36	11	26	35	11	25	263276.914	0.02553		74	11	63	74	10	64	268363.529	0.00415	0.1693
21	15	7	20	14	6	263658.356	-0.00011	0.2229	37	20	17	36	20	16	268590.867	-0.04432	0.5
21	15	6	20	14	6	263658.356	-0.00012	0.2771	37	20	18	36	20	17	268590.867	-0.04297	0.5
21	15	6	20	14	7	263658.356	-0.00023	0.2229	44	1	43	43	1	42	268604.401	0.00181	0.4534
21	15	7	20	14	7	263658.356	-0.00022	0.2771	44	1	43	43	2	42	268604.401	0.00181	0.0466
26	11	15	25	10	15	263834.777	-0.01001		44	2	43	43	1	42	268604.401	0.00181	0.0466
44	0	44	43	0	43	264087.815	-0.00857	0.4519	44	2	43	43	2	42	268604.401	0.00181	0.4534
44	0	44	43	1	43	264087.815	-0.00857	0.0481	35	11	24	34	11	23	268705.779	0.0229	
44	1	44	43	0	43	264087.815	-0.00857	0.0481	41	5	36	40	6	35	268946.680	0.00526	0.0386
44	1	44	43	1	43	264087.815	-0.00857	0.4519	41	6	36	40	6	35	268946.680	0.00513	0.4614
36	16	21	35	16	20	264140.416	-0.01145		41	5	36	40	5	35	268946.680	0.00495	0.4614
36	16	20	35	16	19	264160.816	-0.04232		41	6	36	40	5	35	268946.680	0.00482	0.0386
20	16	4	19	15	5	264341.407	0.02413	0.2297	24	13	11	23	12	11	268950.701	0.03982	
20	16	5	19														



Comprehensive analysis of Isobutyraldehyde: millimetre-wave spectroscopy as an approach to ISM detection

38	9	29	37	10	28	270101.518	-0.02724			46	1	46	45	0	45	275944.039	0.02209	0.0482
28	8	20	27	7	20	270194.036	0.00554			46	1	46	45	1	45	275944.039	0.02209	0.4518
38	10	29	37	10	28	270224.423	-0.00635			39	10	30	38	10	29	276064.729	0.00738	
42	4	38	41	4	37	270318.917	0.01198	0.4591		39	9	30	38	9	29	276127.297	0.00483	
42	4	38	41	5	37	270318.917	0.01198	0.0409		38	20	18	37	20	17	276142.921	-0.04157	0.5
42	5	38	41	4	37	270318.917	0.01198	0.0409		38	20	19	37	20	18	276142.921	-0.03749	0.5
42	5	38	41	5	37	270318.917	0.01198	0.4591		38	10	28	37	10	27	276164.258	0.00181	
38	9	29	37	9	28	270347.645	-0.00943			43	4	39	42	4	38	276248.296	0.01343	0.4589
22	15	8	21	14	7	270775.228	0.03135	0.2196		43	4	39	42	5	38	276248.296	0.01343	0.0411
22	15	7	21	14	8	270775.228	0.03076	0.2196		43	5	39	42	4	38	276248.296	0.01343	0.0411
22	15	8	21	14	8	270775.228	0.03082	0.2804		43	5	39	42	5	38	276248.296	0.01343	0.4589
22	15	7	21	14	7	270775.228	0.03128	0.2804		27	5	23	26	4	23	276441.632	-0.57728	0.5
37	17	21	36	17	20	270851.699	-0.01715			27	4	23	26	3	23	276441.632	0.54995	0.5
37	17	20	36	17	19	270856.161	-0.03616			30	10	20	29	9	20	276634.894	-0.02055	
37	10	27	36	10	26	270890.959	0.00607			38	19	20	37	19	19	276814.636	-0.02047	0.5
27	6	21	26	5	21	271082.285	0.00169			38	19	19	37	19	18	276814.636	-0.08715	0.5
39	8	31	38	9	30	271136.895	-0.00429			40	9	32	39	9	31	277022.933	0.01159	
39	9	31	38	9	30	271141.991	0.0054			40	8	32	39	8	31	277025.695	0.01903	
39	8	31	38	8	30	271147.867	0.00423			37	14	23	36	14	22	277028.857	0.05295	
21	16	5	20	15	6	271483.001	-0.00898	0.227		38	18	21	37	18	20	277629.587	-0.02194	
21	16	6	20	15	5	271483.001	-0.00898	0.227		44	3	41	43	3	40	277644.393	-0.00321	0.4569
21	16	6	20	15	6	271483.001	-0.00898	0.273		44	3	41	43	4	40	277644.393	-0.00321	0.0431
21	16	5	20	15	5	271483.001	-0.00898	0.273		44	4	41	43	3	40	277644.393	-0.00321	0.0431
43	3	40	42	3	39	271714.695	0.0084	0.4572		44	4	41	43	4	40	277644.393	-0.00321	0.4569
43	3	40	42	4	39	271714.695	0.0084	0.0428		36	12	24	35	12	23	277664.938	0.04492	
43	4	40	42	3	39	271714.695	0.0084	0.0428		28	7	21	27	6	21	277796.653	-0.04059	
43	4	40	42	4	39	271714.695	0.0084	0.4572		23	15	9	22	14	8	277876.439	-0.00614	0.2162
37	16	22	36	16	21	271996.704	-0.01583			23	15	8	22	14	8	277876.439	-0.00644	0.2838
37	16	21	36	16	20	272042.715	-0.02468			23	15	9	22	14	9	277876.439	-0.00845	0.2838
20	17	4	19	16	3	272139.395	-0.0073	0.2327		23	15	8	22	14	9	277876.439	-0.00874	0.2162
20	17	4	19	16	4	272139.395	-0.0073	0.2673		29	11	18	28	10	18	277884.143	0.00743	
20	17	3	19	16	3	272139.395	-0.0073	0.2673		41	8	34	40	7	33	278183.089	-0.11466	0.0339
20	17	3	19	16	4	272139.395	-0.0073	0.2327		41	7	34	40	7	33	278183.089	-0.04963	0.4661
29	9	20	28	8	20	272182.592	0.00634			41	8	34	40	8	33	278183.089	0.03511	0.4661
40	8	33	39	7	32	272275.269	-0.24103	0.0335		41	7	34	40	8	33	278183.089	0.10014	0.0339
40	7	33	39	7	32	272275.269	-0.09126	0.4665		27	3	24	26	2	24	278363.062	0.02596	0.5
40	8	33	39	8	32	272275.269	0.10097	0.4665		27	4	24	26	3	24	278363.062	-0.02133	0.5
40	7	33	39	8	32	272275.269	0.25075	0.0335		22	16	6	21	15	7	278615.629	0.00849	0.2239
38	31	7	37	31	6	272718.428	-0.05402	0.5		22	16	7	21	15	6	278615.629	0.00851	0.2239
38	31	8	37	31	7	272718.428	-0.05402	0.5		22	16	7	21	15	7	278615.629	0.0085	0.2761
19	18	2	18	17	1	272770.555	-0.00528	0.2376		22	16	6	21	15	6	278615.629	0.00851	0.2761
19	18	2	18	17	2	272770.555	-0.00528	0.2624		38	17	22	37	17	21	278639.878	-0.04751	
19	18	1	18	17	1	272770.555	-0.00528	0.2624		38	17	21	37	17	20	278650.511	-0.03178	
19	18	1	18	17	2	272770.555	-0.00528	0.2376		45	2	43	44	2	42	279050.949	-0.00353	0.455
38	30	9	37	30	8	272882.618	0.00313	0.5		45	2	43	44	3	42	279050.949	-0.00353	0.045
38	30	8	37	30	7	272882.618	0.00313	0.5		45	3	43	44	2	42	279050.949	-0.00353	0.045
27	11	17	26	10	17	272977.800	0.00889			45	3	43	44	3	42	279050.949	-0.00353	0.455
38	29	9	37	29	8	273063.200	0.0276	0.5		21	17	5	20	16	4	279288.403	0.00586	0.2303
38	29	10	37	29	9	273063.200	0.0276	0.5		21	17	5	20	16	5	279288.403	0.00586	0.2697
44	2	42	43	2	41	273122.019	0.00081	0.4552		21	17	4	20	16	4	279288.403	0.00586	0.2697
44	2	42	43	3	41	273122.019	0.00081	0.0448		21	17	4	20	16	5	279288.403	0.00586	0.2303
44	3	42	43	2	41	273122.019	0.00081	0.0448		37	11	26	36	11	25	279360.026	0.00558	
44	3	42	43	3	41	273122.019	0.00081	0.4552		42	7	36	41	7	35	279459.252	0.0002	0.4633
38	28	10	37	28	9	273262.809	0.03361	0.5		42	6	36	41	6	35	279459.252	-0.00169	0.4633
38	28	11	37	28	10	273262.809	0.03361	0.5		42	7	36	41	6	35	279459.252	-0.00302	0.0367
37	12	26	36	12	25	273335.423	0.01086			42	6	36	41	7	35	279459.252	0.00153	0.0367
37	15	23	36	15	22	273405.291	-0.00582			64	2	62	64	2	63	279579.394	-0.01959	0.3447
38	27	12	37	27	11	273484.618	0.03387	0.5		64	3	62	64	1	63	279579.394	-0.01959	0.3447
38	27	11	37	27	10	273484.618	0.03387	0.5		64	3	62	64	2	63	279579.394	-0.01959	0.1553
41	7	35	40	7	34	273538.648	0.00431	0.4637		64	2	62	64	1	63	279579.394	-0.01959	0.1553
41	6	35	40	6	34	273538.648	-0.00019	0.4637		38	12	27	37	12	26	279737.276	0.00581	
41	7	35	40	6	34	273538.648	-0.0034	0.0363		38	16	23	37	16	22	279908.594	-0.02065	
41	6	35	40	7	34	273538.648	0.00752	0.0363		20	18	3	19	17	2	279927.225	-0.0106	0.2354
28	11	17	27	10	17	273643.452	-0.02293			20	18	3	19	17	3	279927.225	-0.0106	0.2646
38	26	12	37	26	11	273732.482	0.03636	0.5		20	18	2	19	17	2	279927.225	-0.0106	0.2646
38	26	13	37	26	12	273732.482	0.03636	0.5		20	18	2	19	17	3	279927.225	-0.0106	0.2354
37	15	22	36	15	21	273779.721	-0.00185			39	31	8	38	31	7	280001.333	-0.03831	0.5
38	25	13	37	25	12	274011.101	0.00553	0.5		39	31	9	38	31	8	280001.333	-0.03831	0.5
38	25	14	37	25	13	274011.101	0.00553	0.5		38	16	22	37	16	21	280008.339	0.00124	
26	12	14	25	11	14	274051.751	-0.0036			39	30	10	38	30	9	280178.565	-0.00432	0.5
38	24	14	37	24	13	274326.450	0.0073	0.5		39	30	9	38	30	8	280178.565	-0.00432	0.5
38	24	15	37	24	14	274326.450	0.0073	0.5		28	11	18	27	10	18	280201.357	-0.03554	
26	12	15	25	11	15	274336.863	0.00463			39	29	10	38	29	9	280373.670	0.03292	0.5
36	11	25	35	11	24	274382.669	0.03843			39	29	11	38	29	10	280373.670	0.03292	0.5
45	2	44	44	2	43	274533.403	-0.00624	0.4534		27	12	15	26	11	15	280451.528	-0.0028	
45	1	44	44	1	43	274533.403	-0.00624	0.4534		46	1	45	45	1	44	280460.995	0.01991	0.4533
45	1	44	44	2	43	274533.403	-0.0											



Comprehensive analysis of Isobutyraldehyde: millimetre-wave spectroscopy as an approach to ISM detection

27	12	15	26	11	16	281269.737	0.02192			40	10	30	39	10	29	287232.927	0.0303	
39	25	14	38	25	13	281399.898	0.00516	0.5		40	31	9	39	31	8	287292.677	0.00603	0.5
39	25	15	38	25	14	281399.898	0.00516	0.5		40	31	10	39	31	9	287292.677	0.00603	0.5
38	15	24	37	15	23	281409.454	-0.00227			40	29	11	39	29	10	287694.122	0.04507	0.5
39	10	29	38	10	28	281630.782	0.02008			40	29	12	39	29	11	287694.122	0.04507	0.5
39	24	15	38	24	14	281742.087	-0.00409	0.5		20	19	1	19	18	2	287707.493	-0.01577	0.2376
39	24	16	38	24	15	281742.087	-0.00409	0.5		20	19	2	19	18	1	287707.493	-0.01577	0.2376
47	0	47	46	0	46	281869.892	-0.00868	0.4518		20	19	2	19	18	2	287707.493	-0.01577	0.2624
47	0	47	46	1	46	281869.892	-0.00868	0.0482		20	19	1	19	18	1	287707.493	-0.01577	0.2624
47	1	47	46	0	46	281869.892	-0.00868	0.0482		41	9	32	40	10	31	287746.231	0.04648	
47	1	47	46	1	46	281869.892	-0.00868	0.4518		41	10	32	40	10	31	287760.092	0.01478	
40	9	31	39	10	30	281879.967	0.01627			41	9	32	40	9	31	287775.340	0.00529	
28	6	22	27	5	22	281899.565	0.06078			41	10	32	40	9	31	287789.253	0.02623	
40	10	31	39	10	30	281909.116	0.01651			48	0	48	47	0	47	287794.257	-0.01231	0.4518
40	9	31	39	9	30	281940.268	0.00499			48	0	48	47	1	47	287794.257	-0.01231	0.0482
28	7	22	27	6	22	282010.722	-0.02159			48	1	48	47	0	47	287794.257	-0.01231	0.0482
39	23	17	38	23	16	282132.718	-0.03202	0.5		48	1	48	47	1	47	287794.257	-0.01231	0.4518
39	23	16	38	23	15	282132.718	-0.03202	0.5		28	12	17	27	11	17	287804.674	-0.0116	
38	15	23	37	15	22	282139.845	0.02174			31	11	20	30	10	20	287825.049	-0.00227	
44	4	40	43	4	39	282176.544	0.01728	0.4587		39	16	24	38	16	23	287874.326	0.0091	
44	4	40	43	5	39	282176.544	0.01728	0.0413		40	28	12	39	28	11	287927.071	0.04465	0.5
44	5	40	43	4	39	282176.544	0.01728	0.0413		40	28	13	39	28	12	287927.071	0.04465	0.5
44	5	40	43	5	39	282176.544	0.01728	0.4587		39	16	23	38	16	22	288082.185	-0.01105	
30	11	19	29	10	19	282361.087	0.00649			45	4	41	44	4	40	288103.580	-0.00128	0.4585
38	13	26	37	13	25	282408.243	0.03786			45	4	41	44	5	40	288103.580	-0.00128	0.0415
39	22	18	38	22	17	282582.593	-0.05124	0.5		45	5	41	44	4	40	288103.580	-0.00128	0.0415
39	22	17	38	22	16	282582.593	-0.05127	0.5		45	5	41	44	5	40	288103.580	-0.00128	0.4585
38	14	25	37	14	24	282654.073	0.01019			40	27	14	39	27	13	288186.333	0.03261	0.5
29	8	21	28	7	21	282728.318	0.04557			40	27	13	39	27	12	288186.333	0.03261	0.5
26	13	14	25	12	13	282738.731	-0.0357			40	26	14	39	26	13	288476.556	0.02808	0.5
26	13	13	25	12	13	282745.036	0.03422			40	26	15	39	26	14	288476.556	0.02808	0.5
26	13	14	25	12	14	282771.227	-0.00648			39	11	28	38	11	27	288744.233	-0.00091	
41	9	33	40	9	32	282908.850	-0.00041			40	25	15	39	25	14	288803.437	-0.0106	0.5
41	8	33	40	8	32	282910.113	-0.01197			40	25	16	39	25	15	288803.437	-0.0106	0.5
39	21	18	38	21	17	283106.029	-0.05688	0.5		28	3	25	27	2	25	288859.121	0.02774	0.5
39	21	19	38	21	18	283106.029	-0.05621	0.5		28	4	25	27	3	25	288859.121	0.00864	0.5
45	3	42	44	3	41	283572.785	0.00059	0.4568		29	7	22	28	6	22	289004.229	-0.01144	
45	3	42	44	4	41	283572.785	0.00059	0.0432		40	24	16	39	24	15	289174.218	-0.05265	0.5
45	4	42	44	3	41	283572.785	0.00059	0.0432		40	24	17	39	24	16	289174.218	-0.05265	0.5
45	4	42	44	4	41	283572.785	0.00059	0.4568		39	13	27	38	13	26	289345.104	0.0286	
39	20	19	38	20	18	283722.606	-0.05877	0.5		39	15	25	38	15	24	289416.780	0.01301	
39	20	20	38	20	19	283722.606	-0.04691	0.5		29	8	22	28	7	22	289540.193	0.01184	
38	11	27	37	11	26	284029.148	0.02159			40	23	18	39	23	17	289598.210	-0.01118	
42	8	35	41	7	34	284092.512	-0.06022	0.0344		43	8	36	42	7	35	290003.117	-0.01439	0.0348
42	7	35	41	7	34	284092.512	-0.03221	0.4656		43	7	36	42	7	35	290003.117	-0.00241	0.4652
42	8	35	41	8	34	284092.512	0.00481	0.4656		43	8	36	42	8	35	290003.117	0.01362	0.4652
42	7	35	41	8	34	284092.512	0.03281	0.0344		43	7	36	42	8	35	290003.117	0.02559	0.0348
69	5	64	69	5	65	284146.194	-0.0406	0.3409		40	22	19	39	22	18	290087.325	-0.01273	0.5
69	6	64	69	4	65	284146.194	-0.0406	0.3409		40	22	18	39	22	17	290087.325	-0.01283	0.5
69	6	64	69	5	65	284146.194	-0.0406	0.1591		39	14	26	38	14	25	290350.763	0.03973	
69	5	64	69	4	65	284146.194	-0.0406	0.1591		28	2	26	27	1	26	290468.071	0.01244	0.5
39	19	21	38	19	20	284460.188	0.04238	0.5		28	3	26	27	2	26	290468.071	0.01192	0.5
39	19	20	38	19	19	284460.188	-0.13681	0.5		40	21	19	39	21	18	290657.698	-0.05288	0.5
28	6	23	27	5	23	284737.056	-0.0452			40	21	20	39	21	19	290657.698	-0.05086	0.5
29	10	20	28	9	20	284953.643	-0.02356			39	15	24	38	15	23	290774.841	0.03565	
24	15	10	23	14	9	284959.011	0.0095	0.213		47	2	45	46	2	44	290904.544	0.01221	0.4549
24	15	9	23	14	9	284959.011	0.00825	0.287		47	2	45	46	3	44	290904.544	0.01221	0.0451
24	15	10	23	14	10	284959.011	0.0003	0.287		47	3	45	46	2	44	290904.544	0.01221	0.0451
24	15	9	23	14	10	284959.011	-0.00096	0.213		47	3	45	46	3	44	290904.544	0.01221	0.4549
46	2	44	45	2	43	284978.464	-0.00368	0.455		26	14	12	25	13	12	290992.444	0.02362	
46	2	44	45	3	43	284978.464	-0.00368	0.045		26	14	13	25	13	13	290994.222	-0.01799	
46	3	44	45	2	43	284978.464	-0.00368	0.045		44	6	38	43	6	37	291300.018	0.0131	0.4626
46	3	44	45	3	43	284978.464	-0.00368	0.455		44	7	38	43	6	37	291300.018	0.01288	0.0374
30	9	21	29	8	21	285124.502	0.00179			44	6	38	43	7	37	291300.018	0.01365	0.0374
39	18	22	38	18	21	285359.475	-0.01609			44	7	38	43	7	37	291300.018	0.01343	0.4626
43	6	37	42	6	36	285379.790	0.02171	0.463		28	1	27	27	0	27	291867.179	-0.03239	0.5
43	7	37	42	6	36	285379.790	0.02116	0.037		28	2	27	27	1	27	291867.179	-0.0324	0.5
43	6	37	42	7	36	285379.790	0.02304	0.037		38	12	26	37	12	25	291939.480	0.03803	
43	7	37	42	7	36	285379.790	0.02249	0.463		40	12	29	39	12	28	291958.723	0.03171	
23	16	7	22	15	8	285737.136	-0.0055	0.221		25	15	11	24	14	10	292019.391	0.01911	0.2096
23	16	8	22	15	8	285737.136	-0.00549	0.279		25	15	10	24	14	10	292019.391	0.01422	0.2904
23	16	7	22	15	7	285737.136	-0.00543	0.279		25	15	11	24	14	11	292019.391	-0.01479	0.2904
23	16	8	22	15	7	285737.136	-0.00543	0.221		25	15	10	24	14	11	292019.391	-0.01968	0.2096
39	12	28	38	12	27	285928.428	0.02254			42	13	29	41	14	28	292116.423	-0.03679	
29	9	21	28	8	21	286322.204	-0.02866			40	19	22	39	19	21	292141.587	0.18172	0.5
47	1	46	46	1	45	286387.104	0.03831	0.4533		40	19	21	39	19	20	292141.587	-0.2824	0.5
47	1	46	46	2	45	286387.104	0.03831	0.0467										

Comprehensive analysis of Isobutyraldehyde: millimetre-wave spectroscopy as an approach to ISM detection

40	18	22	39	18	21	293139.503	-0.0327			41	21	21	40	21	20	298235.641	-0.03094	0.5
23	17	7	22	16	6	293565.707	-0.00417	0.2251		46	5	41	45	5	40	298573.117	0.00683	0.4601
23	17	7	22	16	7	293565.707	-0.00417	0.2749		46	5	41	45	6	40	298573.117	0.00683	0.0399
23	17	6	22	16	6	293565.707	-0.00417	0.2749		46	6	41	45	5	40	298573.117	0.00683	0.0399
23	17	6	22	16	7	293565.707	-0.00418	0.2251		46	6	41	45	6	40	298573.117	0.00683	0.4601
42	10	33	41	10	32	293618.246	0.00972			42	11	32	41	11	31	298600.791	0.02181	
42	9	33	41	9	32	293625.589	-0.00198			42	10	32	41	10	31	298674.473	0.00969	
40	11	29	39	11	28	293688.522	0.00063			42	11	32	41	10	31	298747.282	0.0067	
49	0	49	48	0	48	293717.085	-0.00859	0.4518		41	11	30	40	11	29	298888.386	0.01987	
49	0	49	48	1	48	293717.085	-0.00859	0.0482		26	15	12	25	14	11	299053.662	0.08096	0.206
49	1	49	48	0	48	293717.085	-0.00859	0.0482		26	15	11	25	14	11	299053.662	0.06332	0.294
49	1	49	48	1	48	293717.085	-0.00859	0.4518		26	15	12	25	14	12	299053.662	-0.035	0.294
46	4	42	45	4	41	294029.391	-0.00267	0.4584		26	15	11	25	14	12	299053.662	-0.05265	0.206
46	4	42	45	5	41	294029.391	-0.00267	0.0416		43	10	34	42	10	33	299483.204	0.00826	
46	5	42	45	4	41	294029.391	-0.00267	0.0416		43	9	34	42	9	33	299486.689	-0.00361	
46	5	42	45	5	41	294029.391	-0.00267	0.4584		50	0	50	49	0	49	299638.314	-0.029	0.4518
29	11	18	28	10	19	294138.076	-0.02711			50	0	50	49	1	49	299638.314	-0.029	0.0482
22	18	5	21	17	4	294229.495	-0.02403	0.2311		50	1	50	49	0	49	299638.314	-0.029	0.0482
22	18	5	21	17	5	294229.495	-0.02403	0.2689		50	1	50	49	1	49	299638.314	-0.029	0.4518
22	18	4	21	17	4	294229.495	-0.02403	0.2689		32	10	22	31	9	22	299695.800	-0.00873	
22	18	4	21	17	5	294229.495	-0.02403	0.2311		41	19	23	40	19	22	299861.210	-0.02325	
40	17	24	39	17	23	294373.585	-0.01103			25	16	9	24	15	10	299937.423	-0.06063	0.215
41	32	9	40	32	8	294405.282	-0.01302	0.5		25	16	10	24	15	9	299937.423	-0.0592	0.215
41	32	10	40	32	9	294405.282	-0.01302	0.5		25	16	9	24	15	9	299937.423	-0.05937	0.285
40	17	23	39	17	22	294426.986	-0.02177			25	16	10	24	15	10	299937.423	-0.06046	0.285
30	10	21	29	9	21	294546.053	-0.04055			47	4	43	46	4	42	299953.924	0.00905	0.4581
41	31	10	40	31	9	294592.646	0.01238	0.5		47	4	43	46	5	42	299953.924	0.00905	0.0419
41	31	11	40	31	10	294592.646	0.01238	0.5		47	5	43	46	4	42	299953.924	0.00905	0.0419
43	8	35	42	9	34	294692.690	0.36059	0.0323		47	5	43	46	5	42	299953.924	0.00905	0.4581
43	9	35	42	9	34	294692.690	0.14932	0.4677		30	8	23	29	7	23	300294.910	-0.00382	
43	8	35	42	8	34	294692.690	-0.11432	0.4677		44	9	36	43	8	35	300588.937	-0.13211	0.0329
43	9	35	42	8	34	294692.690	-0.32559	0.0323		44	8	36	43	8	35	300588.937	-0.03894	0.4671
30	8	22	29	7	22	294789.846	0.00007			44	9	36	43	9	35	300588.937	0.07915	0.4671
21	19	2	20	18	3	294863.252	-0.01656	0.2357		44	8	36	43	9	35	300588.937	0.17232	0.0329
21	19	3	20	18	2	294863.252	-0.01656	0.2357		42	39	3	41	39	2	300669.025	-0.01673	0.5
21	19	3	20	18	3	294863.252	-0.01656	0.2643		42	39	4	41	39	3	300669.025	-0.01673	0.5
21	19	2	20	18	2	294863.252	-0.01656	0.2643		24	17	8	23	16	7	300690.682	0.01432	0.2225
32	11	21	31	10	21	294882.669	0.003			24	17	8	23	16	8	300690.682	0.01432	0.2775
41	29	12	40	29	11	295024.863	0.0521	0.5		24	17	7	23	16	7	300690.682	0.01432	0.2775
41	29	13	40	29	12	295024.863	0.0521	0.5		24	17	7	23	16	8	300690.682	0.01431	0.2225
41	28	13	40	28	12	295275.930	0.03273	0.5		41	18	24	40	18	23	300956.925	-0.03314	
41	28	14	40	28	13	295275.930	0.03273	0.5		41	18	23	40	18	22	300969.585	-0.03079	
29	6	24	28	5	24	295329.259	0.00468			48	3	45	47	3	44	301349.632	0.00059	0.4565
47	3	44	46	3	43	295425.438	-0.00061	0.4565		48	3	45	47	4	44	301349.632	0.00059	0.0435
47	3	44	46	4	43	295425.438	-0.00061	0.0435		48	4	45	47	3	44	301349.632	0.00059	0.0435
47	4	44	46	3	43	295425.438	-0.00061	0.0435		48	4	45	47	4	44	301349.632	0.00059	0.4565
47	4	44	46	4	43	295425.438	-0.00061	0.4565		23	18	6	22	17	5	301372.688	-0.0198	0.2284
20	20	0	19	19	0	295481.727	-0.02192	0.2603		23	18	6	22	17	6	301372.688	-0.0198	0.2716
20	20	0	19	19	1	295481.727	-0.02192	0.2397		23	18	5	22	17	5	301372.688	-0.0198	0.2716
20	20	1	19	19	0	295481.727	-0.02192	0.2397		23	18	5	22	17	6	301372.688	-0.0198	0.2284
20	20	1	19	19	1	295481.727	-0.02192	0.2603		42	33	9	41	33	8	301516.214	-0.05515	0.5
41	27	15	40	27	14	295555.630	0.04125	0.5		42	33	10	41	33	9	301516.214	-0.05515	0.5
41	27	14	40	27	13	295555.630	0.04125	0.5		30	12	19	29	11	19	301519.586	-0.01992	
30	11	20	29	10	20	295803.494	-0.02426			42	32	10	41	32	9	301700.344	0.01758	0.5
41	26	15	40	26	14	295868.973	0.00865	0.5		42	32	11	41	32	10	301700.344	0.01758	0.5
41	26	16	40	26	15	295868.973	0.00865	0.5		45	7	38	44	7	37	301826.338	0.00793	0.4644
44	8	37	43	8	36	295914.494	0.01418	0.4648		45	8	38	44	7	37	301826.338	0.00579	0.0356
44	7	37	43	7	36	295914.494	0.00729	0.4648		45	7	38	44	8	37	301826.338	0.01302	0.0356
44	8	37	43	7	36	295914.494	0.00221	0.0352		45	8	38	44	8	37	301826.338	0.01087	0.4644
44	7	37	43	8	36	295914.494	0.01926	0.0352		22	19	3	21	18	4	302015.948	-0.00279	0.2335
40	13	28	39	13	27	296001.877	0.04676			22	19	4	21	18	3	302015.948	-0.00279	0.2335
73	6	67	73	6	68	296069.878	0.01739	0.3394		22	19	4	21	18	4	302015.948	-0.00279	0.2665
73	7	67	73	5	68	296069.878	0.01739	0.3394		22	19	3	21	18	3	302015.948	-0.00279	0.2665
73	7	67	73	6	68	296069.878	0.01739	0.1606		41	17	25	40	17	24	302323.315	0.01536	
73	6	67	73	5	68	296069.878	0.01739	0.1606		42	29	13	41	29	12	302366.211	0.03988	0.5
41	25	16	40	25	15	296222.312	-0.02597	0.5		42	29	14	41	29	13	302366.211	0.03988	0.5
41	25	17	40	25	16	296222.312	-0.02597	0.5		41	13	29	40	13	28	302401.198	0.03312	
40	16	24	39	16	23	296302.619	0.01296			40	12	28	39	12	27	302449.245	0.03621	
28	13	16	27	12	16	296357.392	-0.0158			42	28	14	41	28	13	302636.473	0.0417	0.5
41	24	17	40	24	16	296623.636	-0.04418	0.5		42	28	15	41	28	14	302636.473	0.0417	0.5
41	24	18	40	24	17	296623.636	-0.04418	0.5		21	20	1	20	19	1	302638.535	-0.02475	0.2625
48	2	46	47	2	45	296829.096	-0.01747	0.4548		21	20	1	20	19	2	302638.535	-0.02475	0.2375
48	2	46	47	3	45	296829.096	-0.01747	0.0452		21	20	2	20	19	1	302638.535	-0.02475	0.2375
48	3	46	47	2	45	296829.096	-0.01747	0.0452		21	20	2	20	19	2	302638.535	-0.02475	0.2625
48	3	46	47	3	45	296829.096	-0.01747	0.4548		29	13	16	28	12	16	302719.762	-0.01652	
30	9	22	29	8	22	296888.281	0.01595			49	2	47	48	2	46	302752.177	-0.	





Comprehensive analysis of Isobutyraldehyde: millimetre-wave spectroscopy as an approach to ISM detection

15	2	13	14	2	12	95436.9928	-0.0088		26	4	22	25	4	21	165738.684	-0.01098
14	3	11	13	3	10	95582.1109	0.01189		27	4	24	26	4	23	166905.148	-0.03344
17	0	17	16	0	16	97831.6282	-0.0581	0.5	28	3	26	27	3	25	168232.115	0.06037
17	1	17	16	1	16	97831.6282	0.04622	0.5	28	2	26	27	2	25	168232.115	0.0246
16	3	14	15	3	13	100724.127	-0.00207		29	2	28	28	2	27	169604.501	-0.01806
16	3	14	15	3	13	100724.129	0.00081		29	1	28	28	1	27	169604.501	-0.01839
16	2	14	15	2	13	100941.297	-0.01354		30	0	30	29	0	29	170991.482	0.01074
18	0	18	17	0	17	103460.248	-0.0195	0.5	30	1	30	29	1	29	170991.482	0.01074
18	1	18	17	1	17	103460.248	0.02557	0.5	27	5	23	26	5	22	171276.401	-0.02561
16	3	13	15	3	12	106324.691	-0.04074		27	4	23	26	4	22	171310.389	-0.00542
17	3	15	16	3	14	106375.04	-0.00658		29	2	27	28	2	26	173854.641	-0.01188
17	2	15	16	2	14	106491.197	0.00433		29	3	27	28	3	26	173854.641	0.00419
16	5	12	15	5	11	107050.32	0.01509		30	2	29	29	2	28	175229.875	-0.00048
18	2	17	17	2	16	107717.982	0.00295		30	1	29	29	1	28	175229.875	-0.00062
18	1	17	17	1	16	107720.551	-0.00524		27	5	22	26	5	21	176072.775	0.0339
19	0	19	18	0	18	109088.742	-0.01926	0.5	31	0	31	30	0	30	176617.725	-0.00734
19	1	19	18	1	18	109088.742	0.00008	0.5	31	1	31	30	1	30	176617.725	-0.00734
17	3	14	16	3	13	111585.862	-0.02251		28	5	24	27	5	23	176877.84	-0.02619
21	1	21	20	1	20	120345.418	0.03889	0.5	28	4	24	27	4	23	176895.354	0.01513
21	0	21	20	0	20	120345.418	0.03539	0.5	30	3	28	29	3	27	179477.246	-0.01133
20	3	18	19	3	17	123259.231	0.01811		30	2	28	29	2	27	179477.246	-0.0185
20	2	18	19	2	17	123274.524	0.05334		31	2	30	30	2	29	180855.021	0.00051
19	5	15	18	5	14	125665.746	-0.00262		31	1	30	30	1	29	180855.021	0.00045
22	1	22	21	1	21	125973.469	-0.00526	0.5	32	0	32	31	0	31	182243.752	0.00638
22	0	22	21	0	21	125973.469	-0.00674	0.5	32	1	32	31	1	31	182243.752	0.00638
20	4	17	19	4	16	127578.7	-0.00567		29	4	25	28	4	24	182488.769	-0.009
20	3	17	19	3	16	127806.149	-0.02393		31	2	29	30	2	28	185099.851	-0.01085
19	4	15	18	4	14	128158.187	-0.03461		31	3	29	30	3	28	185099.851	-0.00767
21	3	19	20	3	18	128880.322	-0.01881		32	2	31	31	2	30	186479.949	0.00795
21	2	19	20	2	18	128887.807	-0.00234		32	1	31	31	1	30	186479.949	0.00792
22	2	21	21	2	20	130222.901	0.04953	0.5	33	0	33	32	0	32	187869.492	-0.00898
22	1	21	21	1	20	130222.901	-0.06118	0.5	33	1	33	32	1	32	187869.492	-0.00898
20	5	16	19	5	15	131587.431	0.03479		30	5	26	29	5	25	188083.411	0.01472
23	1	23	22	1	22	131601.399	-0.00673	0.5	30	4	26	29	4	25	188087.803	-0.01124
23	0	23	22	0	22	131601.399	-0.00735	0.5	32	2	30	31	2	29	190722.375	-0.02383
21	4	18	20	4	17	133214.994	-0.01143		32	3	30	31	3	29	190722.375	-0.02243
20	4	16	19	4	15	133316.457	-0.01468		33	2	32	32	2	31	192104.607	-0.01528
21	3	18	20	3	17	133338.306	-0.03144		33	1	32	32	1	31	192104.607	-0.01529
22	3	20	21	3	19	134501.101	-0.03492		34	0	34	33	0	33	193494.992	0.00069
22	2	20	21	2	19	134504.766	0.02831		34	1	34	33	1	33	193494.992	0.00069
23	2	22	22	2	21	135849.126	0.05462	0.5	31	4	27	30	4	26	193690.665	-0.00214
23	1	22	22	1	21	135849.126	0.00537	0.5	32	4	29	31	4	28	194986.071	0.02539
24	0	24	23	0	23	137229.136	-0.02518	0.5	32	3	29	31	3	28	194986.071	-0.02163
24	1	24	23	1	23	137229.136	-0.02492	0.5	33	2	31	32	2	30	196344.815	-0.01683
21	5	17	20	5	16	137401.016	-0.02582		33	3	31	32	3	30	196344.815	-0.01621
16	5	11	15	4	11	138748.791	0.02286		34	2	33	33	2	32	197729.06	0.00821
22	4	19	21	4	18	138837.444	-0.01936		34	1	33	33	1	32	197729.06	0.00821
22	3	19	21	3	18	138902.659	0.02587		31	5	26	30	5	25	198131.033	0.0156
20	5	15	19	5	14	139165.855	0.02933		35	0	35	34	0	34	199120.201	-0.00672
23	3	21	22	3	20	140122.082	-0.03799		35	1	35	34	1	34	199120.201	-0.00672
24	2	23	23	2	22	141475.261	0.00774		32	5	28	31	5	27	199295.164	0.00823
25	1	25	24	1	24	142856.74	0.00763	0.5	32	4	28	31	4	27	199296.205	-0.01214
25	0	25	24	0	24	142856.74	0.00752	0.5	33	4	30	32	4	29	200603.759	-0.0007
22	5	18	21	5	17	143133.251	0.00985		33	3	30	32	3	29	200603.759	-0.02223
22	4	18	21	4	17	143811.698	0.0118		34	2	32	33	2	31	201967.113	-0.01261
23	3	20	22	3	19	144486.813	-0.02129		34	3	32	33	3	31	201967.113	-0.01235
21	5	16	20	5	15	144814.394	-0.02787		35	2	34	34	2	33	203353.236	0.01933
24	3	22	23	3	21	145743.474	0.00336		35	1	34	34	1	33	203353.236	0.01933
24	2	22	23	2	21	145744.317	0.03987		32	5	27	31	5	26	203704.312	0.02765
25	2	24	24	2	23	147101.389	0.0256	0.5	36	0	36	35	0	35	204745.153	0.01052
25	1	24	24	1	23	147101.389	0.01606	0.5	36	1	36	35	1	35	204745.153	0.01052
23	5	19	22	5	18	148808.829	0.00705		34	4	31	33	4	30	206221.715	-0.00115
23	4	19	22	4	18	149203.834	0.00619		34	3	31	33	3	30	206221.715	-0.01093
24	4	21	23	4	20	150066.119	0.01699		35	2	33	34	2	32	207589.253	0.00151
23	3	21	23	3	20	150083.194	-0.01132		35	3	33	34	3	32	207589.253	0.00162
22	5	17	21	5	16	150088.768	-0.01332		33	5	28	32	5	27	209286.694	-0.0288
25	3	23	24	3	22	151365.349	0.14683	0.5	37	0	37	36	0	36	210369.774	-0.01187
25	2	23	24	2	22	151365.349	-0.22836	0.5	37	1	37	36	1	36	210369.774	-0.01187
27	0	27	26	0	26	154111.264	-0.0146	0.5	34	4	30	33	4	29	210512.616	-0.01226
27	1	27	26	1	26	154111.264	-0.01458	0.5	34	5	30	33	5	29	210512.616	0.13174
24	5	20	23	5	19	154448.207	-0.00164		35	4	32	34	4	31	211839.842	0.01671
24	4	20	23	4	19	154670.375	0.02815		35	3	32	34	3	31	211839.842	0.0123
23	5	18	22	5	17	155174.167	0.00429		36	2	34	35	2	33	213211.218	0.03631
25	4	22	24	4	21	155678.558	0.03562		36	3	34	35	3	33	213211.218	0.03636
25	3	22	24	3	21	155687.057	-0.00636		37	2	36	36	2	35	214600.716	0.00959
26	3	24	25	3	23	156987.305	0.0437	0.5	37	1	36	36	1	35	214600.716	0.00959
26	2	24	25	2	23	156987.305	-0.12921	0.5	34	5	29	33	5	28	214875.439	-0.01205
27	2	26	26	2	25	158353.194	-0.05268	0.5	38	0	38	37	0	37	215994.117	-0.01473
27	1	26	26	1	25	158353.194	-0.05448	0.5	38	1	38	37	1	37	215994.117	-0.01473
28	0	28	27	0	27	159738.261	0.02609	0.5	36	4	33	35	4	32	217458.034	0.0198
28	1	28	27	1	27	159738.261	0.0261	0.5	36	3	33	35	3	32	217458.034	0.01782
25	5	21	24	5	20	160066.507	0.01669		37	2	35	36	2	34	218832.918	0.02664
25	4	21	24	4	20	160187.959	0.00018		37	3	35	36	3	34	218832.918	0.02666
24	5	19	23	5	18	160247.729	0.00915		38	2	37	37	2	36	220223.981	-0.02964
26	4	23	25	4	22	161291.411	-0.00703		38	1	37	37	1	36	220223.981	-0.02964
26	3	23	25													

Comprehensive analysis of Isobutyraldehyde: millimetre-wave spectroscopy as an approach to ISM detection

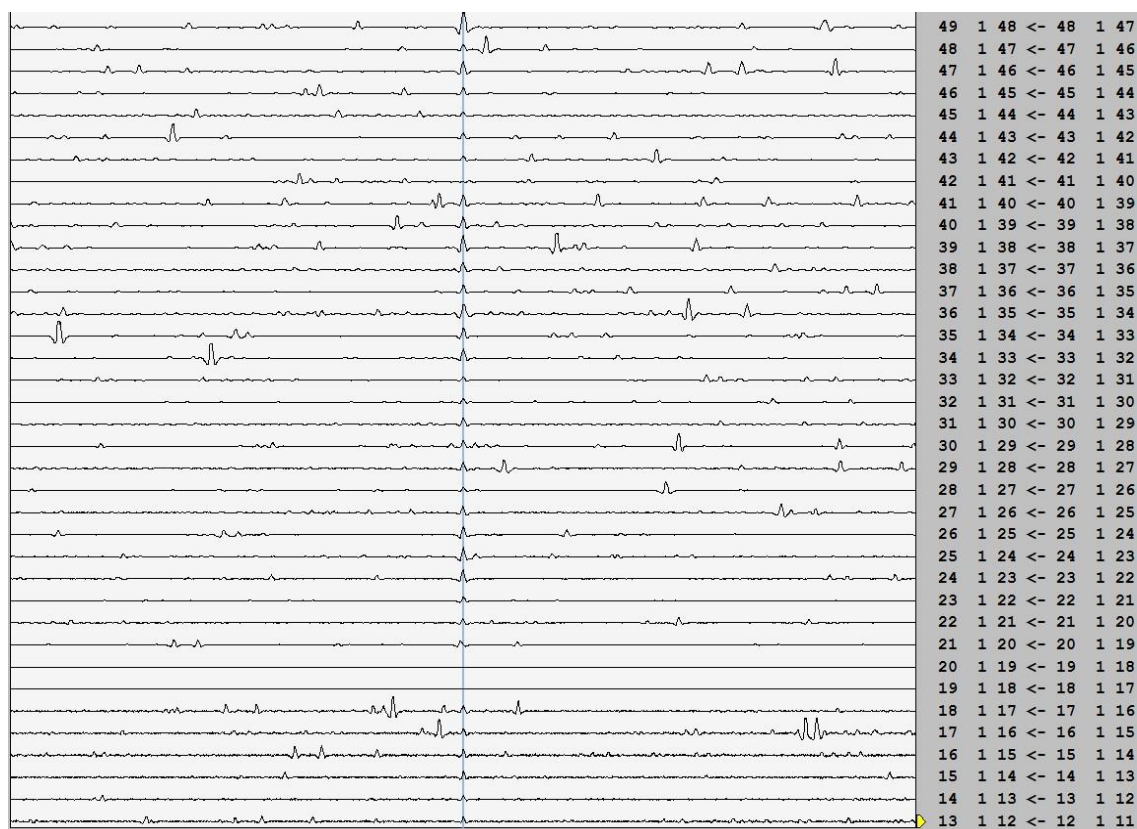
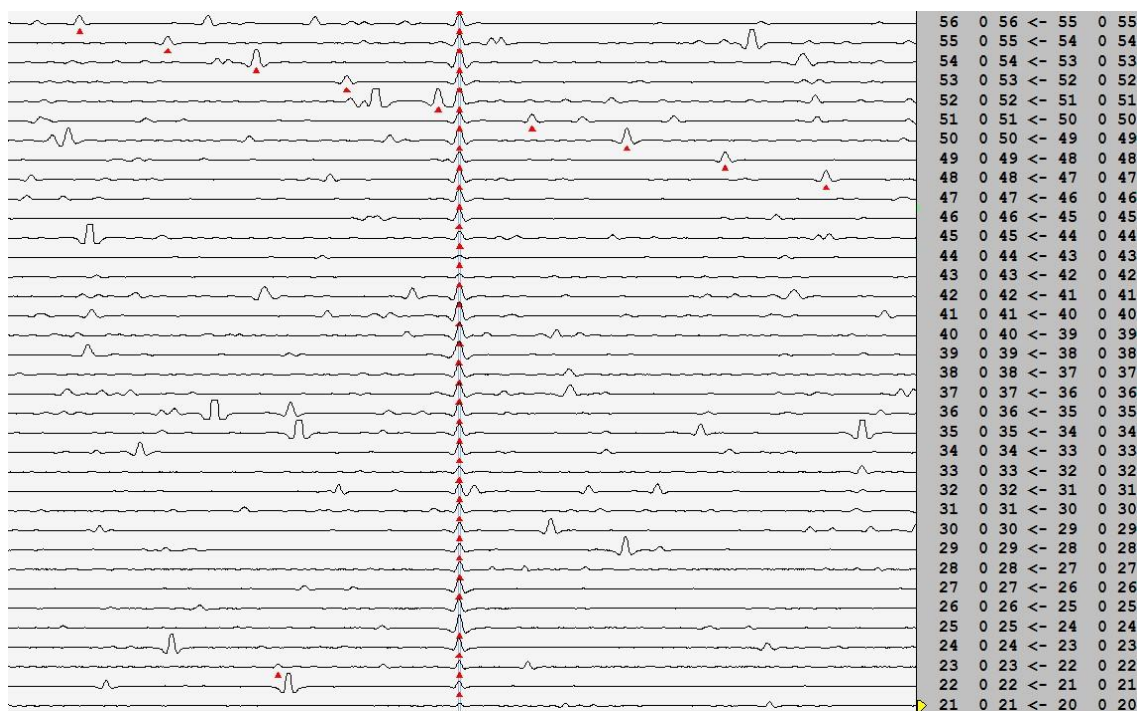
39	1	38	38	1	37	225846.995	-0.01217	0.5	46	5	42	45	5	41	277860.449	0.00076	0.5
39	2	38	38	2	37	225846.995	-0.01217	0.5	47	3	44	46	3	43	279249.672	-0.00516	0.5
36	5	31	35	5	30	226065.139	0.01207		47	4	44	46	4	43	279249.672	-0.00516	0.5
40	0	40	39	0	39	227241.936	0.03976	0.5	48	2	46	47	2	45	280652.201	0.01313	0.5
40	1	40	39	1	39	227241.936	0.03976	0.5	48	3	46	47	3	45	280652.201	0.01313	0.5
37	4	33	36	4	32	227345.423	-0.03172	0.5	49	2	48	48	2	47	282058.011	0.03529	0.5
37	5	33	36	5	32	227345.423	-0.00663	0.5	49	1	48	48	1	47	282058.011	0.03529	0.5
38	3	35	37	3	34	228694.402	0.02385	0.5	50	0	50	49	0	49	283460.086	0.0022	0.5
38	4	35	37	4	34	228694.402	0.02424	0.5	50	1	50	49	1	49	283460.086	0.0022	0.5
39	2	37	38	2	36	230075.567	-0.00424	0.5	47	4	43	46	4	42	283473.013	-0.01594	0.5
39	3	37	38	3	36	230075.567	-0.00423	0.5	47	5	43	46	5	42	283473.013	-0.01593	0.5
40	2	39	39	2	38	231469.671	-0.01585	0.5	48	3	45	47	3	44	284865.545	0.02225	0.5
40	1	39	39	1	38	231469.671	-0.01585	0.5	48	4	45	47	4	44	284865.545	0.02225	0.5
41	0	41	40	0	40	232865.28	-0.01778	0.5	49	2	47	48	2	46	286270.004	0.01545	0.5
41	1	41	40	1	40	232865.28	-0.01778	0.5	49	3	47	48	3	46	286270.004	0.01545	0.5
38	4	34	37	4	33	232957.569	-0.01873	0.5	50	1	49	49	1	48	287676.959	-0.01829	0.5
38	5	34	37	5	33	232957.569	-0.00718	0.5	50	2	49	49	2	48	287676.959	-0.01829	0.5
40	2	38	39	2	37	235696.52	0.01752	0.5	47	5	42	46	5	41	287713.805	-0.01038	0.5
40	3	38	39	3	37	235696.52	0.01752	0.5	47	6	42	46	6	41	287713.805	-0.01014	0.5
41	2	40	40	2	39	237092.031	-0.0067	0.5	51	0	51	50	0	50	289079.824	0.00353	0.5
41	1	40	40	1	39	237092.031	-0.0067	0.5	51	1	51	50	1	50	289079.824	0.00353	0.5
42	0	42	41	0	41	238488.377	0.00683	0.5	48	4	44	47	4	43	289085.429	0.0339	0.5
42	1	42	41	1	41	238488.377	0.00683	0.5	48	5	44	47	5	43	289085.429	0.0339	0.5
39	4	35	38	4	34	238570.104	0.01711	0.5	49	3	46	48	3	45	290481.019	0.00894	0.5
39	5	35	38	5	34	238570.104	0.0224	0.5	49	4	46	48	4	45	290481.019	0.00894	0.5
43	0	43	42	0	42	244111.114	0.01109	0.5	50	2	48	49	2	47	291887.377	-0.00512	0.5
43	1	43	42	1	42	244111.114	0.01109	0.5	50	3	48	49	3	47	291887.377	-0.00512	0.5
40	4	36	39	4	35	244182.83	-0.01377	0.5	51	1	50	50	1	49	293295.564	0.00126	0.5
40	5	36	39	5	35	244182.83	-0.01137	0.5	51	2	50	50	2	49	293295.564	0.00126	0.5
41	3	38	40	3	37	245548.179	0.01287	0.5	48	5	43	47	5	42	293320.952	0.00941	0.5
41	4	38	40	4	37	245548.179	0.0129	0.5	48	6	43	47	6	42	293320.952	0.00951	0.5
42	2	40	41	2	39	246937.464	-0.00425	0.5	49	4	45	48	4	44	294697.517	0.00491	0.5
42	3	40	41	3	39	246937.464	-0.00425	0.5	49	5	45	48	5	44	294697.517	0.00491	0.5
43	2	42	42	2	41	248335.711	-0.01147	0.5	52	0	52	51	0	51	294699.151	0.00253	0.5
43	1	42	42	1	41	248335.711	-0.01147	0.5	52	1	52	51	1	51	294699.151	0.00253	0.5
40	6	35	39	6	34	248470.997	0.04979	0.5	50	3	47	49	3	46	296096.122	-0.0007	0.5
40	5	35	39	5	34	248470.997	-0.00676	0.5	50	4	47	49	4	46	296096.122	-0.0007	0.5
44	0	44	43	0	43	249733.484	-0.00569	0.5	51	2	49	50	2	48	297504.376	0.0173	0.5
44	1	44	43	1	43	249733.484	-0.00569	0.5	51	3	49	50	3	48	297504.376	0.0173	0.5
41	4	37	40	4	36	249795.755	-0.01147	0.5	52	1	51	51	1	50	298913.73	0.00421	0.5
41	5	37	40	5	36	249795.755	-0.01039	0.5	52	2	51	51	2	50	298913.73	0.00421	0.5
43	2	41	42	2	40	252557.488	0.016	0.5	49	5	44	48	5	43	298928.074	0.00603	0.5
43	3	41	42	3	40	252557.488	0.016	0.5	49	6	44	48	6	43	298928.074	0.00607	0.5
44	1	43	43	1	42	253957.026	-0.01069	0.5	50	4	46	49	4	45	300309.372	0.02067	0.5
44	2	43	43	2	42	253957.026	-0.01069	0.5	50	5	46	49	5	45	300309.372	0.02068	0.5
41	6	36	40	6	35	254075.526	-0.0151	0.5	53	0	53	52	0	52	300318.057	0.00019	0.5
41	5	36	40	5	35	254075.526	-0.04165	0.5	53	1	53	52	1	52	300318.057	0.00019	0.5
45	0	45	44	0	44	255355.546	0.02462	0.5	52	2	50	51	2	49	303120.923	0.01452	0.5
45	1	45	44	1	44	255355.546	0.02462	0.5	52	3	50	51	3	49	303120.923	0.01452	0.5
42	4	38	41	4	37	255408.757	-0.01861	0.5	53	1	52	52	1	51	304531.438	-0.01752	0.5
42	5	38	41	5	37	255408.757	-0.01813	0.5	53	2	52	52	2	51	304531.438	-0.01752	0.5
43	3	40	42	3	39	256783.094	0.00905	0.5	50	5	45	49	5	44	304535.127	-0.00528	0.5
43	4	40	42	4	39	256783.094	0.00906	0.5	50	6	45	49	6	44	304535.127	-0.00526	0.5
45	1	44	44	1	43	259577.97	-0.01741	0.5	51	4	47	50	4	46	305920.889	0.00253	0.5
45	2	44	44	2	43	259577.97	-0.01741	0.5	51	5	47	50	5	46	305920.889	0.00253	0.5
42	5	37	41	5	36	259680.859	-0.02666	0.5	54	0	54	53	0	53	305936.536	-0.00388	0.5
42	6	37	41	6	36	259680.859	-0.0143	0.5	54	1	54	53	1	53	305936.536	-0.00388	0.5
46	0	46	45	0	45	260977.175	-0.01579	0.5	52	3	49	51	3	48	307325.156	-0.00995	0.5
46	1	46	45	1	45	260977.175	-0.01579	0.5	52	4	49	51	4	48	307325.156	-0.00995	0.5
43	4	39	42	4	38	261021.809	0.00489	0.5	53	2	51	52	2	50	308737.04	0.0184	0.5
43	5	39	42	5	38	261021.809	0.0051	0.5	53	3	51	52	3	50	308737.04	0.0184	0.5
44	3	41	43	3	40	262400.188	0.01391	0.5	51	5	46	50	5	45	310142.079	-0.00348	0.5
44	4	41	43	4	40	262400.188	0.01392	0.5	51	6	46	50	6	45	310142.079	-0.00347	0.5
45	2	43	44	2	42	263796.45	-0.00638	0.5	54	1	53	53	1	52	310148.75	0.0049	0.5
45	3	43	44	3	42	263796.45	-0.00638	0.5	54	2	53	53	2	52	310148.75	0.0049	0.5
46	2	45	45	2	44	265198.559	-0.00575	0.5	52	4	48	51	4	47	311532.097	0.00726	0.5
46	1	45	45	1	44	265198.559	-0.00575	0.5	52	5	48	51	5	47	311532.097	0.00726	0.5
47	0	47	46	0	46	266598.492	0.00245	0.5	55	0	55	54	0	54	311554.586	-0.00302	0.5
47	1	47	46	1	46	266598.492	0.00245	0.5	55	1	55	54	1	54	311554.586	-0.00302	0.5
44	4	40	43	4	39	266634.785	-0.00828	0.5	53	3	50	52	3	49	312939.043	-0.02334	0.5
44	5	40	43	5	39	266634.785	-0.00818	0.5	53	4	50	52	4	49	312939.043	-0.02334	0.5
45	3	42	44	3	41	268016.976	-0.00801	0.5	54	2	52	53	2	51	314352.671	-0.01749	0.5
45	4	42	44	4	41	268016.976	-0.00801	0.5	54	3	52	53	3	51	314352.671	-0.01749	0.5
46	2	44	45	2	43	269415.413	0.00222	0.5	52	5	47	51	5	46	315748.856	-0.01585	0.5
46	3	44	45	3	43	269415.413	0.00222	0.5	52	6	47	51	6	46	315748.856	-0.01585	0.5
47	2	46	46	2	45	270818.766	0.00501	0.5	55	1	54	54	1	53	315765.561	-0.02554	0.5
47	1	46	46	1	45	270818.766	0.00501	0.5	55	2	54	54	2	53	315765.561	-0.02554	0.5
44	5	39	43	5	38	270893.142	-0.00621	0.5	53	4	49	52	4	48	317142.918	-0.02148	0.5
44	6	39	43	6	38	270893.142	-0.0036	0.5	53	5	49	52	5	48	317142.918	-0.02148	0.5
48	0	48	47	0	47	272219.408	-0.00208	0.5	56								



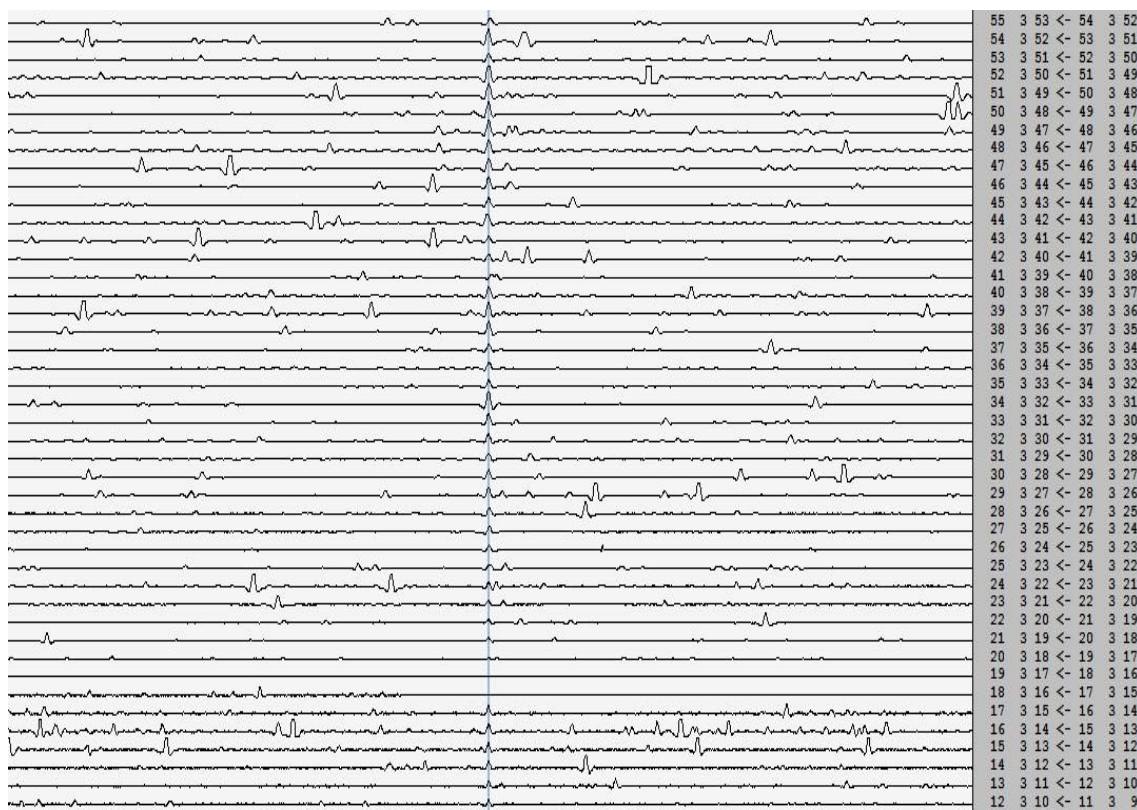
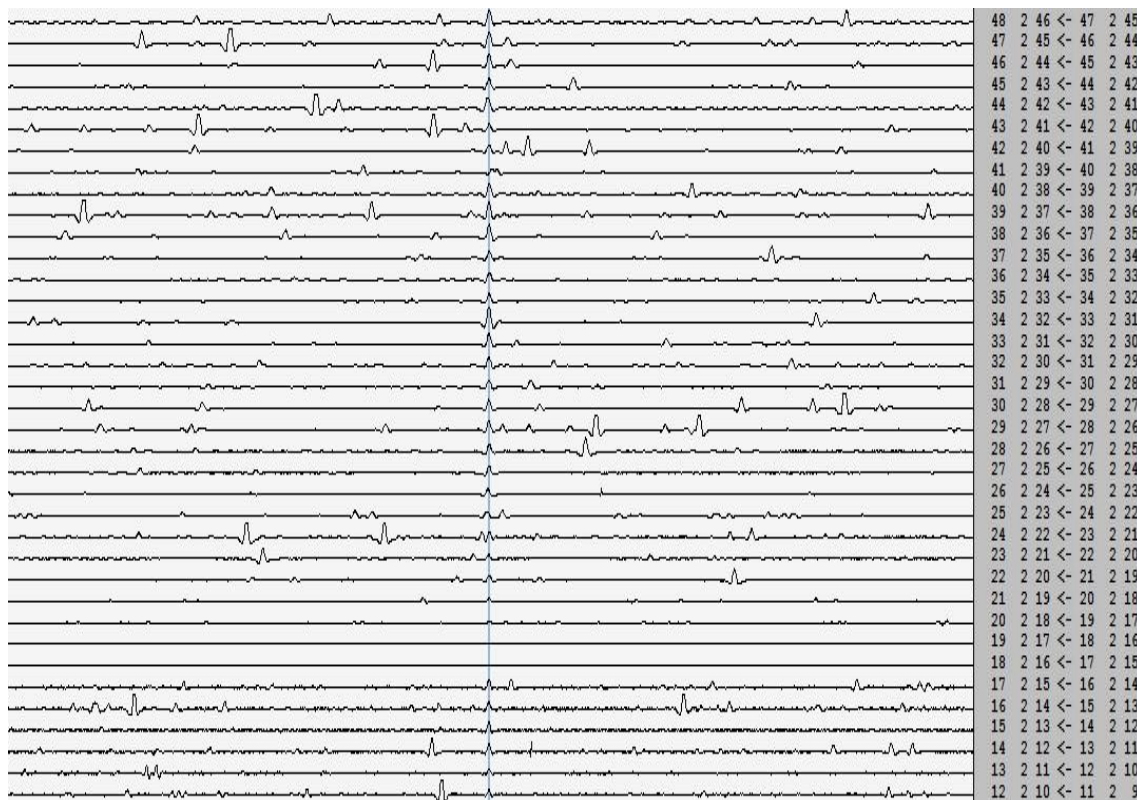


**+ TRANS CONFORMER: LOOMIS-WOOD PLOTS**

Collection of Loomis-Wood plots for the trans conformer from  $K_a=0$  to  $K_a=15$ .

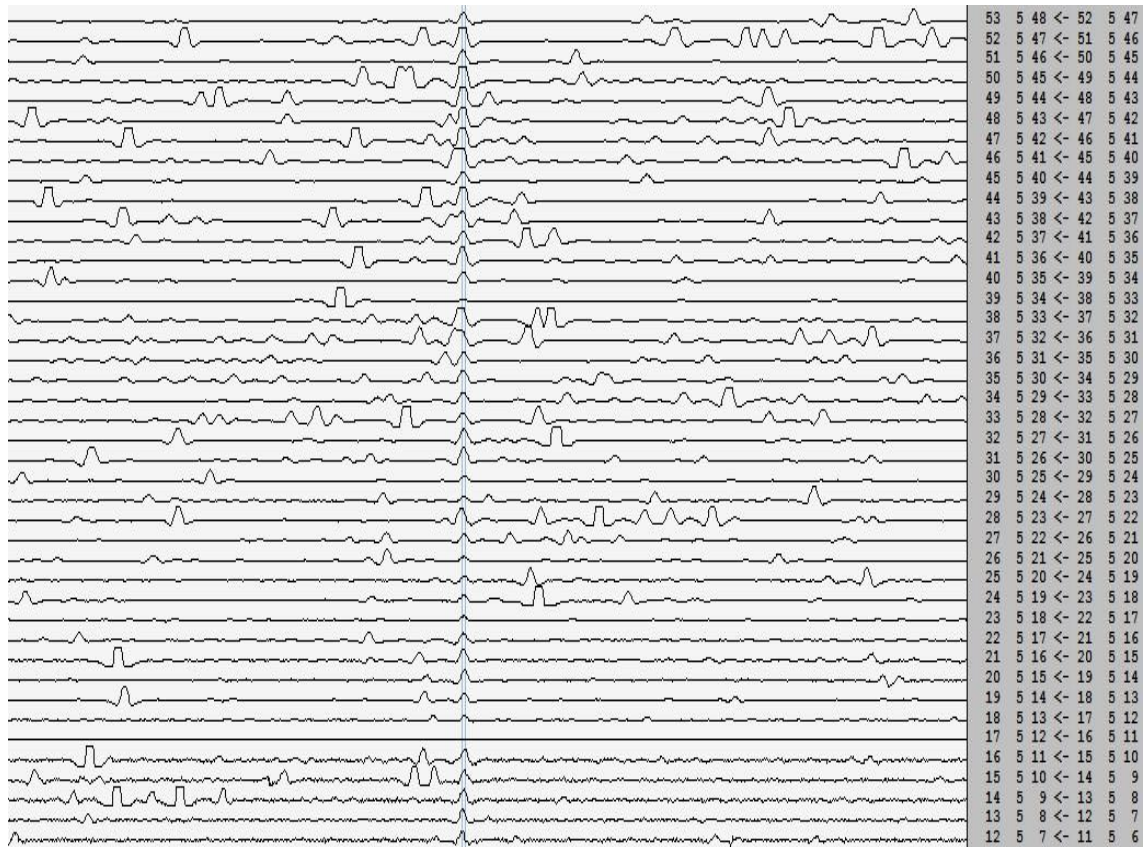
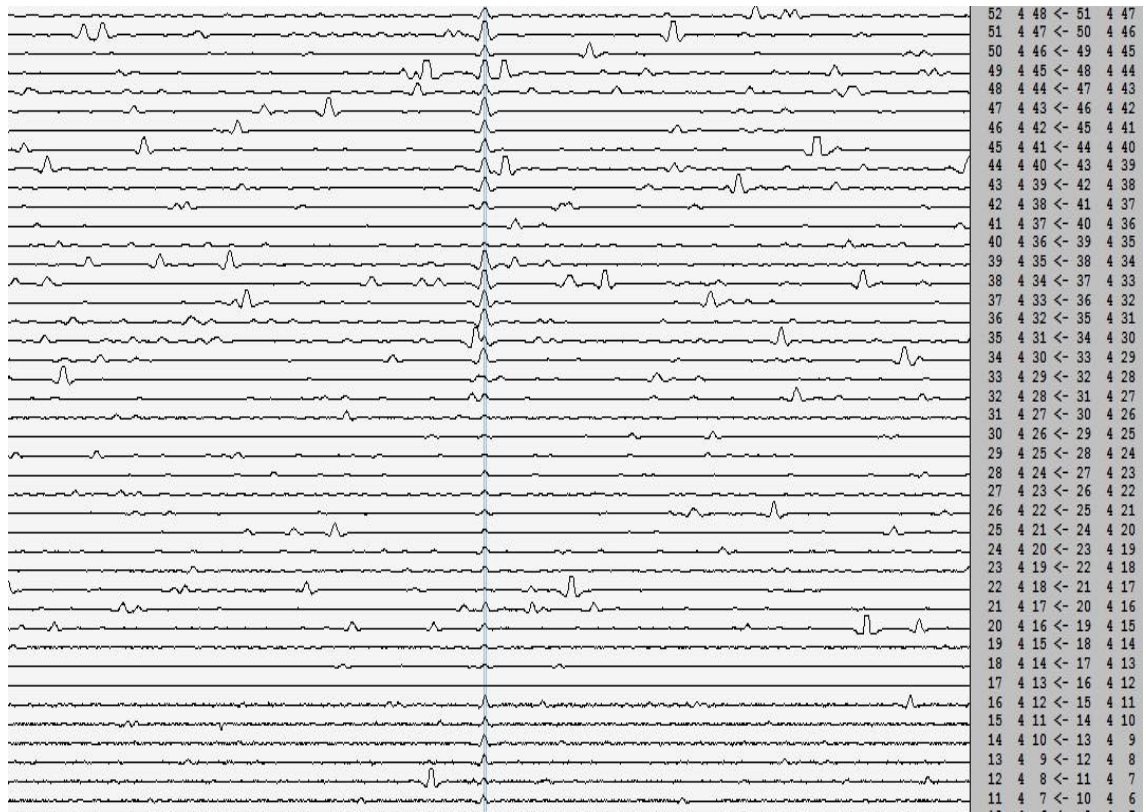


Comprehensive analysis of Isobutyraldehyde: millimetre-wave spectroscopy as an approach to ISM detection





Comprehensive analysis of Isobutyraldehyde: millimetre-wave spectroscopy as an approach to ISM detection



Comprehensive analysis of Isobutyraldehyde: millimetre-wave spectroscopy as an approach to ISM detection

